Technische Universität München

Lehrstuhl für Technische Chemie II

Selective activation of lower alkanes: Selective oxychlorination of methane and oxidative dehydrogenation of ethane

Balkrishna Tope

Vollständiger Abdruck der vom Department für Chemie der Technischen Universität München zur Erlangung des akademischen Grades eines

Doktors der Naturwissenschaften (Dr. rer. nat.)

genehmigten Dissertation.

Acknowledgments

Table of Contents

Chapter 3

Transformation of LaOCl samples to LaCl₃, functional groups and surface chemistry in relation to catalytic activity of methane oxychlorination

Chapter 4

Oxidative dehydrogenation of ethane over Dy₂O₃/MgO supported LiCl containing eutectic chloride catalysts

Chapter 5

Summary

Chapter 1

General introduction (Part A) and (Part B)

1 Motivation

Crude oil is the main source of energy and petrochemical products in the past few decades. However, the world crude oil reserves are limited and non reversible. According to the latest statistics released by BP for the year 2003 as shown in Fig 1, world reserves equivalent to 1147.7 billion barrels (bbl) of oil are available to be tapped [1].
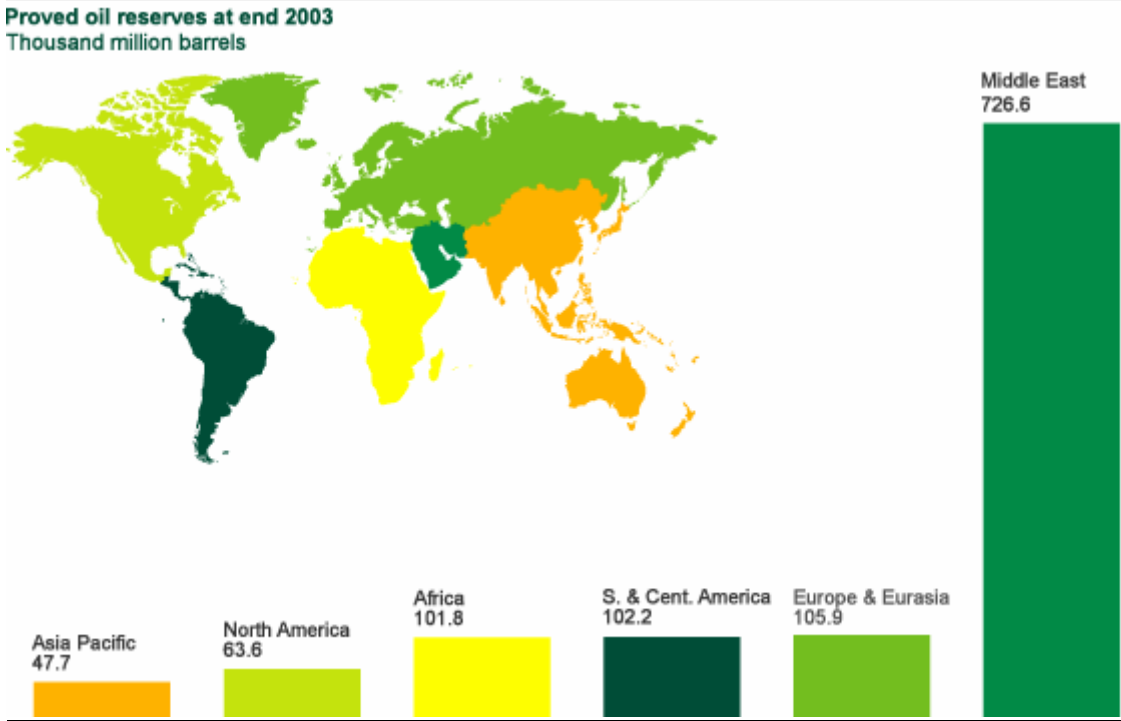
Fig.1. Proved oil reserves at end of 2003 [1]

At current world average production levels of 28 billion bbl per year, the world oil reserves will be completely exhausted within 41 years. Therefore, as ready supplies and access to crude oil are becoming more uncertain, the searching or making use of alternative source for hydrocarbons and fuel becomes more and more important. One possible substitute for crude oil is natural gas. Natural gas is a combustible mixture of hydrocarbon gases. While natural gas is formed primarily of methane. It can also include

ethane, propane, butane and pentane. The composition of natural gas (Table1) can vary widely, but below is a chart outlining the typical makeup of natural gas before refining.

Table1. Typical composition of natural gas

Methane	CH_4	70-90 %
Ethane	C_2H_6	2-8%
Propane	C_3H_8	0-2%
Butane	C_4H_{10}	0-0.8%
Carbon Dioxide	CO_2	0-8%
Oxygen	O_2	0-0.2%
Nitrogen	N_2	0-5%
Hydrogen sulphide	H_2S	0-5%
Rare gases	Ar, He, Ne, Xe	trace

The proven natural gas reserves in the world are 175.77 trillion m^3 shown in Fig. 2. Converting into appropriate units to draw a direct comparison with oil, this amount corresponds to 1105.55 trillion bbl. The energy equivalence of the world natural gas reserves is 1105.55 billion bbl of oil which is the same as the oil reserves.

In its purest form, natural gas is methane. It is considered 'dry', when most of the other commonly associated hydrocarbons are removed, and wet when other hydrocarbons are present respectively. Much of the readily accessible natural gas is already being used in local markets as fuel in residential, commercial and industrial applications. Recently, the conversion of natural gas, containing predominantly low molecular weight alkanes, to higher molecular weight hydrocarbons has received increasing consideration. The challenge arises from the fact that methane like other alkanes exhibits high chemical stability which can be easily explained by its electronic structure. An essential feature of this structure is that the number of valence electrons in methane is equal to the number of

valence orbitals and there are no lone pair and empty orbitals, which are important for heightened reactivity [2].
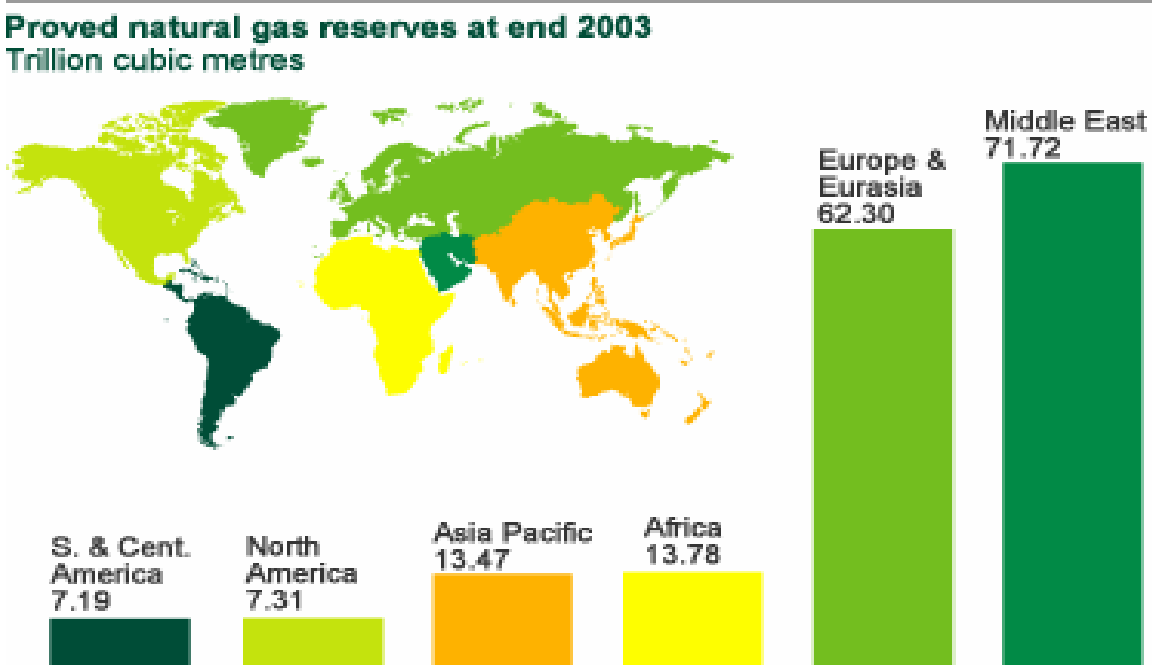
Fig.2. Proven natural gas reserves at end 2003 [1]

Among the factors decreasing the activity of alkanes can also be mentioned a low polarity of the C-H bond and a relatively high binding energy (ca. 100 kcal/mol) together with the tetrahedral arrangement of bonds which imposes steric hindrance for the attack of carbon atom. Thus, the problem of searching for chemical species capable of methane activation is very interesting.

The dominant technology now employed for using remote natural gas reserves involves its conversion to synthesis gas, also commonly referred to as "syngas", a mixture of hydrogen and carbon monoxide [3], with the syngas subsequently being converted to liquid products [4]. Synthesis gas can be converted to syncrude, with Fischer-Tropsch technology, [5-6] and syncrude can then be upgraded to transportation

fuels using typical refining methods. Alternatively, synthesis gas can be converted to liquid oxygenates, such as methanol, which in turn can be converted to more conventional transportation fuels via zeolitic catalysts.

While syngas processing provides a means for converting natural gas into a more easily transportable liquid that in turn can be converted into useful chemical products, the intermediate step involved in such processing, i.e., the formation of the synthesis gas, is disadvantageously costly. The cost occurs in adding oxygen to the substantially inert methane molecule to form the syngas mixture of hydrogen and carbon monoxide, and occurs again in removing the oxygen when hydrocarbons are the desired end-product. Further disadvantages, for methanol preparation from synthesis gas are the high pressure and high temperature to achieve acceptable syngas formation rates. Accordingly, the research for alternative methods of converting methane directly to more valuable chemical feedstocks is under investigation.

A potential alternate route to activating methane involves its oxidative halogenation, where in a first step methyl halide are formed, which can be converted in a second step into valuable commodity chemicals, such as methanol, dimethyl ether, light olefins, and higher hydrocarbons, including gasoline. While converting the methyl halide into higher hydrocarbons, the produced hydrogen halide may then be separated from the hydrocarbon product and recycled back to the halogenation process step. Formation of water as by product, which constitutes 55.6% (by weight) of the products in methanol conversion, is thereby avoided. When applied to chlorine halogenation, this route has been referred to as the "chlorine-assisted" route and it involves the conversion of methane into methyl chloride [2].

2 Processes for the conversion of methane into methyl chloride

The chlorination of paraffins, discovered by Dumas in 1840 [7] is the oldest substitution reaction. Photochemical or thermal chlorination as we today call it radical process lacks selectivity and generally yields mixture of chloroparaffins. In the chlornation of methane all four chloromethanes are obtained.

$$CH_4 \xrightarrow{Cl_2} CH_3Cl \xrightarrow{Cl_2} CH_2Cl_2 \xrightarrow{Cl_2} CHCl_3 \xrightarrow{Cl_2} CCl_4 \qquad (I)$$
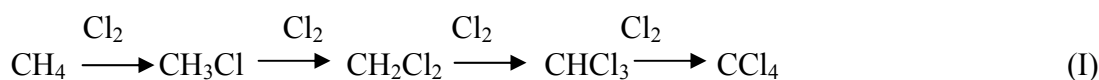
The preferred route to methyl chloride has been the reaction of methanol with HCl. Commercially, methyl chloride is produced by reacting methanol with hydrogen chloride, either by bubbling hydrogen chloride gas through boiling methanol with or without a zinc chloride catalyst, or by passing combined methanol and hydrogen chloride vapours over an alumina catalyst at 350°C [8]. The overall reaction is shown in eq.(II):

$$CH_3OH + HCl \longrightarrow CH_3Cl + H_2O \qquad (II)$$

While, the eq.(II) works with methanol, hydrogen chloride does not react directly with methane (see eq.(III)) and no catalyst is available for this process yet.

$$CH_4 + HCl \xcancel{\longrightarrow} CH_3Cl + H_2O \qquad (III)$$

Oxychlorination, as shown in eq.(IV), involves the catalytic reaction of methane with a mixture of oxygen and hydrogen chloride to produce methyl chloride [2]. The reaction is not thermodynamically limited. Depending on the catalyst used, methyl

chloride is produced highly selectively and in yields that make the process commercially viable. The greatest advantage of this process is that the methyl chloride can be converted to different products in a subsequent process and the resulting hydrogen chloride can be recycled to the oxychlorination reactor.

$$2\ CH_4 + 2\ HCl + O_2 \longrightarrow\ 2\ CH_3Cl + 2\ H_2O\ \text{(highly selective)} \qquad\qquad \text{(IV)}$$
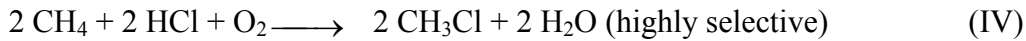
2.1   Process of oxychlorination of hydrocarbons

Oxidative chlorination of hydrocarbons for selective production of chlorinated products is a new chemistry with the potential to reduce significantly feed and capital costs in hydrocarbon functionalization. Specifically, this technology allows the use of cheap alkane-alkene mixtures or pure alkanes as a feed, instead of pure alkenes, and to achieve selective chlorination in a single stage. The overall chemistry can be described by eq.(V):

$$R\text{-}H + HCl + {}^1\!/_2O_2 \longrightarrow R\text{-}Cl + H_2O \qquad\qquad\qquad \text{(V)}$$

Research efforts for this chemistry are divided into three main areas based on the hydrocarbon feed: C_1, C_2, and C_{3+} [2, 9]. Currently, the research on the C_2 system, as represented by the ethane to vinyl chloride technology (E2V), is being transferred from laboratory to miniplant stage. In E2V, the overall reaction is:

$$C_2H_6\ (\text{or } C_2H_4) + HCl + O_2 \longrightarrow C_2H_3Cl + 2\ H_2O \qquad\qquad \text{(VI)}$$
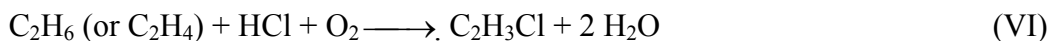
The reaction proceeds over a rare-earth chloride catalyst at about 400°C with a selectivity higher than 50% [9]. The main side products are CO and CO2. In the case of methane (C_1) oxychlorination the main product is CH_3Cl as seen in eq. (IV). Extensive research has been carried out on this reaction because natural gas is cheaper and easily available.

Initially oxychlorination reactions were mainly studied on Cu, Fe, Cr, K chloride catalysts. In traditional oxychlorination chemistry, for example over Cu, the metal changes its oxidation state on hydrocarbon chlorination, and then the metal is reoxidized by oxygen in presence of a chlorine source [10 - 12]:

$$2 CuCl_2 + C_2H_4 \longrightarrow 2 CuCl + C_2H_4Cl_2 \hspace{3cm} \text{(VII)}$$
$$4 CuCl + O_2 + 4 HCl \longrightarrow 4 CuCl_2 + 2 H_2O \hspace{2.5cm} \text{(VIII)}$$
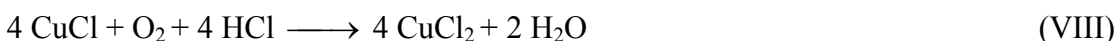
2.2   Catalysts for oxychlorination of methane

Extensive studies have been carried out on the catalyzed oxidative halogenation of methane to halogenated methane's [13-16]. Catalysts for this process are typically based on first row transition metal halides, particularly, copper chloride, with promoters, such as potassium and lanthanum chlorides, supported on silica or alumina [17-21]. Chlorination of methane has also been reported over other catalysts such as active carbon and Kieselguhr, pumice [22, 23]. Besides this certain Pd based catalysts supported on various materials have been studied [24-30].

All the catalysts stated above produce an unacceptable quantity of per halogenated product, such as carbon tetrachloride, which is less desirable among C_1 halogenated products, such as methyl chloride and dichloromethane. As a further disadvantage, these

processes produce an unacceptable quantity of deep oxidation products, specifically carbon monoxide and carbon dioxide (CO_x). The production of lower value perhalogenated products and undesirable oxidized products irretrievably wastes the methane and creates product separation and by-product disposal problems. Additionally, many of the transition metal halides, used as catalysts, exhibit significant vapour pressure at reaction temperatures, that is, these catalysts are volatile. The volatility generally produces a decline in catalyst activity and/or deposition of corrosive materials in downstream parts of the process equipment. Methyl chloride can also be produced by reacting methane with chlorine gas over supported acid or platinum metal catalysts [31-32]. The supported acid catalysts include ferric oxychloride, tantalum oxyfluoride, niobium oxyfluoride, zirconium oxyfluoride, and antimony oxyfluoride, supported on alumina. Disadvantageously, these catalysts exhibit reaction rates and lifetimes that are too low for practical use. As a further disadvantage, the hydrochloric acid formed must be converted back to chlorine gas and water, which makes the process uneconomical for most applications. Since the direct chlorination of methane with chlorine gas is substantially non-selective for methyl chloride, and since the catalytic oxidative chlorination of methane is either non-selective for methyl chloride or impractical, the current method of preparing methyl chloride depends on the reaction of methanol with hydrochloric acid and does not solve the problem of activation of methane. Accordingly, if C_1 chemistry based on the oxidative chlorination of methane to methyl chloride and other lower chlorinated methane's is to advance, then various improvements in the above catalytic processes will be required. Specifically, an increase in selectivity to methyl chloride is needed. Likewise, a reduction in selectivities to perchlorinated and oxygenated

9

products is needed. Also needed is an increase in catalyst activity and catalyst lifetime. With these improvements, the conversion of methane to methyl chloride will be more attractive. Likewise, downstream applications, particularly, of methyl chloride to methanol, dimethyl ether, vinyl halide monomer, acetic acid, light olefins, and higher hydrocarbons, including gasoline, will also be more attractive, thereby increasing the overall value of the direct conversion of methane to methyl chloride [33-35].Copper-based catalysts have proven to be active for this reaction though these catalysts are originally used in the industrial oxychlorination of ethylene [36]. Since copper based catalysts are known to be also active for Deacon chemistry [37], oxidation of HCl to Cl_2, methane activation through liberation of elemental chlorines is possible. Therefore, methane chlorination proceeds, at least partially, *via* a radical gas-phase mechanism and the selectivity to methyl chloride is usually low at significant methane conversion level [37]. Another drawback is that copper salts are volatile at the usual temperatures required for the methane activation. By adulation of KCl, which can lower the melting point of copper chloride and promotes the copper redox steps, the stability of copper catalysts has been greatly enhanced [38-40]. Moreover, in order to prevent melt segregation of copper and potassium chlorides at high reaction temperatures, $LaCl_3$ has been used as a stabilizing promoter [41, 42].

Recently, researchers at Dow Chemicals, USA, discovered that certain rare earth metal catalysts exhibit extremely high selectivities for CH_3Cl at acceptable CH_4 conversions in the methane oxychlorination process [40]. LaOCl has been found to be particularly effective providing a plausible solution to the above stated problems in the methane oxychlorination process and hence is at the core of our study.

3 Industrial process for converting methane into higher hydrocarbons using methyl chloride as intermediate

The industrial process for converting methane into higher hydrocarbons using methyl chloride as intermediate is shown in Fig 3. Methane (11) along with oxygen (13) and recycled gases including HCl (15) are preheated and introduced into the oxychlorination reactor (17). The methane oxychlorination reaction is carried out under optimum temperature and pressure conditions over a $LaCl_3$ catalyst.
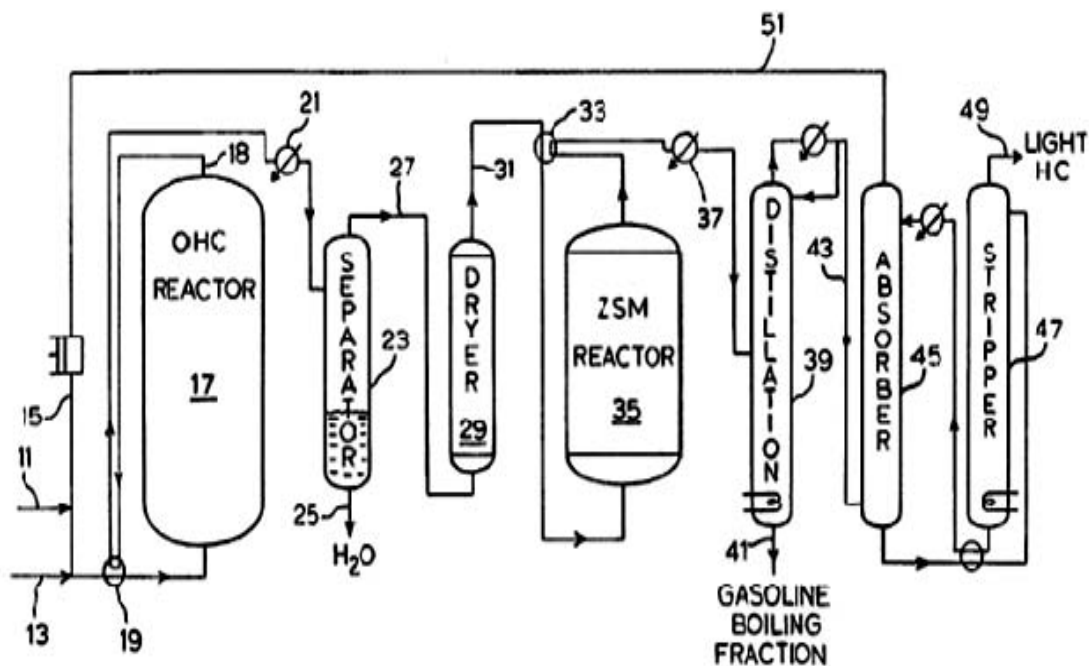
Fig.3. Process flow diagram for the conversion of methane into higher hydrocarbons

The heat from the intermediate gaseous products (18) is exchanged with the incoming feed in a preheater (19). The cooled intermediate gases are passed into a condenser (21) to start water removal at 30°C – 40°C. Water, possibly with small amounts of methylene chloride, chloroform and unreacted HCl, is collected in the

separator (23) and withdrawn from the process (25). If required for economy reasons, these chlorinated materials can be recovered by fractionation and returned to the process. The intermediate gaseous mixture (27) is further dried over a molecular sieve or an alumina desiccant in a dryer (29) to obtain a dew point of at least -40°C. Drying is enhanced by pressures in the range of 10 to 20 atmospheres. The dried reactants including methyl chloride and methylene chloride are preheated in a preheater (33) and passed into a second reactor (35) for contact with a crystalline aluminosilicate catalyst. Preferably a shape selective catalyst in the hydrogen or iron promoted form of ZSM-5 is employed. The reaction product gases are further processed by cooling and condensing at about 30°C – 40°C (37). They are then fed into a fractionating column (39) from which gasoline boiling fraction (41) is obtained. The gasoline boiling fraction typically includes hydrocarbons from the C_5 to C_{10} range with an average molecular weight of about 90 to 100, boiling at temperatures of about 30°C to 200°C. The column overhead (43) passes to an absorber (45) stripper (47) combination for separating the light hydrocarbons (49) from HCl excess, methane and inert gases (51). Light hydrocarbons can include C_3-C_5 hydrocarbons and possibly some ethane. This light fraction can be withdrawn for other use or advantageously recycled with the HCl and unreacted methane (51) to the oxychlorination reactor. Recovering and recycling all HCl allows this process to be installed in remote location.

4   Scope of the thesis

There are abundant natural gas reserves in the world. However, most of the natural gas is concentrated in relatively remote part of the world; transportation of this gas to the local market is always a problem. Therefore, techniques for transformation of methane, the major component of the natural gas, into easy transportable or value added products, such as methanol, ethylene, aromatics, and liquid hydrocarbon fuels are high industrially interested. However, selective activation of C-H bond in methane is difficult because of low polarity of C-H bond and a relatively high binding energy together with tetrahedral arrangement of the bonds. Hence, selective activation of methane presents a formidable challenge to the chemical industry. A viable process for the conversion of methane into a more useful intermediate is required if the natural gas reserves located in remote parts of the world have to be fully exploited. The low pressure and low temperature conversion of methane to methyl chloride offers a plausible solution to this problem. In a further step methyl chloride can be used for the production of olefins and other useful chemicals. Over the years many catalysts have been studied for this process but so far none has been industrially viable. Only recently, in a remarkable breakthrough by DOW Chemicals, lanthanum oxychloride based catalysts have been found to show promising results for methane oxychlorination. In line with this discovery, the objective of this thesis is the characterization and correlate physicochemical properties of new, innovative lanthanum based catalysts for the conversion of methane into methyl chloride.

Four lanthanum oxychloride based catalyst precursors were supplied by Dow Chemical Company USA. To identify the key factors that influence the catalytic behaviour, a combination of physicochemical techniques were applied. Textural characteristics (surface area, dimension and shape of the particles) were investigated by

BET analysis and SEM. Structural characterization was carried out by XRD. EDX was used to determine the chemical composition of the catalytic materials. The basic and acidic properties of the samples were investigated by CO_2 - and NH_3 TPD respectively. Raman measurements were carried out to understand surface characteristics of the catalyst. IR spectroscopy used to identify functional groups and to study the surface chemistry. The catalytic behaviour and activity were studied using a plug flow reactor under various conditions. The gas stream was analyzed by online gas chromatography. Temperature programmed activation and chlorination experiments were carried out to study the transformation of LaOCl to $LaCl_3$.

1   Motivation (Part B)

Ethylene and propylene are important building blocks of chemical industry. These light olefins are currently produced from catalytic or steam cracking of various petroleum fractions and catalytic cracking (FCC) of heavy oil. While these two routes are very well developed and commercialized, they have several limitations. These processes are already are operated under severe conditions with disadvantages including thermodynamic limitations, which in the case of ethane need to operate at extremely high temperatures, high input requirements for the strongly endothermic reaction and formation of coke on the catalyst [43].

To surpass these limitations, the driving force which stimulates new breakthrough for the alkane commercialization involves better engineering of the process and better tuning of the catalyst activity and selectivity. A conceptually interesting way that has been propose to overcome theses limitations, is called oxidative dehydrogenation and has widely been studied in the literature [44-46]. ODH is exothermic and can be operated at lower temperatures (T < 650ºC) reducing so the energy input. Presence of oxygen in the feed limits coking and extends catalyst life time hence frequent catalyst generation is not necessary. The feedstock for ODH, light alkanes, is easily available and competitively cheaper. Despite these advantages industrial scale application of ODH has not been successful till date due to low olefin selectivity shown by catalysts employed. The development of an appropriate catalyst proved to be difficult, since CO_x the main byproducts is thermodynamically favored and the olefins produced are generally more reactive than alkanes. Consequently, catalysts that can, activate ethane effectively, while maintain high ethene selectivity would be highly desirable.

2   Current methods for olefin production

Ethylene is one of the primary building blocks for the manufacture of chemicals and its demand increases 2 to 3 % every year. The olefins are mainly used for production of plastic, surface coating materials, synthetic polymers and synthetic fibers. The main route to ethylene and propylene production is by the thermal cracking of hydrocarbons, other methods include catalytic cracking and catalytic dehydrogenation. A brief description of these industry processes is given below [43, 47, 48]

Steam cracking

The majority of olefin production comes from thermal cracking of various petroleum hydrocarbons, most often LPG and naptha with steam. The process is called pyrolysis or steam cracking. The main products of steam cracking are ethene and propene. Thermal cracking reaction also produces valuable by-products including propylene, butadiene, benzene, gasoline and hydrogen. Some of the less valuable co products include methane and fuel oil. The schematic of a steam cracking reactor is shown in Figure 4. Thermal cracking of hydrocarbons takes place in tubular coils placed in the center of a fired radiant box. Steam is added to reduce the partial pressure of the hydrocarbons in the radiant coils. The cracked effluents leave the radiant coils at a temperature of 750 to 900°C,
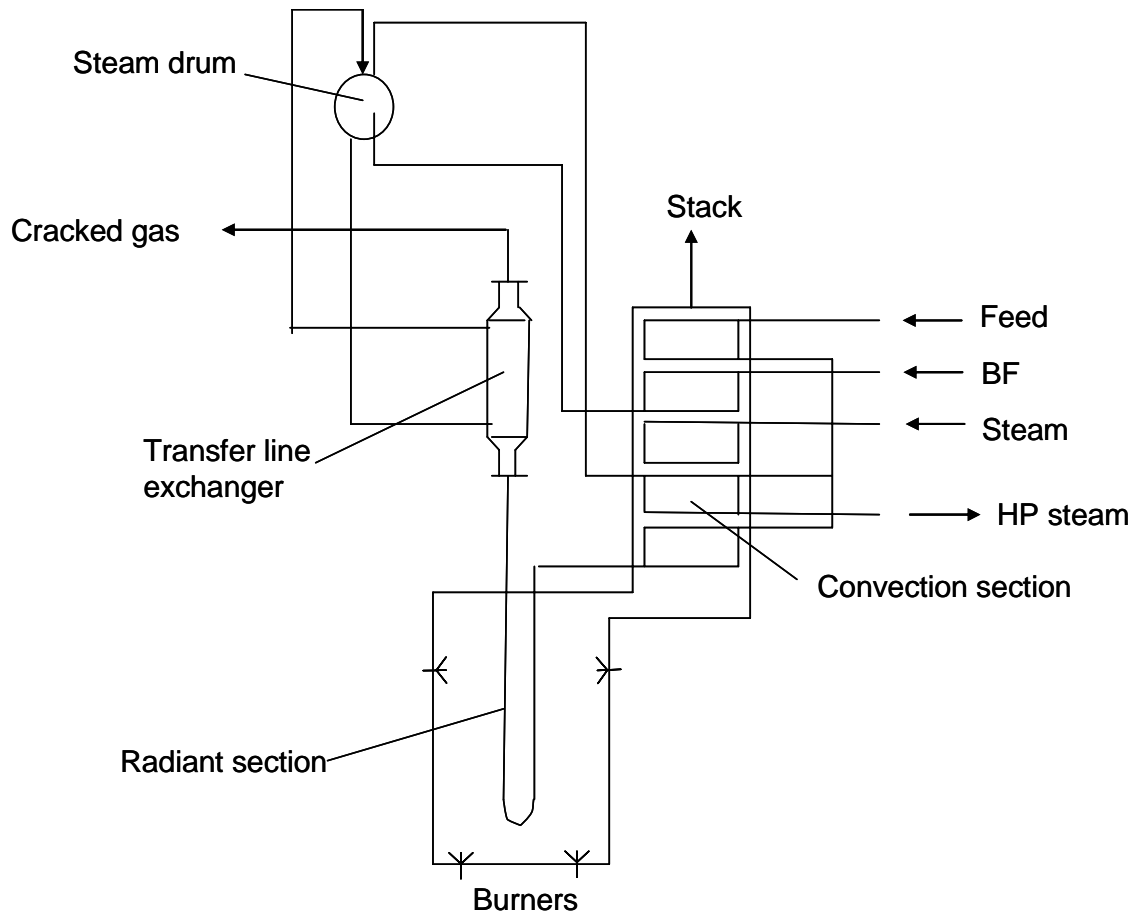
Fig.4. The schematic diagram of a steam cracking reactor.

depending on feedstock, cracking severity and selectivity. In order to maintain the overall process efficiency, it is required to efficiently recover the heat in the cracked effluents. The cracked effluents also need to be quenched quickly to stop secondary reactions that yield degradation. Since the conversion of saturated hydrocarbons to olefins in the radiant tube is highly endothermic, high energy input rates are needed. The reaction product leaving the radiant tube at 750 to 900°C are cooled to 550-650°C within 0.02-0.1 s to prevent degradation of the highly reactive products by secondary reaction. The feed stock is cracked into smaller molecules like ethylene, other olefins and diolefins. Those products are separated by using a complex sequence of separation and chemical-treatment.

3   The catalytic oxidative dehydrogenation of lower alkanes

The modern petrochemical industry heavily depends on the ethylene and propylene. Ethylene is mainly used for the production of low density polyethylene (LDPE), high density polyethylene (HDPE) and ethyl dichloride, ethylene oxide, linear LDPE and ethyl benzene among other compounds. However the cost and availability of feedstock can seriously limit the process involving olefin because the raw materials constitute 60-70 % of the costs of production. This creates strong dependence on the raw materials. Therefore, more abundant and economic sources for the production of olefin must be find out. Ethane is the second major component of natural gas which makes it a potential source for the production of olefins. However activation of ethane is difficult due to the strong C-H bond and hence requires high activation energy to break that bond. Both carbons in ethane are primary carbons and which possesses the second highest C-H bond energy (Table 2).

Table 2. Dissociation energy of C-H bond and charge on H of some light hydrocarbons.

Hydrocarbon	Weakest C-H bond	C-H bond E_{disoc}(kJ/mol)	Atomic charge on H
Methane	Primary	440	+0.087
Ethane	Primary	420	+0.002
Propane	Secondary	401	-0.051
Isobtane	Tertiary	390	-0.088

This makes it less reactive than its larger homologues. Although it is difficult activate, their large reserves underline the economic interest in their conversion. Hence the oxidation of lower alkanes is a key issue in the use of natural gas and volatile

petroleum fractions. Although oxidative dehydrogenation (ODH) offers many advantages compared to steam cracking and direct dehydrogenation. ODH of alkanes continue to pose major development challenges. Research efforts on ethane ODH have led to catalytic systems with yield approaching those that could compete with the current non oxidative technology, indicating the probability of a viable process. Research efforts are being made to limit the formation of CO_x by increasing the selectivity to olefin at appreciable conversion.

Catalysts for ODH is extensively studied in the literature and many review article are published on this topic. In a review article Kung et al. [49] mentioned that selectivity of alkenes decreases with increasing conversion. Reaction proceeds with a sequential mechanism in which alkanes are dehydrogenated to produce alkenes, which could react further at catalysts surface to produce carbon oxides. Banares et al. [44] stated in review that ODH of ethane may be highly selective as ethylene is less reactive than ethane in some catalytic system. This is assumed to be the difference cause by different reactivity's of both reactant paraffin and formed olefins make the olefin formation and degradation different in two cases. Cavani et al. [45] suggested that two reaction mechanisms existed simultaneously for ODH of ethane. Heterogeneous surface initiated mechanism favored at low temperature and homogeneous gas phase mechanism proceeds at higher temperature. Burch et al. [50] also highlighted the lower reactivity of ethylene as compared to ethane for catalytic conversion. He further pointed out that the contribution from non-catalytic homogeneous reaction was evident for ODH of alkanes at temperature above 650°C. Thus for high temperature catalytic measurement, blank reaction data in the absence of catalyst are necessary for a reliable evaluation of catalytic performance.

The acid-base properties of catalysts play a very important role for the initial activation of the C-H bond in the hydrocarbon. The acid-base interaction between the hydrocarbon molecule and the surface of catalysts can promotes the approach of the hydrocarbon to the active sites [51, 52]. The surface acid-base features of an oxide depend on the charge and radius of the cation. The charges on the most reactive hydrogen atom of the hydrocarbons shown in Table 2 were calculated by Busca et al. [52]. A new concept related to selectivity in mild oxidation catalysis of hydrocarbons was established by Bordes et al. [53]. He found relationship between optical basicity and selectivity. Cavani et al classified catalysts for ODH into two groups a) reducible transition metal oxides, b) ions and oxides of Group IA/IIA metals.

The first group materials are reducible transition metal oxides, based on V and Mo oxides, which can operate at temperatures below 550 ºC [54-60]. The second groups are non-reducible alkali metal-based oxide catalysts that are active at a temperature above 600 ºC [61-71]. The transition metal oxides with redox properties have not seen promising because of their highly active nature, re-adsorption of olefins leads to total oxidation and hence limit ethylene selectivity and yield. The mechanism for the transition metal oxide and other metal oxide believed to proceed through a classical Mar-van Krevelen red-ox cycle. Catalysts for group IA and group IIA operates at high temperature in which a homogeneous gas-phase radical mechanism controls.

3.1 Reducible metal oxide catalysts (Redox catalysts)

The mechanism for the transition metal oxides and or other easily reducible metal oxides which operates below 600°C is believed to proceed through a classical Mar-van Krevelen red-ox cycle. Lower alkanes from gas phase are activated by the lattice oxygen

20

of the catalyst to ultimately form olefins through several possible intermediate species. Gas phase oxygen serve as role of re-oxidizing the catalyst surface. The mechanism is presented in Scheme 1.1, in which O_1 represents lattice oxygen and V^* is a surface vacancy.

$$C_nH_{2n+2} \quad C_nH_{2n+2} + H_2O \quad O_{2(gas)}$$

$$C_nH_{2n+2\,(ads)} + O_1 \quad 2V^* \longrightarrow 2O_1$$

Oxide catalysts surface
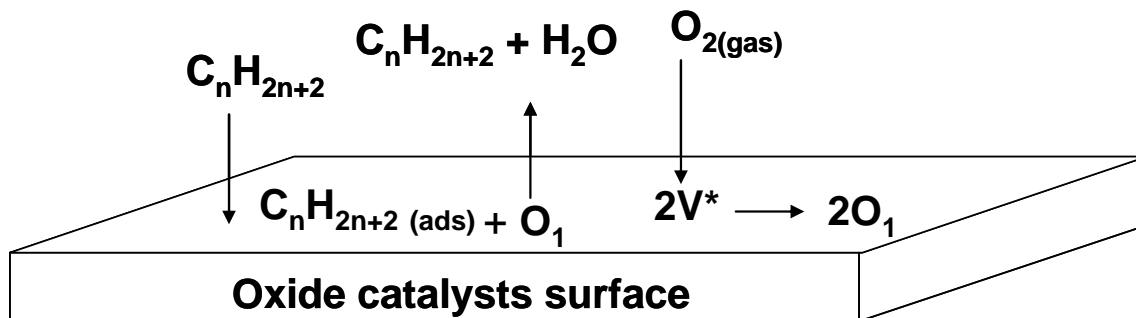
Scheme 1.1 The mars van Krevelen red-ox mechanism

Although mars van Krevelen red-ox cycle is believed to be the dominant mechanism over selective ODH catalyst. There are several unselective mechanistic steps on the catalyst surface and in the gas phase, consequently overall mechanism could be quite complicated [49]. There are several routes [Scheme 1.2] by which reaction can proceed for ODH. For higher alkanes product distribution is more complicated.

$$C_nH_{2n+2} \xrightarrow{r_1} C_nH_{2n}$$
$$r_3 \searrow \qquad \swarrow r_2$$
$$CO_x$$
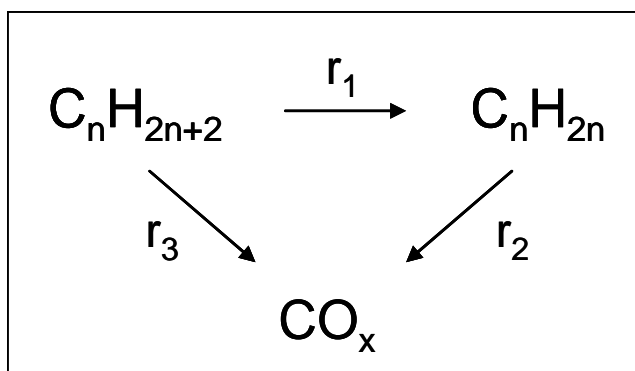
Scheme 1.2 Possible pathways for alkanes ODH

V-containing catalysts are extensively studied for Oxidative dehydrogenation (ODH) of ethane [72-75]. A change in the support changes the catalytic performance for ethane oxidation by one order of magnitude in the sequence. $TiO_2 > ZrO_2 >> Al_2O_3 > Nb_2O_5 > CeO_2$-$SiO_2$ [76]. Both acid-base and redox properties affect the conversion of ethane. Lopez-Nieto and coworkers [77-78] have reported the equilibrium required between reducibility and the acid-base character of the sites. Silica supported molybdenum oxide catalysts are tested for ODH with nitrous oxide instead of oxygen [79]. Catalytic activity is very low if molecular oxygen is used instead of nitrous oxide. Erdohelyi and Solymosi [80-83] evaluated the performance of alkali metal on silica supported vanadium oxide and alkali-molybdates supported on silica for ODH of ethane. All catalysts undergo deactivation slowly during the oxidation of ethane with N_2O. Catalysts are reactivated by oxidation. Merzouki et al [84] evaluated the performance of phosphorous containing VPO catalysts and the activity was found to be very low under low temp conditions. Conversely, Pd-doped catalysts increases ethane conversion and ethylene becomes the main oxidation product with selectivity above 90% at ca 12% conversion.

The group of Otsuka [85] studied the performance of many oxides for ODH of ethane which includes oxides of B, Mg, Al, Si, Ca, Ti, V, Cr, Mn, Fe, Co, Ni, Cu, Zn, Ga, Sr, Y, Zr, Nb, Mo, Cd, In, Sn, Sb, Te, Ba, La, Ce, W, Pb, and Bi. However most of the oxides produces mainly CO_x . Supporting Boria on alumina, magnesia, lanthanum and P_2O_5 improves catalytic performance of boria and the yield of ethylene was nearly 14.5%.The use of mixed oxide catalyst is a very versatile method to tailor the catalytic properties. Thorsteinson et al [86] showed its applicability for ethane oxidation using

22

mixed oxides of V and Mo, together with other transition metal oxides. The MoVNb formulation appeared to be efficient for the production of ethylene. Recently many researchers varied mixed oxide composition and studied for ODH of ethane. The activity results were found to be significant when MoVTe(Sb)Nb oxides were used [87, 88].

3.2 Non-reducible metal oxide catalysts

The second group is non-reducible alkali metal-based oxide catalysts which are active also active for methane coupling [89-91] and these catalysts activate ethane at a temperature above 600 ºC. The most successful of these catalysts is the Li/MgO. The conversion of ethane on Li-doped magnesia is a heterogenous-homogeneous catalytic process due to its ability to generate ethyl radicals. This strongly promotes selectivity since oxidation of ethylene on Li/MgO catalysts is non-selective. Non reducible oxides for ethane oxidation run through a different mechanism than on reducible oxides because of the absence of redox functionality. The Selectivity for ethylene is higher for non-reducible catalysts than reducible catalysts. A redox catalyst promotes further non selective oxidation.

The activity of Li/MgO can be significantly increased by addition of small amount of chlorine-containing compounds in the feed or by direct incorporation of chlorine into the catalyst [92, 93]. Lunsford et al [93] investigated the effect of chloride ions on Li/MgO catalysts, ethylene yields of 58% (77% selectivity at 75% conversion) have been maintained for up to 50 h on stream at 620°C. A surface model has been proposed in which lithium is mainly present as LiCl on the MgO support. Au et al [94] studied $BaBr_2/Ho_2O_3$ catalysts which show significant deactivation during the first 4h of operation (from 88% selectivity of ethylene at 71% of conversion after 1h on stream to

64% selectivity of ethylene at 52% conversion after 4h on stream). After this deactivation the yield of ethylene remains constant at 33%. Further they used F-doped catalysts and achieved yield 32.9% and for Cl-doped catalysts 50.8% yield at 680°C which was stable on stream for about 48h [95].

Recently, Wang et al. [96] greatly improved the catalytic performance for ethane ODH by modifying silica and zirconia based catalysts with lithium chloride and sulfur. Carbon dioxide has also tried as oxidant instead of molecular oxygen. For silica-based catalysts $LiCl/SiO_2$ gave 99% ethane conversion and 80% ethylene selectivity at 600°C, however it shows rapid deactivation. For zirconia-based catalysts [97-99], sulfated zirconia doped with lithium was found to be effective giving over 90% selectivity to ethylene and 25% ethylene yield at 650°C. Addition of chlorine to LiCl/sulfated zirconia catalysts gave 97.6% conversion of ethane and 69.0% selectivity to ethylene. The activity of Li/MgO can be further improved by addition of SnO_2, La_2O_3, Nd_2O_3 or Dy_2O_3 as promoter [67-68]. Ethene yields up to 77% have been obtained when Dy_2O_3 is used as a promoter [68].

From previous study in our group, it has been found [68] that high selectivity is obtained, once the reaction temperature approaching the melting point of LiCl. To further study this phenomenon and the effect of melting point on the ODH of alkanes, a series of catalyst were prepared by adding alkali or alkaline earth metal chloride to the $LiCl/Dy_2O_3/MgO$ catalyst. Various physicochemical characterization techniques are used together with the catalytic tests for the OHD of ethane in order to establish structure-activity relations.

4   Scope of the thesis (Part B)

The aim of this thesis is to produce ethene selectively from ethane at lower temperature through oxidative dehydrogenation. To achieve this goal it is necessary to formulate catalysts composition to reduce the melting temperature of LiCl melt which is selective towards olefin production, by addition of alkali metal chloride and alkaline chloride metal.

To explore the possibility of tailoring a catalyst that is highly selective at lower temperature. A series of catalyst were prepared by adding alkali or alkaline earth metal chloride to the $LiCl/Dy_2O_3/MgO$ catalyst. Theses catalysts are characterized by various physicochemical characterization techniques such as N_2 adsorption measurement, XRD, TG-DSC. Basic properties of the sample were investigated by CO_2 TPD and by IR spectroscopy. Catalytic activity for ODH of ethane was studied on theses catalysts. The correlation between melting temperature, basicity and activity was established. This knowledge would lay ground work for developing highly selective catalysts at low temperature.

References

[1]   BP Statistical Review of World Energy 2004.

[2]   G. M. Zhidomirov, V. I. Avdeev, N. U. Zhanpeisov, I. I. Zakharov, I.V.Yudanov, Catalysis Today., 24 (1995) 383.

[3]   J.R. Rostrup-Nielsen, Catal. Today., 18 (1993) 305.

[4]   Sustainable Strategies for the Upgrading of Natural Gas: Fundamentals, Challenges and Opportunities. Proceedings of the NATO Advanced Study Institute, held in Vilamoura, Portugal, July 6-July18, 2003.

[5]   Kirk-Othmer Encyclopedia of Chemical Technology, Fourth Edition., 121 (1995) 55.

[6]   I.E. Maxwell, J.E. Naber, Catal. Lett., 12 (1992) 105.

[7]   J.B. Dumas, Ann. Chim. Phys., 73 (1840) 2.

[8]   D.A. Evans, T.R.Watson, P.W. Robertson, J.Chem.Soc.,16 (1950) 24.

[9]   M. E. Jones, J.P.Henley, D. A. Hickman, WO 01/38272 A1 2000.

[10]   P. R. Arganbright, W. F. Yates, J. Org. Chem., 27 (1962)1205.

[11]   R. Zhang, App. Chem., 3 (1986) 23.

[12]   F. Chen, Petrochemical Eng., 23 (1994) 421.

[13]   R.P. Noceti, C.E. Taylor, US 4769504 1998.

[14]   W. L. Borkowski, P.E. Oberdorfer, D. Claymount, W.H. Seitzer, US 3172915, 1965

[15]   R. J. Blake, G.W. Roy, US 3657367, 1972.

[16]   T. Imai, P.T. Barger, A. H. Eck, US 4795843 1989.

[17]   M.A Mcdonald, M.F. Zarochak, W.J. Graham, Chem Eng Sci., 49 (1994) 4627.

[18]   E. M. Fortini, C. L.Garcia, D.E. Resasco, J. Catal., 99 (1986) 12.

[19]   W.J.M. Pieters, W.C. Conner, E.J. Carlson, Appl. Catal.,11 (1984) 35.

[20]   W.C. Conner, W.J.M. Pieters, A.J. Signorelli, Appl. Catal.,11 (1984) 59.

[21]   W.C. Conner, W.J.M. Pieters, W. Gates, J.E. Wilkalis, Appl. Catal., 11 (1984) 49.

[22]   C. Morterra, G. Magnacca, Catal. Today, 27 (1996) 497.

[23]   M. Girodani. Ann. Chim. Appl., 25 (1935) 163.

[24]   L. K. Volkova, E. S. Rudakov, V.P. Tret'yakov, Kinet. Katal., 37 (1996) 540.

[25]   L. K. Volkova, V.P. Tret'yakov, E. S. Rudakov, Kinet. Katal., 36 (1995) 373.

[26]   L. K. Volkova, V.P. Tret'yakov, Teor. Eksp. Khim., 31 (1995) 29.

[27]   V. P. Tret'yakov, L. K. Volkova, E. S. Rudakov,. Eksp. Khim., 30 (1994) 163.

[28]   V. P. Tret'yakov, L. K. Volkova, G.P. Zimtseva, E. S. Rudakov,. Kinet. Katal., 34
        (1993) 183.

[30]   V. P. Tret'yakov, G.P. Zimtseva, E. S. Rudakov, Kinet. Katal. 32 (1991)1022.

[31]   G. A. Olah US 4523040 1985.

[32]   I. T. Horvath, J.M.Millar, R.A.Cook, US 5354916 1994.

[33]   C. E. Taylor, Stud. Surf. Sci, Catal., 130D (2000) 3633.

[34]   C. E. Taylor, Am. Chem. Soc., Div. Fuel Chem., 39 (1994)1228.

[35]   C. E. Taylor, Noceti, P. Richard, Proc.-Int. Congr. Catal. 9th 2 (1988) 990.

[36]   B. R. Crum, R. F. J. Jarvis, A. I. T. B. M. Naasz, EP 0720975 A1 1996.

[37]   F. Wattimena, W. M. H. Sachtler, Stud. Surf. Sci. Catal. 7 (1982) 816.

[38]   A. J. Rouco, J. Catal., 157 (1995) 380.

[39]   C. Kenney, Catal. Rev.-Sci. Eng.,11 (1975) 197.

[40]   C. L. Garcia, D. E. Resasco, Appl. Catal., 46 (1989) 251.

[41]   C. L. Garcia, D. E. Resasco, J. Catal.,122 (1990) 151.

[42]   W. J. M. Pieters, W. C. Conner, E. J. Carlson, Appl. Catal.,11 (1984) 35.
         814.

[43]   M. M. Bhasin, J. H. McCain, B. V. Vora, T. Imai, P. R. Pujado, Appl. Catal. A:
        Gen., 221 (2001) 397.

[44]   M. A. Banares, Catal. Today., 51 (1999) 319.

[45]   F. Cavani, F. Trifiro, Catal. Today., 24 (1995) 307.

[46]   P. Botella, A. Dejoz, J. M. L. Nieto, P. Concepcion, M. I. Vazquez, Appl. Catal.
        A: Gen., 298 (2006) 16.

[47]   Ullmann's Encyclopedia of Industrial Chemistry, Sixth ed. Wiley-VCH
         :Weinheim, 2002.

[48]   Kirk-Othmer Encyclopedia of Chemical Technology, Wiley-VCH, Weinheim,
         2002.

[49]   H. H. Kung, Adv. Catal., 40 (1994) 1.

[50]   R. Burch, E. M. Crabb, Appl. Catal., 97(1993) 49.

[51]   S. Albonetti, F. Cavani, F. Trifiro, Catal. Rev.-Sci. Eng., 38 (1996) 413.

[52] G. Busca, E. Finochio, G. Ramis, G. Ricchiardi, Catal. Today., 32 (1996) 133.

[53]   P.Moriceau, A. Libouteiller, E. Bordes and P.Courtine, Phys. Chem. Chem. Phys., 1(1999) 5735.

[54] P. Botella, E. Garcia-Gonzalez, A. Dejoz, J. M. L. Nieto, M. I. Vazquez, J. Gonzalez-Calbet, J. Catal., 225 (2004) 428.

[55] J. M. L. Nieto, P. Botella, M. I. Vazquez, A. Dejoz, Chem. Commun., 17 (2002) 1906.

[56] D. Siegel, J. Biophys., 45 (1986) 399.

[57] E. M. Thorsteinson, T. P. Wilson, F. G. Young, P. H. Kasai, J. Catal., 52 (1978) 116.

[58] W. Ueda, N. F. Chen, K. Oshihara, Chem. Commun., (1999) 517.

[59] E. Heracleous, A. A. Lemonidou, J. Catal., 237 (2006) 162.

[60] E. Heracleous, A. F. Lee, K. Wilson, A. A. Lemonidou, J. Catal., 231 (2005) 159.

[61] E. Morales, J. H. Lunsford, J. Catal., 118 (1989) 255.

[62] J. A. Roos, S. J. Korf, R. H. J. Veehof, J. G. van Ommen, J. R. H. Ross, Catal. Today., 4 (1989) 441.

[63] J. B. M. S. S. Hong, Catal. Lett., 40 (1996) 1.

[64] S. Sugiyama, N. Kondo, K. Satomi, H. Hayashi, J. B. Moffat, J. Mol. Catal. A: Chem., 95 (1995) 35.

[65] S. J. Conway, J. H. Lunsford, J. Catal., 131 (1991) 513.

[66] D. J. Wang, M. P. Rosynek, J. H. Lunsford, J. Catal., 151 (1995) 155.

[67] S. J. Conway, D. J. Wang, J. H. Lunsford, Appl. Catal., 79 (1991) L1.

[68] S. Gaab, M. Machli, J. Find, R. K. Grasselli, J. A. Lercher, Top. Catal., 23 (2003) 151.

[69] H. M. Swaan, A. Toebes, K. Seshan, J. G. van Ommen, J. R. H. Ross, Catal. Today, 13 (1992) 629.

[70] S. B. Wang, K. Murata, T. Hayakawa, S. Hamakawa, K. Suzuki, Catal. Lett., 62 (1999)

[71] S. B. Wang, K. Murata, T. Hayakawa, S. Hamakawa, K. Suzuki, Chem. Commun., 1 (1999) 103.

[72]   E.A. Mamedov, V. Cortes Corberan, Appl. Catal. A, 127 (1995) 1.

[73] C. Hallett, BP European Patent, 0480594 A2 (1992).

[74] M. Kitson, BP European Patent, 0407091 A1 (1991).

[75] P. Barthe, European Patent, 0479692 A1 (1992).

[76] M. A. Banares, X. GaO, J.L.G. Fierro, I. E. Wachs, R. K. Grasselli, S.T. Oyama, A. M. Gaffney, J.E. Lyons, Stud. Surf. Sci. Catal, 110 (1997) 295.

[77] P.Concepcion, A.Galli, J.M.Lopez Nieto, A.Dejoz, M.I.Vazquez, Topics Catal., 3 (1996) 451.

[78] P.Concepcion, A.Corma, J.M.Lopez Nieto, J. Perez-Pariente, Appl. Catal. A, 143 (1996) 17.

[79] M.B.Ward, M.J. Lin, J.H. Lunsford, J. Catal., 50 (1977) 306.

[80] A.Erdohelyi, F. Mate, F. Solymosi, J.Catal., 135 (1992) 563.

[81] A.Erdohelyi, F. Solymosi, J. Catal., 129 (1991) 497.

[82] A.Erdohelyi, J.Csrenyi, F. Solymosi, ACS Symp. Ser., 523 (1993) 368.

[83] A.Erdohelyi, K. Fodor, F. Solymosi, J.Catal., 166 (1997) 244.

[84] M.Merzouki, B.Taouk, L.Tessier, E.Bordes, P.Courtine, L.Guczi, F.Solymosi, P.Tetenyi, New Frontiers in Catalysis, Stud. Surf. Sci. Catal., 75 (1993) 1875.

[85] Y. Murakami, K. Otsuka, Y. Wada, Bull. Chem. Soc. Jpn., 63(1990) 340.

[86] E. M. Thorsteinson, T. P. Wilson, F. G. Young, P. H. Kasai, F. Catal., 52(1978) 116.

[87] J.M. Lopez Nieto, P. Botella, M. I. Vazquez, A. Dejoz, Chem. Commun., (2002) 1906.

[88] J.M. Lopez Nieto, P. Botella, M. I. Vazquez, A. Dejoz, WO patent 03/064035, 2003

[89] E. Morales, J.H.Lunsford, J.Catal., 118(1989) 255.

[90] R.Burch, S.C.Tsang, Appl.Catal., 65(1990) 259.

[91] G.A.Martin, A.Bates, V.Ducarme, C.Mirodatos, Appl.Catal. 47 (1989) 287.

[92] S. J. Conway, J. H. Lunsford, J. Catal., 131 (1991) 513.

[93] D. J. Wang, M. P. Rosynek, J. H. Lunsford, J. Catal., 151 (1995) 155.

[94] C.T. Au, K.D. Chen, H.X. Daik, Y.W. Liu, J.Z. Luio, C.F. Ng, J. Catal., 179 (1998) 300.

[95]   H.X. Dai, C.T. Au, Y.Chan, K.C. Hui, Y.L. Leung, Appl. Catal. A: General., 213 (2001) 91.

[96]   S. Wang, K. Murata, T. Hayakawa, S. Hamakawa, K. Suzuki, Energy & Fuels., 14 (2000) 899.

[97]   S. Wang, K. Murata, T. Hayakawa, S. Hamakawa, K. Suzuki, J. Chem. Tech. Biotech., 74 (1999) 988.

[98]   S. Wang, K. Murata, T. Hayakawa, S. Hamakawa, K. Suzuki, Chem. Eng. Tech., 23 (2000) 1099.

[99]   S. Wang, K. Murata, T. Hayakawa, S. Hamakawa, K. Suzuki, J. Chem. Tech. Biotech, 76 (2001) 265.

Chapter 2

Acid-base properties of LaOCl precursors for the CH$_4$ oxychlorination

Abstract

Four commercial LaOCl catalyst precursors have been characterized and compared for their activity in the methane oxychlorination (MOC). All samples were characterized with X-ray diffraction (XRD), N$_2$ sorption measurement, scanning electron microscopy (SEM), temperature programmed desorption (TPD), Raman and infrared (IR) spectroscopy. TPD of adsorbed NH$_4$ and 2, 6-dimethylpyridine (DMP) showed that only one type of weak acid sites presented on all sample surfaces and their acid sites decreased in the following order GRII>SCI>SCIIIB >SCII. Three desorption peaks were detected in CO$_2$ TPD measurement, indicating the existence of three different basic sites. The concentration of total basic sites was exactly opposite to the sample's acid sites. IR spectra indicated that different types of carbonate species were formed after adsorption of CO$_2$. Combining IR and TPD results, it was deduced that monodentate and bidentate carbonates were the main species and the minor species was the hydrogen carbonates. All catalysts have been compared for their performance at different temperatures for MOC and the trend for the activity was found to be SCII > SCIIIB > SCI > GRII. SCII sample showed best activity. A correlation between acidity, basicity and catalytic performance revealed that a strong basicity and low acidic character of LaOCl enhances the MOC activity. The high activity for the more basic sample is probably related to its basic surface which can be easily chlorinated.

1. Introduction

There are abundant natural gas reserves in the world. However, most of the natural gas is concentrated in relatively remote part of the world; transportation of this gas to the local market is always a problem. Therefore, techniques for transformation of methane, the major component of the natural gas, into easy transportable or value added products, such as methanol, ethylene, aromatics, and liquid hydrocarbon fuels are highly interested industrially. However, selective activation of C-H bond in methane is difficult because of low polarity of C-H bond and a relatively high binding energy together with tetrahedral arrangement of the bonds. Hence selective activation of methane presents a formidable challenge to the chemical industry [1, 2]. The dominant technology used for production of chemicals from methane involves its conversion to a mixture of carbon monoxide and hydrogen. This is usually referred to as synthesis gas or syngas. Synthesis gas can be converted back to liquid hydrocarbon. Although this is the only commercialized technique, it has its own disadvantages like huge capital input, high energy consumption, extremely high operation temperature and so on. Other promising techniques under developing include oxidative coupling of methane and oxidation of methane to methanol.

Oxidative halogenation of methane or methane oxychlorination (MOC) to methyl halide is also an attractive technique. In this reaction, methane is reacted with HCl and O_2 to produce chloromethane and H_2O. Copper-based catalysts have proven to be active for this reaction though these catalysts are originally used in the industrial oxychlorination of ethylene [3]. Since copper based catalysts are known to be also active for Deacon chemistry [4], oxidation of HCl to Cl_2, methane activation through liberation of elemental chlorines is possible. Therefore, methane chlorination proceeds, at least partially, *via* a radical gas-phase mechanism and the selectivity to methyl chloride is usually low at significant methane conversion level [4]. Another drawback is that copper salts are volatile at the usual temperatures required for the methane activation. By adulation of KCl, which can lower the melting point of copper chloride and promotes the copper redox step, the stability of copper catalysts has been greatly enhanced [5-7]. Moreover, in order to prevent melt segregation of copper and potassium chlorides at high reaction temperatures, $LaCl_3$ has been used as a stabilizing promoter [8, 9].

32

Recently, it was found that catalysts based exclusively on LaOCl, which is converted to LaCl$_3$ in the presence of HCl under reaction conditions, were active, selective, and importantly stable for oxidative chlorination [10]. This is surprising because La^{3+} cannot change their oxidation state and hence was believed to be not active for MOC. Combining activity measurements and density-functional theory (DFT) calculations, Peringer et al. [11] in our group proposed that a transient OCl$^-$ anion, formed by oxidation of Cl$^-$ in LaOCl and LaCl$_3$ with molecular oxygen, was the active site for the initial step of methane activation. However, the effect of surface as well as bulk LaOCl precursor properties on catalytic activity is not studied in detail.

In this study, different techniques like X-ray diffraction (XRD), N$_2$ sorption measurement, scanning electron microscopy (SEM), temperature programmed desorption (TPD), and Raman and infrared (IR) spectroscopy were employed to characterize four commercial LaOCl precursor samples. Our main goal is to establish a link between acid-base properties of precursor LaOCl and catalytic activity.

2. Experimental

2.1 Materials

Four commercial LaOCl samples named SCI, SCII, SCIIIB and GRII were kindly supplied in powder form by Dow Chemical Company USA. The specific surface area of the samples was determined by N$_2$ adsorption at -196°C on a Micromeritics ASAP 2000 apparatus. Samples were degassed at 400°C for 6h before measurement. The chemical compositions of these samples were analyzed by energy dispersive X-ray spectroscopy (EDX) on a JEOL 500 SEM microscope.

2.2 Powder X-ray diffraction (XRD)

The phase purity of the La-based materials was checked with X-ray diffraction (XRD). XRD pattern of the LaOCl samples were recorded at ambient conditions using Philips X'Pert Pro (CuK$_{\alpha 1}$-radiation, λ = 0.154056 nm) at 40 kV/ 40 mA. Measurements were performed on a spinner in the angle range from 5° to 75° 2θ (0.05 °/min) with a ¼" slit.

2.3 IR Spectroscopy

The IR spectra of the samples in the hydroxyl (3000-4000 cm^{-1}) region were recorded on a Brucker IFS 88 spectrometer at 4 cm^{-1} resolution. The spectrometer was equipped with a flow cell and a vacuum cell and the signals were detected with a MCT detector. For the experiment, about 8 mg sample was pressed into self-supporting wafer and placed in a gold sample holder in the center of stainless steel chamber equipped with CaF_2 window, which was evacuated ($<10^{-6}$ mbar). The temperature was raised to 400 °C stepwise and a spectrum was recorded at RT, 100, 200, 300 and 400 °C.

Infrared spectra of adsorbed CO_2 were recorded on a Bruker IFS 88 IR spectrometer with a resolution of 4 cm^{-1}. The sample, about 8 mg, was pressed into a self-supported wafer, pretreated at 400°C under vacuum ($<10^{-6}$ mbar) for 2h, and cooled to 30°C to record a spectrum. The sample was equilibrated with CO_2 at 0.4 mbar and 1mbar for 1h before recording a spectrum.

2.4 Raman Spectroscopy

Raman experiments were recorded in the region 3500 to 50 cm^{-1} using a RENISHAW Series 1000 laser Raman spectrometer equipped with a CCD detector. The Raman measurement was conducted using the 514 nm line of a 20mW Ar laser for excitation. The samples were activated at 400°C for 2h in He before recording a spectra.

2.5 Temperature programmed desorption (TPD)

TPD of DMP, NH_3 and CO_2 were performed in a tubular reactor with the effluent analyzed by a Balzers QMG 420 mass spectrometer. The sample (~200 mg) was pretreated at 500°C for 1h under vacuum followed by adsorption of a probe gas at 30°C. After evacuation of the sample at 30°C for 1h under 10^{-3} mbar, desorption of the adsorbed gases was monitored by mass spectrometry during heating up to 700°C with a rate of 10°C /min.

2.6 Catalytic test

Methane oxychlorination reaction was performed in a conventional fixed bed down stream reactor under atmospheric pressure. The reactor was made up of stainless steel tube (glass lining inside) with 4mm i.d and approximately 43.5 cm long. The catalyst 0.5 g was placed in the middle of the reactor supported in between a plug of glass wool. The remaining dead volume of the reactor was filled with the glass beads of size between 0.63 to 0.75 mm to minimize void space. Before each run the catalyst was activated at 550°C for 1h in He to remove adsorbate, like CO_2 and water. After decreasing the temperature to 400°C, a flow of HCl (10 ml/min) was added to the He flow and passed over the catalyst for 2h, to convert the lanthanum oxychloride catalyst to lanthanum trichloride. Then the feed gas flow was switched to a mixture of He, CH_4 HCl, O_2, N_2 with a ratio of 2 :1:1:0.5:0.5. The total flow was 20 ml/min.The catalytic test was performed under integral condition within the temperature range of 400-540 °C. At each temperature the reaction was run for 1.5 h before product analysis by online GC. The lines were heated at 130°C to avoid the condensation of the liquid HCl inside the lines which could result in corrosion and plugging of the lines. Teflon tubing and fitting were used to avoid corrosion due to hydrogen chloride. The outlet of the effluent lines was connected to a 4M NaOH solution to neutralize the HCl and other acidic gases coming out of the reactor. The effluent was further purified by passing through activated charcoal.

The products distribution was analyzed by a Siemens online GC equipped with a thermal-conductivity detector (TCD). Six columns were used for separating product effluent gases.

3. Results

3.1 Physicochemical characterization of LaOCl materials

The physicochemical properties of the LaOCl materials are presented in Table 1.

Table 1. Physicochemical properties of LaOCl precursor samples.

Samples	La/O	La/Cl	Phase(s) by XRD/Raman	Surface area (m^2/g)
SCII	0.28	2.40	LaOCl	20
SCIIIB	0.30	1.61	LaOCl	28
SCI	0.36	1.58	LaOCl	34
GRII	0.32	2.82	LaOCl, $La_2O_2CO_3$	35

The N_2 sorption results show that GRII has a higher surface area (35m^2/g) than all other samples. SCII possesses relatively low surface area and pore volume. The elemental composition of the LaOCl materials does not correspond to stoichiometric ratio of pure LaOCl. That means in addition to La, Cl and O some other dopants may also be present in negligible amount. In this respect it is important to compare the La/Cl mol ratio to understand the nonstoichiometry exhibited by the different samples as given in Table 1.

Note that La/Cl ratio is highest for GRII samples, which indicate that more amount of dopants present in GRII sample. The O mole percentage is comparable in all samples. GR II has comparatively the highest mole percentage of oxygen followed by SCII. SCI shows the lowest amount of oxygen. It is also interesting to note that there seems to be good trend among SC samples. Lanthanum mole percentage decreases from SCI > SCIIIB > SCII while La/Cl mole ratio increases in the order SCI < SCIIIB < SCII. Among SC samples, a SCII sample shows the highest stoichiometric ratio which replicates more impurity in the samples.

The phase purity of the LaOCl sample is checked with XRD because LaOCl is easily contaminated by other compound like La_2O_3 and $LaCl_3$. XRD patterns of LaOCl are presented in Fig 1. Intense and sharp reflection is observed for SCI and SCIIIB pointing out the high crystallinity of these samples. On the contrary, the XRD patterns of SCII and GRII feature broad reflections of very low intensity. This indicates that SCII and GRII either contain more amorphous phase or have smaller particles size.
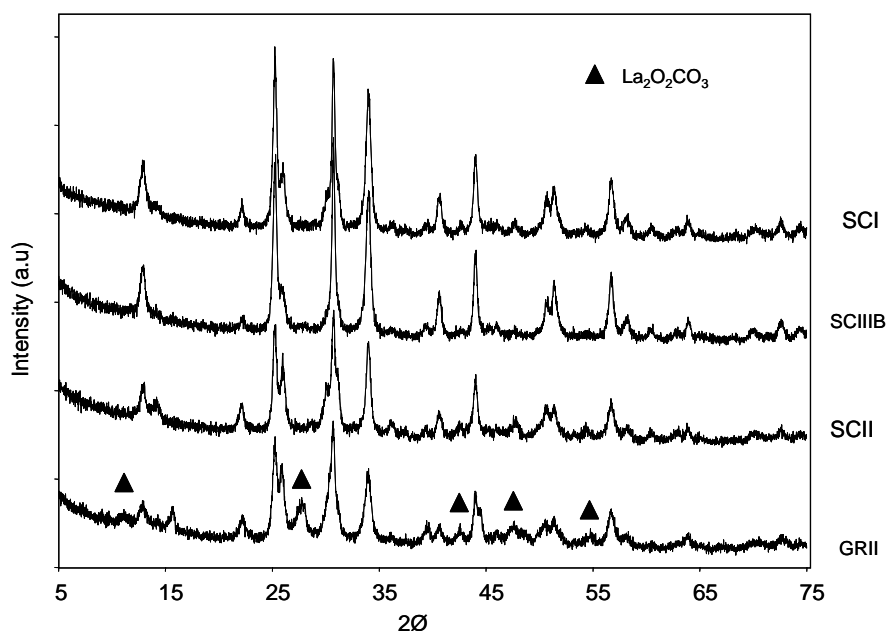
Fig.1. X-ray diffractograms of LaOCl samples recorded at RT.

Therefore, the XRD peak positions and intensities for SCII and GRII are compared with $LaCl_3$ and $La_2O_2CO_3$. A large amount of $La_2O_2CO_3$ was found to be present in GRII sample. This is also evident from EDX analysis having highest La/Cl ratio 2.82 for GRII that means GRII is highly impure among the four samples. All samples resemble that of LaOCl [12]. The presence of additional reflexes and broadening of the XRD peaks is attributed to the presence of an impurity in the sample. Hence from EDX analysis and XRD we are able to rank the purity of the samples in the following order SCI >SCIIIB > SCII > GRII. The lanthanum carbonates are most likely formed with CO_2 from water or from air during precipitation. The detail study about the stability and the role of carbonate in all LaOCl samples were done in our group for the methane oxychlorination reaction. The carbonates are very stable and remain in the materials up to very high temperature. The phase transformation from lanthanum carbonate to lanthanum oxide is presented in equation 1.

$$La_2(CO_3)_3 \xrightarrow[-CO_2]{\sim 480°C} La_2O(CO_3)_2 \xrightarrow[-CO_2]{\sim 530°C} La_2O_2CO_3 \xrightarrow[-CO_2]{725°C} La_2O_3 \qquad (1)$$

37
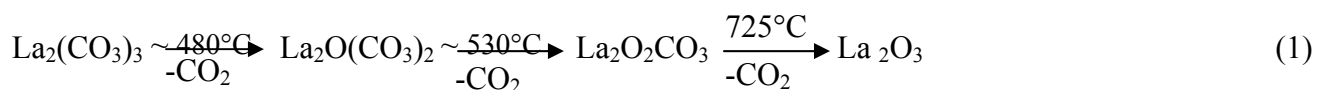
The surface morphology of four LaOCl precursors SCI, SCII, SCIIIB and GRII are presented in Fig 2. Sample SCI (Fig.2a) shows a very homogeneous distribution of needle-shaped particles with length of ca.1μm and thickness of ca.0.2μm.
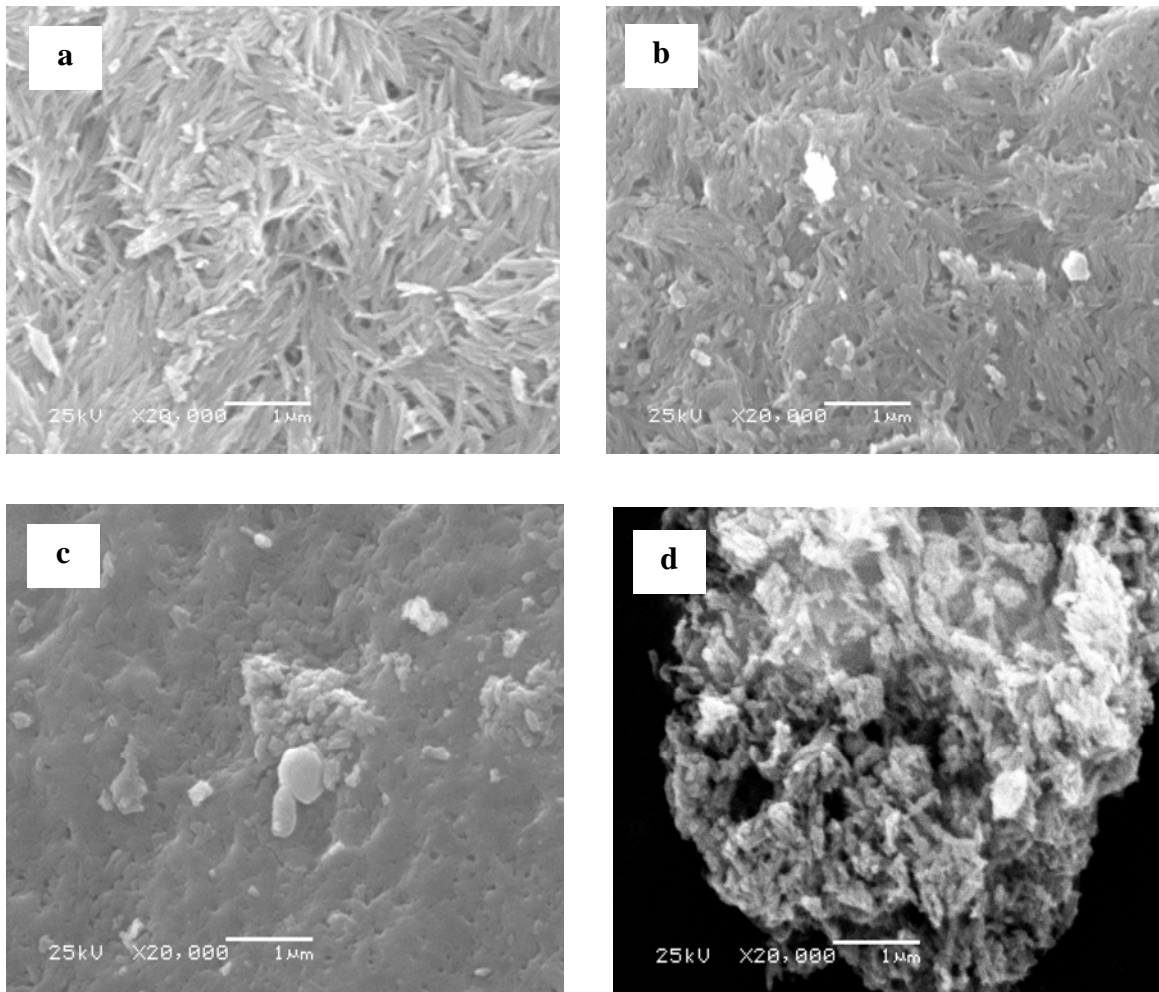
Fig.2. Scanning electron micrographs of LaOCl samples: (a) SCI, (b) SCIIIB, (c) SCII, and (d) GRII.

This particular shape of the grains reflects well layered crystalline structure of LaOCl. The morphology of sample SCIIIB (Fig.2b) is similar to that of SCI except that the length of its needle-shaped crystals is shorter. The particle size of sample SCII is very small and is aggregated (Fig. 2c). It's hard to differentiate one particle from the other based on SEM images. Sample GRII (Fig. 2d) shows completely different morphology from other samples. It seems that small crystallites are aggregated together. The difference in morphology could be due to many factors including lanthanum source, precipitation process, and calcinations procedure. Here the difference is temporarily attributed to the

presence of impurities such as lanthanum carbonates which are confirmed by XRD. The lanthanum carbonates could be introduced during sample precipitation and calcination.

Raman spectroscopy is a sensitive technique to probe the local structure and can be used to study the impurity introduced into the lattice, which could give an indication for the active sites present on the surface. Fig3. shows the characteristic Raman bands of LaOCl at 122, 185, 209, 333 and 438 cm^{-1} appear in all four samples.
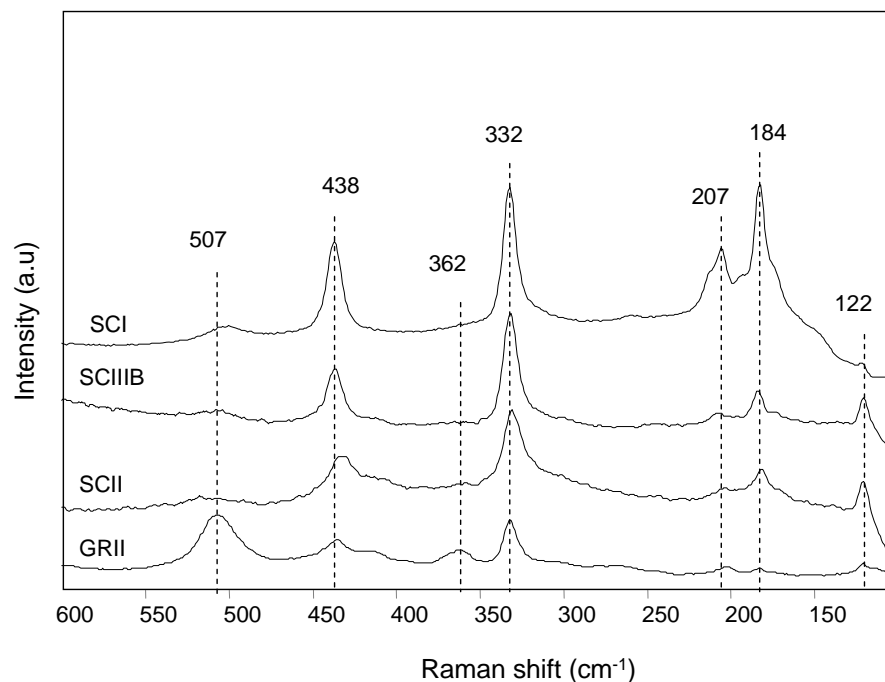
Fig.3. Raman spectra of SCI, SCIIIB, SCII and GRII recorded at RT.

According to Hase *et al.* [13] bands at 438 and 333 cm^{-1} are assigned to the oxygen site translations belonging to the E_g and B_{1g} species respectively. The bands at 185 and 209 cm^{-1} are assigned to the A_{1g} and E_g fundamentals of the chlorine site translation. The bands at 122 cm^{-1} and 69 cm^{-1} are assigned to the A_{1g} and E_g fundamental bands due to the lanthanide site translation. This observation shows that LaOCl is dominant in all samples which was also substantiate by XRD results. However the sample GRII shows additional Raman bands at 1086, 697 and 658cm^{-1}. The band at 1086 cm^{-1} can be assigned to the presence of Lanthanum dioxycarbonate. The assignment for other two bands (not shown here) is not sure at the moment.

Temperature dependent IR studies

39

IR spectroscopy is a sensitive technique to identify the different type of species present on the surface of the sample.
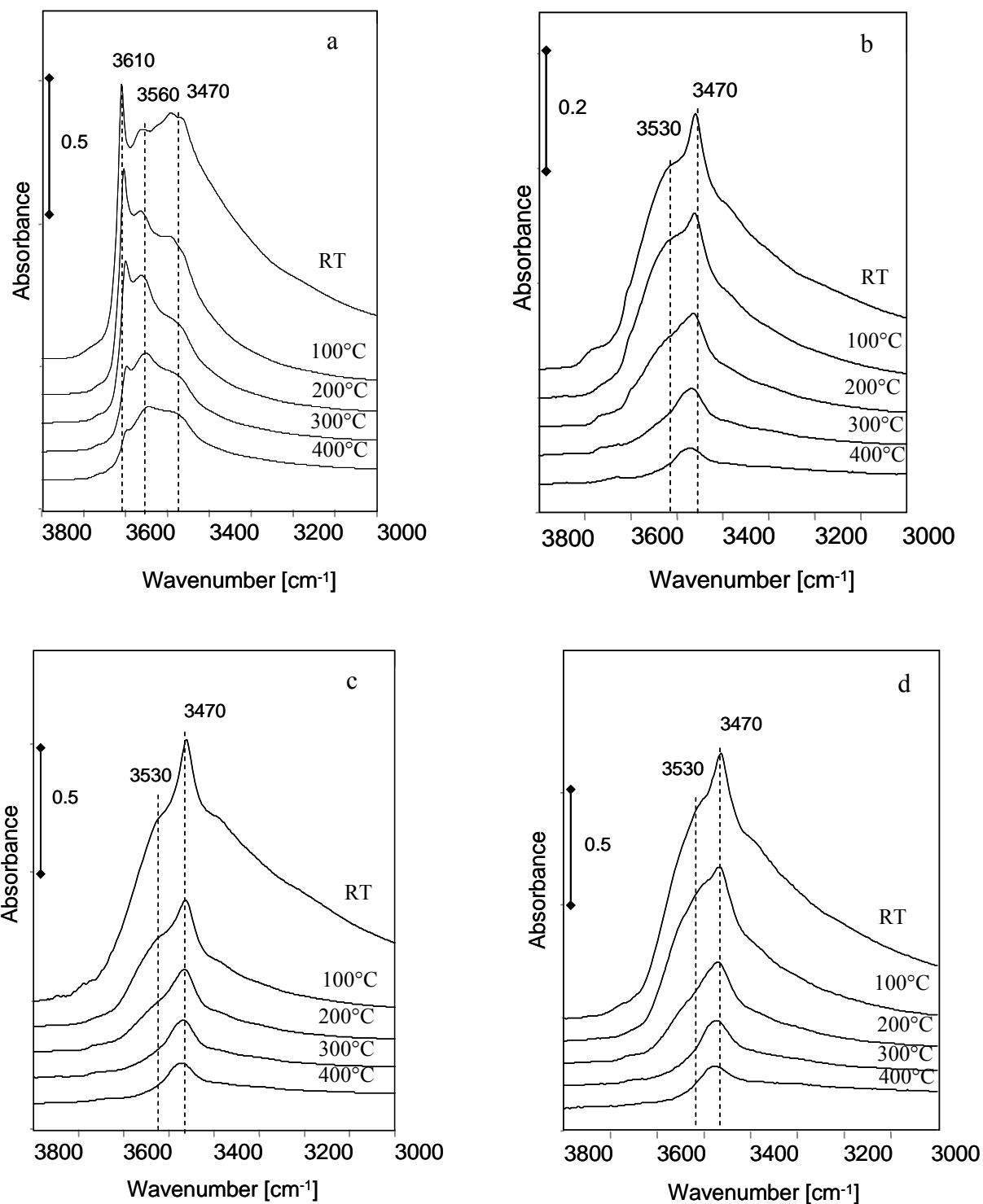
Fig.4. IR spectra of (a) GRII, (b) SCIIIB, (c) SCI, and (b) SCII recorded in vacuum from RT to 400°C.

In order to gain insights into the type of OH groups, carbonate and identify their thermal stability the samples were subjected to temperature dependent IR investigation. The in-situ IR spectra

of all samples are recorded from RT to 400°C and presented in Fig 4 a-d. At RT temperature all the SC samples show a broad band centered at 3470 cm^{-1} with a shoulder at 3530 cm^{-1}. The band at 3470 cm^{-1} can be assigned to the OH stretching vibration of LaO(OH) type species [14,15]. Whereas the second type of hydroxyl band at 3530 cm^{-1} can be attributed to La(OH) species [16]. Upon heating the samples the intensity of the hydroxyl groups decreases but persists up to 400°C. The loss of the intensity is due to the evaporation of hydroxyl groups. GRII sample shows three types of hydroxyl groups on the surface. Besides the OH stretching bands at 3470 and 3560 cm^{-1} similar to SC samples which can be assigned to LaO(OH) and La(OH) type species, another band at 3610 cm^{-1} is detected. This band is very sharp and can be assigned to the strongly bound OH groups in La(OH)$_3$ [14,17]. The intensity of the band at 3610 cm^{-1} vanished upon heating to 400°C, indicative of its labile property. From XRD and Raman studies it is clear that GRII is the most impure sample containing high amount of lanthanum dioxycarbonate. In a separate experiment, the pure lanthanum carbonate from Aldrich also shows OH bands at 3612, 3545 and 3475 cm^{-1}, which further confirms that there is lanthanum carbonate impurity in sample GRII. The OH bending mode should be visible around 1600 cm^{-1} but it is probably hidden by intense carbonate bands. However, the role of hydroxyl group and carbonate are explored in detail for the methane oxychlorination reaction in next chapter.

TPD of adsorbed DMP and ammonia

Temperature programmed desorption of ammonia was used to measure the total acid sites of the samples and the results are presented in Fig. 5 (a-d). For all samples, only one desorption peak, which appeared around 185°C, were observed. This implies that only one type of weak acid sites is present in all samples.

Table 2. Amount of basic sites determined by CO_2 TPD and acid sites determined by ammonia TPD and DMP TPD.

Sample	Basic sites (μmol g^{-1}) by CO_2	Acid sites (μmol g^{-1}) by ammonia	Acid sites (μmol g^{-1}) by DMP
SCII	25.2	2.4	1.7
SCIIIB	13.5	2.9	2.4
SCI	12.4	3.3	2.9
GRII	12.0	3.5	3.1

However, the amount of ammonia desorbed per unit weight (Table 2) decreases in the following order: GRII >SCI >SCIIIB >SCII, which means the acidity of samples decreased in the same order. SCII possesses the lowest acidity while GRII has the highest acidity.
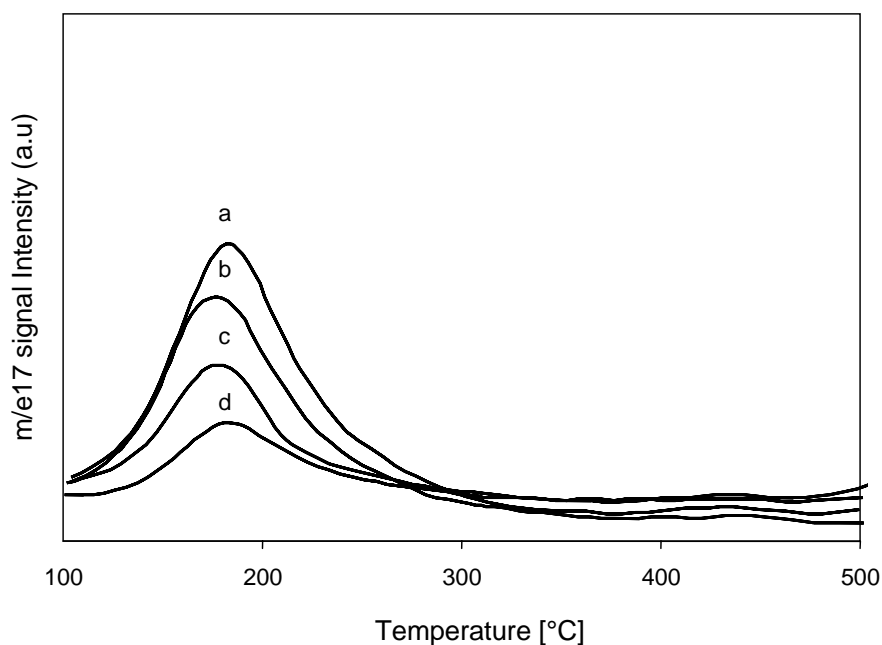
Fig.5. TPD profiles of ammonia adsorbed on: (a) GRII, (b) SCI, (c) SCIIIB and (d) SCII.

TPD of DMP for all LaOCl samples is presented in Fig 6 (a-d). DMP could be used to distinguish the strength of acid sites of different samples. All LaOCl samples show only one desorption maxima at around 130°C. Ammonia adsorption on these samples shows similar results with only one desorption peak, however desorption peak is ~50°C lower than ammonia.
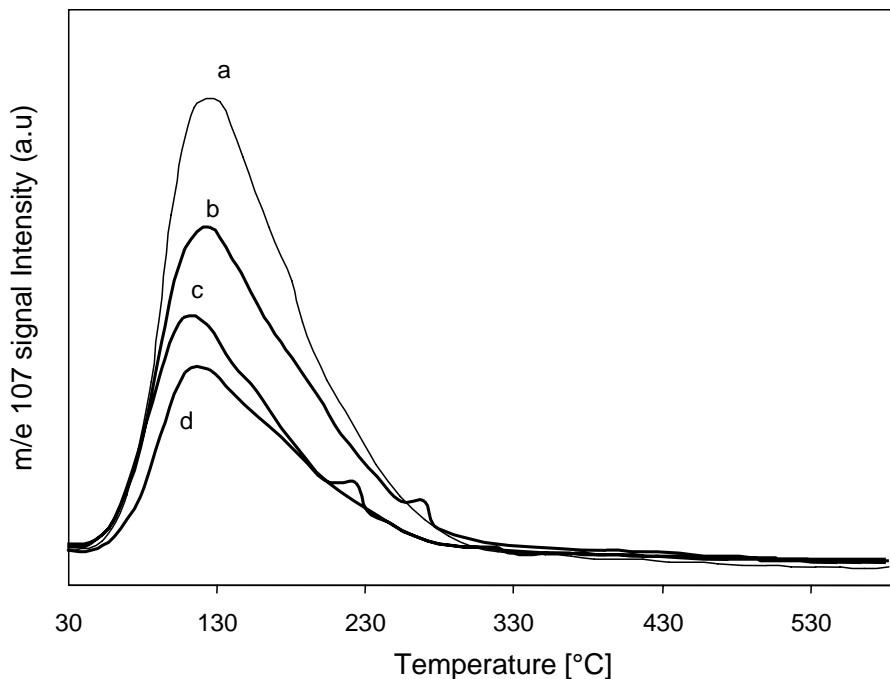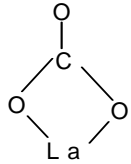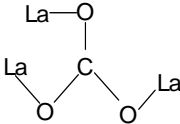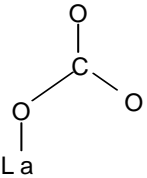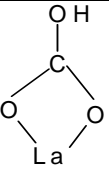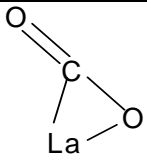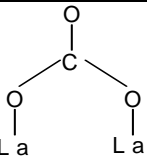
Fig.6. TPD profiles of adsorbed DMP on: (a) GRII, (b) SCI, (c) SCIIIB and (d) SCII.

Which is quiet expected as ammonia is stronger base than DMP and can interact with surface acid sites more strongly. DMP adsorption results are in agreement with the ammonia adsorption and hence confirming the same acidity ranking in LaOCl. Concentration of acid sites decreased in the sequence GRII >SCI >SCIIIB > SCII. From adsorption results clearly shows that desorption maxima shifts to higher temperature with increase in temperature. Hence it is possible to distinguish the strength of acid sites in different LaOCl which was not possible in case of ammonia adsorption. Strength of Lewis acid sites decreased in the order GRII >SCI >SCIIIB > SCII. The amount of acid sites determined either by ammonia or DMP is small, indicating that only weak acid sites are present on LaOCl samples.

IR spectra of adsorbed CO_2

CO_2 is an amphoteric molecule. It can adsorb on surface basic oxygen ions to form various carbonate species. It can also adsorb on basic hydroxyl groups to generate hydrogen carbonate species. Moreover, it can act as a Lewis base and adsorb on metal ions to form carboxylates. The possible species due to the CO_2 adsorption are summarized Table 3.

Table 3. Vibrational frequencies of carbonate species on the surface of LaOCl upon adsorption of CO_2.

	Surface species	$v_{as}(CO_3)$ (cm^{-1})	$v_s(CO_3)$ (cm^{-1})	δ (OH) (cm^{-1})
Bidentate carbonate		1546, 1619	1278, 1335	-
Polydentate carbonate		(N.O)	(N.O)	-
Monodente carbonate		1499	1416	-
Hydrogen carbonate		1654	-	1208
Carboxylate		(N.O)	(N.O)	-
Bridged carbonate		(N.O)	(N.O)	-

(N.O) not observed

In this study, CO_2 is used as a probe molecule to study the basicity of the LaOCl samples. The IR spectra of three representative LaOCl SC samples after adsorption of CO_2 are shown in Fig 7. Since all samples present similar type of IR spectra upon adsorption of CO_2, we choose SCII as a representative for all samples.
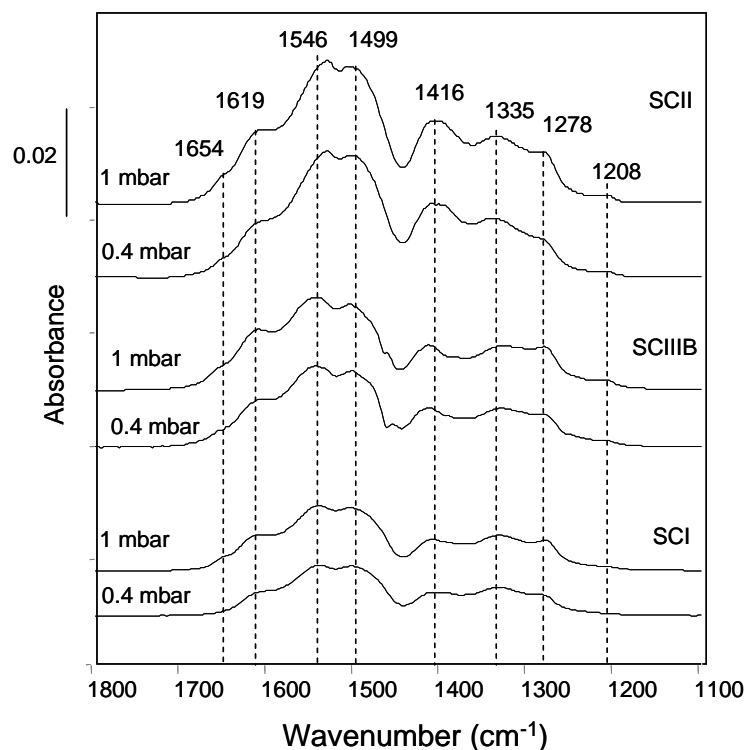
Fig.7. IR spectra of CO_2 adsorbed on LaOCl and equilibrated under 1mbar and 0.4 mbar.

For SCII, main adsorption bands detected are presented at 1619, 1546, 1499, 1416, 1335, and 1278cm^{-1}. Two minor bands at 1654 and 1208 cm^{-1} are also observed. The main bands can be grouped into two sets of bands. One set of bands is present between 1654 and 1499 cm^{-1}, and another set of bands between1416 and 1278 cm^{-1}. Each set consists of bands due to antisymmetric and symmetric stretching modes. Their assignments are shown in Table 3. The bands located at 1619 and 1335 cm^{-1} are ascribed to the $v_{as}(CO_3)$ and $v_s(CO_3)$ modes of bidentate carbonate species because the band splitting for this pair of band ($\Delta v_3 = 268$ cm^{-1}) is in close agreement to the 300 cm^{-1} splitting mentioned in literature for metal oxides [15,16,18-21]. The bands at 1546 and 1278 cm^{-1} are assigned to bidentate species as the difference between this pair is 284 close to 300 cm^{-1} [22]. The bands at 1499 and 1416 cm^{-1} could be assigned to either monodentate or polydentate carbonates because it has been shown that the bands with $\Delta v_3 = 100$ cm^{-1} are indicative of either monodentate or polydentate carbonates. Unfortunately IR spectroscopy is not able to distinguish between mono- and polydentate carbonates. To differentiate these species, CO_2 TPD was performed. This will be discussed in the next section. Besides major bands, minor asymmetric $v_{as}(CO_3)$ stretching band at 1654 cm^{-1} and $v(OH)$ bending mode at 1208 cm^{-1} are detected and can be assigned to hydrogen carbonate formed by coordinating CO_2 toward the surface

45

hydroxyl groups [23]. Therefore, upon adsorption of CO_2, a high concentration of bidentate and either mono or polydentate carbonates coupled with a low concentration of hydrogen carbonate species are expected to be present.

Although all samples show similar type of IR spectra after adsorption of CO_2 in the carbonate region, the concentration of basic sites vary on different samples. The relative intensity of adsorbed CO_2 under different pressure is integrated (Table 4) and it is found that the relative intensity of samples decrease in the order SCII > SCIIIB > SCI.

Table 4. Relative basicity from IR spectra of adsorbed CO_2.

Sample	Rel. basicity (1 mbar)*	Rel. basicity (0.4 mbar)*
SCII	171	156
SCIIIB	137	122
SCI	119	98

*Sum of band intensities in the range 1700-1200 cm^{-1}.

It is interesting to found that the relative intensity decreases as the pressure decreases from 1mmbar to 0.4 mmbar; however, the bands persist even after evacuation below 10^{-5}mmbar. This shows that all carbonate species are stable at ambient temperature.

TPD of CO_2

In order to discriminate between monodentate and polydentate carbonates, TPD of CO_2 is performed. The basicity of different material can be compared on the basis of interaction with CO_2. TPD of CO_2 would be a choice to find the concentration and strength of basic sites. Adsorption of CO_2 results in formation of different type of basic sites on LaOCl, which could be investigated by using temperature programmed desorption. TPD profiles of four LaOCl are presented in Fig. 8. Three desorption bands are observed indicating three types of basic sites on LaOCl materials.
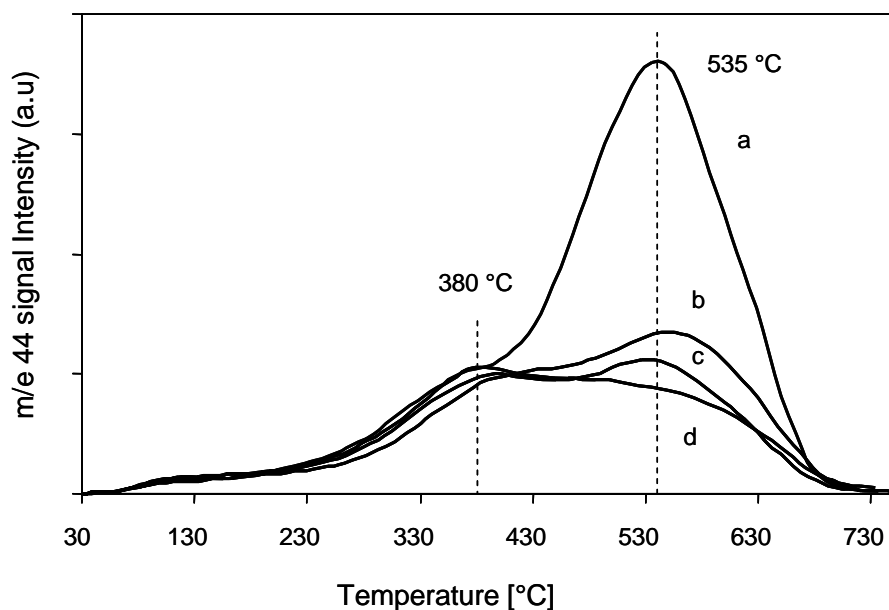
Fig.8. TPD profiles of CO_2 adsorbed on: (a) SCII, (b) SCIIIB, (c) SCI and (d) GRII

The first desorption band is observed below 100°C and can be assigned to physisorbed CO_2 and hydrogen carbonates. The second peak maxima appeared at about 380°C. According to Van der Heijden [24], this peak could be assigned to bidentate or bridged carbonate species. However bridged carbonates tend to convert to polycarbonates at around 622°C as a result of CO_2 desorption but a desorption peak at temperature higher than 600°C was not observed. Therefore, this peak is assigned to desorption of bidentated carbonate species. This is in agreement with IR study as bridged carbonates were not detected. The third CO_2 desorption peak is observed at 535°C. For the reason stated above, this could not be the desoption peak of polycarbonates. Here it is assigned to desorption of monodentate carbonates. The intensity of this desorption peak is much higher for SCII than for the other samples, featuring its higher basic properties. The total amount of CO_2 desorbed in the temperature range from 25 to 700 °C increases according to the order GRII < SCI < SCIIIB < SCII, which is in agreement with IR results on increase in basicity. Combining TPD with IR results, it can be concluded that a large amount of bidentate and monodentate carbonate species coupled with a small amount of hydrogen carbonates present on four commercial LaOCl samples after adsorption of CO_2.

3.2 Catalytic activity

The four commercial LaOCl samples were tested for the methane oxychlorination in the temperature range from 400 to 540°C. For methane oxychlorination reaction methyl chloride is the primary product followed by methylene chloride, CO, and CO_2 as secondary products and trace amount of $CHCl_3$ and CCl_4 as minor by-products. The catalytic results are presented in Fig 9.
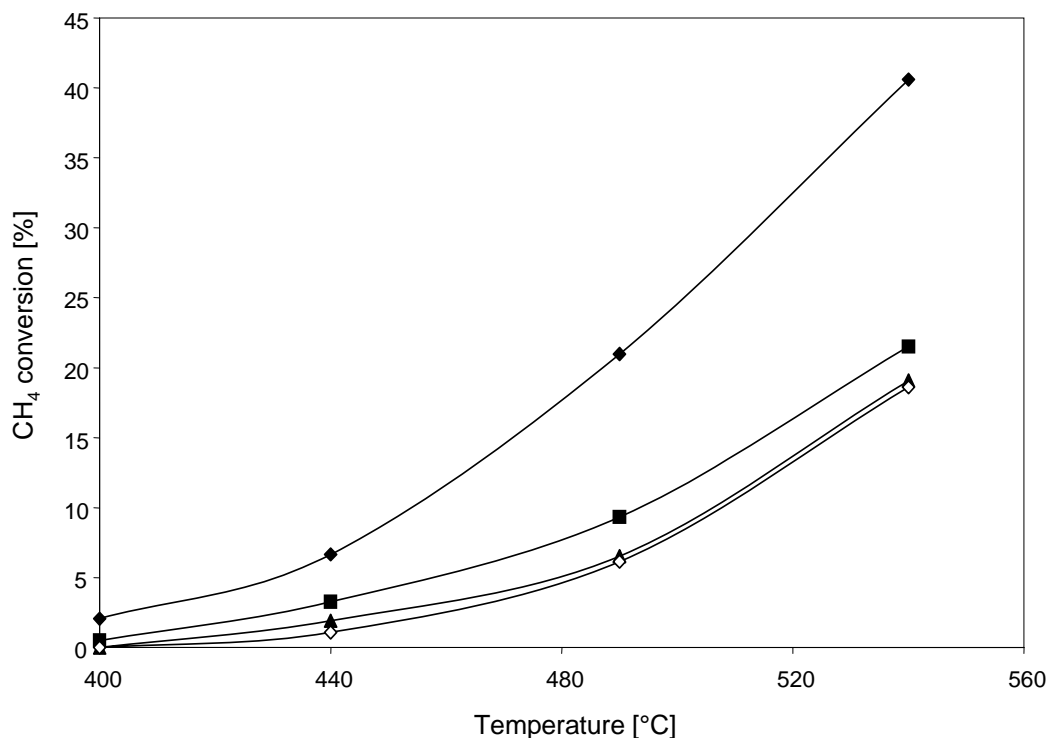
Fig.9. Conversion of methane at different temperatures: (◆) SCII, (■) SCIIIB, (▲) SCI and (Δ) GRII.

It was found that sample SCII was the most active catalyst for MOC reaction and its activity was nearly twice compared to the other samples. The highest conversion for this sample was 40.6% obtained at 540°C. Sample SCI and GRII showed lowest activity and their activity was similar at same reaction temperatures. Sample SCIIIB was slightly more active than SCI and GRII.

However, sample SCII showed the lowest selectivity to methyl chloride and its selectivity decreased from 92% at 400 °C to 55.6% at 540°C. Sample SCI and GRII presented relatively high selectivity. Their selectivity was as high as 80% even at 540°C. The selectivity of sample SCIIIB was in between. Methane oxychlorination is a sequential reaction. Methane is first converted to methyl chloride, then to methylene chloride and can be further converted to $CHCl_3$ and CCl_4. However, $CHCl_3$

and CCl$_4$ are too active in our reaction conditions. Once they are formed, immediately oxidized to CO$_x$, Therefore, only trance amount of CHCl$_3$ and CCl$_4$ are detected and their selectivity in our experiment is always less than 0.5%. During our catalytic test, all samples were first subject to the treatment of HCl, this treatment transformed LaOCl totally or partially to LaCl$_3$ according to the following equilibrium:

$$LaOCl + 2HCl \rightleftharpoons LaCl_3 + H_2O \tag{2}$$

In the following methane chlorination, the surface LaCl$_3$ will catalytically active. It is obvious that the acid-base properties of precursor LaOCl can affect the structure and state of LaCl$_3$ and accordingly have an effect on the catalyst activity.
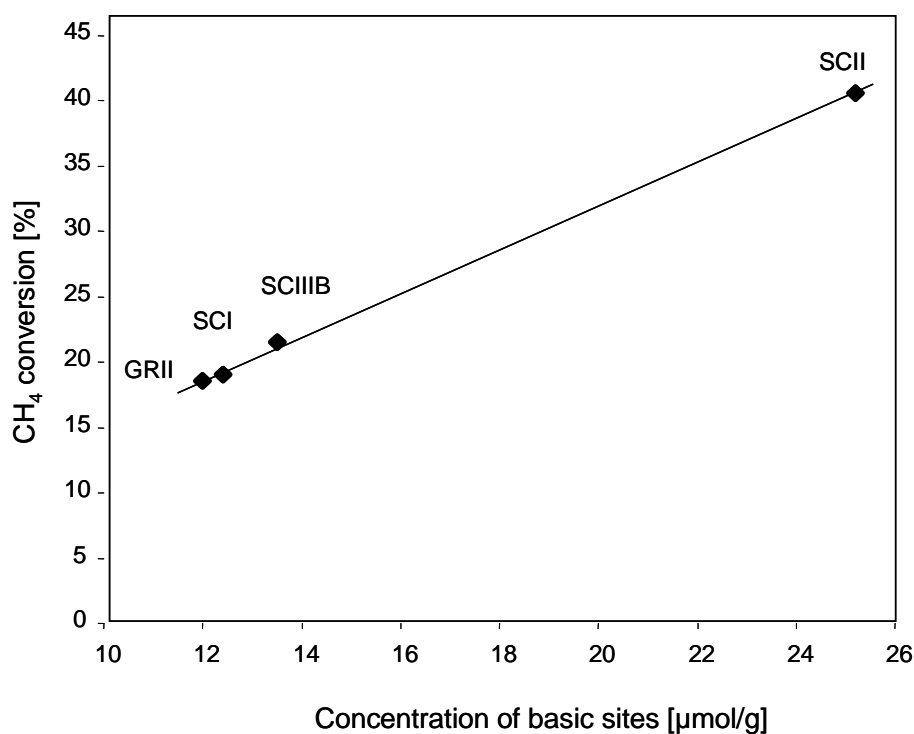
Fig.10. Correlation between the catalytic activity and the amount of basic sites.

In order to explore the effect of the acid-base properties of the samples, the methane conversion was plotted either as a function of basic sites (Fig.10) or as a function of acidic sites (Fig.11).
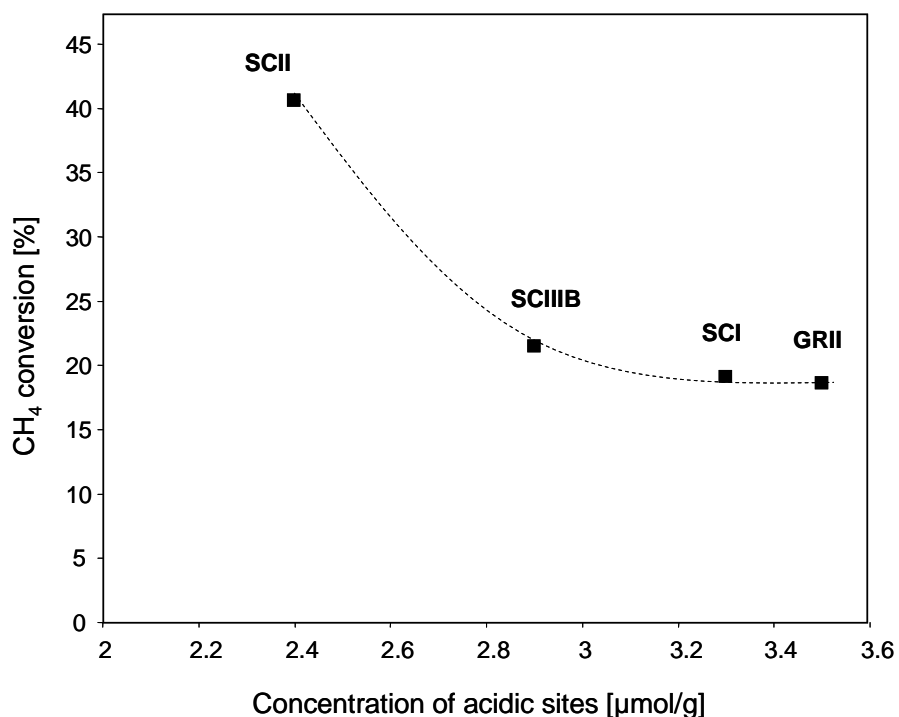
Fig.11. Correlation between the catalytic activity and the concentration of acid sites.

A linear relationship was found between methane conversion and basic sites. Sample SCII, which have more basic sites, presented higher activity. However, the more acidic samples like SCI and GRII showed lower MOC activity. It is considered that sample SCII is more basic, its surface LaOCl is much easier to be chlorinated and hence the Cl$^-$ added to the surface is more labile in nature, which makes this sample more active.

The dependence of product selectivities on methane conversion is shown for SCII sample in Fig.12. Selectivity to methyl chloride decreased with increase in methane conversion. While the selectivity to CH_2Cl_2, on the contrary increased. Such dependence suggests that CH_2Cl_2 is formed from CH_3Cl as a secondary product. The selectivity to CO_2 and CO increased slightly with methane conversion. It is postulated that the CH_2Cl_2 is formed through consecutive reaction of CH_3Cl.

50
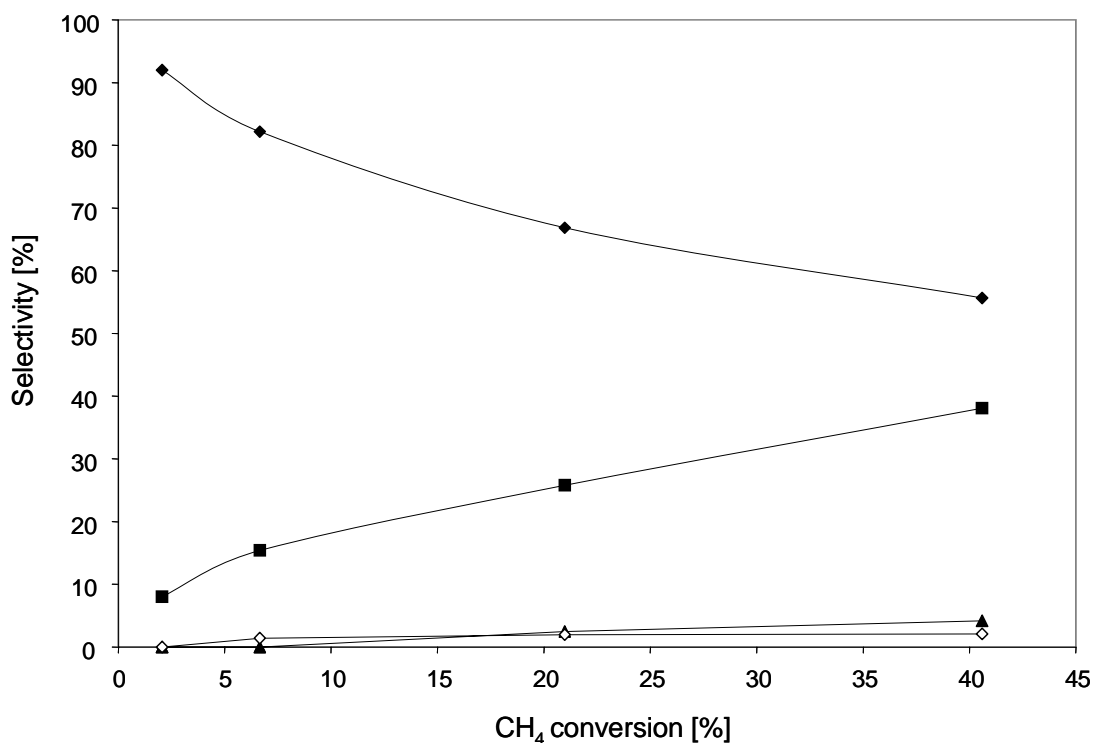
Fig.12. Selectivity to different products at various conversions over sample SCII. (♦)CH$_3$Cl, (■)CH$_2$Cl$_2$, (◊) CO and (▲) CO$_2$.

4. Discussion

The surface area of LaOCl samples depends on the preparation conditions, precipitating agent, solvent used, and calcination temperature. As it is mentioned above CO$_2$ and water has a big influence on the characteristic of the sample, since water easily adsorbs on the LaOCl surface and easily hydroxylate the surface whereas CO$_2$ from water and from atmosphere during synthesis forms carbonate in the sample, which get converted to different phases during the calcination treatment. Like lanthanum monoxy dioxycarbonate and later dioxycarbonate and at high temperature lanthanum oxide (Eq. 1). Low temperature leads to impure phase like lanthanum carbonate and La(OH)Cl$_2$ whereas high temperature leads to Lanthanum oxide. Therefore calcinations pretreatment should be optimised. High calcination temperatures lowers the surface area. However, the presence of carbonate also influences the surface area. LaOCl sample with surface area up to 127 cm^2/g has also been prepared in our lab and tested such sample for methane oxychlorination reaction, however activity could not be improved on such sample as conversion to LaCl$_3$ lowers the surface area. Hence, we could not find any activity relationship with

51

surface area of sample. LaOCl material changes dynamically under reaction conditions according to the equation 2.

This equilibrium shifts towards right, which is towards bulk chloride under the reaction condition. Since $LaCl_3$ is hygroscopic, it is very difficult to accurately characterize the state of the working catalyst. Specially, the structure sensitivity of the reaction could not be ascertained because the surface area of the catalyst changes under the reaction conditions and thus its influence on the reaction rate could not be established. Therefore, it is desirable to correlate catalytic activity with properties of initial LaOCl materials. As a result we have decided to characterize LaOCl deeply and correlate its acid-base properties with activity.

Methane is a highly stable hydrocarbon with high binding energy (ca.100 kcal/mol). It is very difficult to activate such molecule; hence chemical species like oxygen is present in the reaction system as one component capable of activating methane. The effect of presence of CH_4, O_2, and HCl on the reaction is studied by temperature programmed reaction (not shown). The reaction carried out in the absence of HCl shows the formation of chlorinated products which implies that Cl from the catalyst, rather than HCl from the reactant is necessary in chlorinating CH_4. Hence, the role of hydrogen chloride is just to maintaining the catalyst surface chlorinated. As first product CH_3Cl is observed at comparatively low temperature (400°C) indicating that the CH_3Cl is primary product of the reaction according to the following equation.

$$CH_4 + HCl + ½\ O_2 \longrightarrow CH_3Cl + H_2O \tag{3}$$

100% CH_3Cl selectivity at low conversion justifies this hypothesis. The CH_3Cl selectivity decreases with increase in selectivity of CH_2Cl_2 indicating that the CH_2Cl_2 is a secondary product and that the reaction follows a consecutive mechanism. CH_2Cl_2 is further oxidized to CO. Furthermore the formation of lattice oxygen sites during the dechlorination is suggested which can be attributed to an increase in the formation of CO and CO_2, responsible for the reduced catalyst selectivity. By partial

dechlorination of the LaCl₃ surface by water at higher temperature, oxygen sites can be produced by shifting the equation to the LaOCl site (Eq.2).

Even bulk LaCl₃ can be converted to LaOCl by calcinations for an appropriate amount of time. Which suggest that the LaOCl phase is responsible for the formation of CO_x and reduced catalyst selectivity. Negligible quantity of CO_2 is produced under the reaction conditions. Thus, its formation is of minor importance to understand the mechanism of oxidative chlorination. CO is produced in high selectivity and its formation is studied by TPR experiments. Results show that CO is formed readily from CH_2Cl_2 than from CH_3Cl. The absence of CO or CO_2 at low methane conversion suggests that theses products are formed not directly from methane but through decomposition of chloromethanes. Therefore, it can be concluded that CO is produced by decomposition of multiply substituted chloromethane. This could explain the formation of only trace amount of higher chloromethane such as $CHCl_3$ and CCl_4 because it is too unstable and reactive at the reaction temperature. The rate of chlorination decreases in the order $CCl_4 > CHCl_3 > CH_2Cl_2 > CH_3Cl > CH_4$. Rare-earth metals in oxides and chlorides do not change their oxidation state under usual reaction conditions and as a result they are commonly referred to as irreducible. Since chlorination is a sequential reaction the selectivity of the primary product, CH_3Cl can be enhanced at low methane conversion, by reducing the probability of further reacting of CH_3Cl. This can be achieved by increasing space velocity or increasing the CH_4 ratio in the feed. For experiments carried out without catalyst in the empty reactor results in no product formation, indicating that there is need of catalyst surface for product formation. Separate experiments carried out in the absence of oxygen yielded no product either. This indicates that there is some definite interaction between the catalyst surface and the O_2 in the reactant gases. Au et al. [25] have mentioned that oxygen adsorbs on terminal lattice oxygen sites and generate dioxygen species O_2^{2-}, O_2^{n-}, and O_2^{-} on the surface of LaOCl. These adsorbed species are expected to cause hydrocarbon oxidation. Further more this is supported by the increase of the COx formation after the dechlorination of the catalyst as seen from temperature programmed reaction (not shown). Therefore, LaOCl is not the predominant phase on a system that is highly selective for chlorinated products again confirm our previous

conclusion. Peringer *et al.* [11] suggested by DFT theory calculation that on chlorinated surface ($LaCl_3$) oxygen dissociatively adsorb and oxidize surface chlorine species and expected to form transient OCl^- surface species. In this adsorption step, gas phase O_2 oxidizes surface Cl from -1 to +1. Lanthanum does not change its formal +3 oxidation state. The function of $LaCl_3$ is to supply chlorine anions by maintaining a surface, which can be referred as chlorine sheet. The chlorine anions can be activated with the formation of OCl^- species. CH_4 reacts with the surface highly active OCl^- species by exchanging a proton for the activated Cl, i.e exchanging H^+ by Cl^+. The resulting product are surface OH group and gas-phase CH_3Cl. Surface hydroxyl can react with HCl to form gas-phase H_2O and surface Cl, regenerating the catalytic site. Hence, proposed catalytic cycle thus involves oxidation of surface chlorine without any change in the oxidation state of the lanthanum metal. In a further step CH_3Cl formed adsorbs on the catalyst surface to give the consecutive reaction products (CH_2Cl_2, COx).

From IR and TPD results it is clear that all the samples have the same type of active sites. However they have a different active site density, which responsible for different activities. A direct dependence of activity on basicity (conc. of O^{2-} sites) is observed for all samples. The more active sample SCII showed a higher initial La/Cl ratio have a lower initial amount of Cl and are characterized by a higher amount of HCl during chlorination leading to a substitution of the O^{2-} basic sites. This sample consequently takes up a higher amount of HCl during chlorination leading to a substitution of the O^{2-} by Cl^-. The substituted Cl^- added to the surface is suggested to be labile and is responsible for a higher activity for methane oxychlorination. Above results will help to design catalyst with high activity and high selectivity.

5. Conclusion

Four commercial LaOCl catalysts are characterized for their bulk and surface properties and tested for their catalytic activity and selectivity during methane oxychlorination MOC reaction. The following conclusions can be drawn from this study:

Crystalline LaOCl is the main phase in all samples from XRD and Raman analysis. But in sample GRII, lanthanum dioxycarbonate phase is also detected. This impurity has a great influence on the property of GRII. For example, GRII presented larger surface area, smaller and aggregated crystallites, and relatively large acid sites. IR spectroscopy in combination with TPD of adsorbed probe molecules was employed to assess the acid-base properties of LaOCl samples. TPD of adsorbed NH_4 and DMP shows that all samples have one similar and weak acidic sites. Three types of basic sites, which can be defined as weak, medium, and strong sites, were determined by using CO_2 as probe molecule in all samples and the total basicity decreases in the order: SCII>SCIIIB>SCI>GRII. i.e. Sample SCII is the most basic sample. IR spectra show that a high amount of monodentate and bidentate carbonates and a low amount of hydrogen carbonates present on the catalyst surface after adsorption of CO_2.

Thus, four commercial LaOCl catalysts samples are active for the methane oxychlorination and the following activity trend was observed: SCII>SCIIIB>SCI>GRII. This trend is exactly same as the basicity of LaOCl samples. Therefore, activity is strongly related to the concentration of basic sites. As LaOCl samples are subject to chlorination treatment before reaction, more basic samples are easier to be chlorinated and make the sample surface more labile which facilitates the activation of methane. Four commercial catalysts samples have different surface area; however, the attempt to correlate surface area with activity is not successful.

References

[1]   J. A. Labinger, J. E. Bercaw, Nature., 417 (2002) 507.

[2]   R. A. Periana, O. Mironov, D. Taube, G. Bhalla, C. J. Jones, Science., 301 (2003) 814.

[3]   B. R. Crum, R. F. J. Jarvis, A. I. T. B. M. Naasz, EP 0720975 A1 1996.

[4]   F. Wattimena, W. M. H. Sachtler, Stud. Surf. Sci. Catal., 7 (1982) 816.

[5]   A. J. Rouco, J. Catal., 157 (1995) 380.

[6]   C. Kenney, Catal. Rev.-Sci. Eng., 11 (1975) 197.

[7]   C. L. Garcia, D. E. Resasco, Appl. Catal., 46 (1989) 251.

[8]   C. L. Garcia, D. E. Resasco, J. Catal., 122 (1990) 151.

[9]   W. J. M. Pieters, W. C. Conner, E. J. Carlson, Appl. Catal., 11 (1984) 35.

[10]   A. E. Schweizer, M. E. Jones, D. A. Hickman, US 6452058 B1 2002.

[11]   E. Peringer, S. G. Podkolzin, M. E. Jones, R. Olindo, J. A. Lercher, Top. Catal., 38 (2006) 211.

[12]   L. H. Brixner, E. P. Moore, Acta. Crystallogr. C39 (1983) 1316.

[13]   Y. Hase, P. O. L. Dunstan, M. L. A. Temperini, Spectrochimica Acta, Part A., 37 (1981) 597.

[14]   B. Klingenberg, M. A. Vannice, Chem. Mater., 8 (1996) 2755.

[15]   M. Nieminen, M. Putkonen, L. Niinisto, Appl. Surf. Sci., 174 (2001) 155.

[16]   O. V. Manoilova, S. G. Podkolzin, B. Tope, J. Lercher, E. E. Stangland, J. M. Goupil, B. M. Weckhuysen, J. Phys. Chem., B 108 (2004) 15770.

[17]   M. P. Rosynek, D. T. Magnuson, J. Catal., 46 (1977) 402.

[18]   M. Weihe, M. Hunger, M. Breuninger, H. G. Karge, J. Weitkamp, J. Catal., 198 (2001) 256.

[19]   S. E. Collins, M. A. Baltanas, A. L. Bonivardi, J. Phys. Chem. B 110 (2006) 5498.

[20]   R. Bal, B. B. Tope, T. K. Das, S. G. Hegde, S. Sivasanker, J. Catal., 204 (2001) 358.

[21]   C. Morterra, G. Magnacca, Catal. Today., 27 (1996) 497.

[22]   F. P. Netzer, E. Bertel, Handbook on the Physics and Chemistry of Rare Earths 1982.

[23]   T. Mathew, B. B. Tope, N. R. Shiju, S. G. Hegde, B. S. Rao, Phys. Chem. Chem. Phys., 4 (2002) 4260.

[24]   A. W. A. M. van der Heijden, V. Belliere, L. E. Alonso, M. Daturi, O. V. Manoilova, B. M. Weckhuysen, J. Phys. Chem. B., 109 (2005) 23993.

[25]   C.T. Au, H.He, S.Y.Lai, C.F.Ng, Appl. Catal. A: Gen., 159 (1997) 133.

Chapter 3

Transformation of LaOCl samples to LaCl₃, functional groups and surface chemistry in relation to catalytic activity of methane oxychlorination

Abstract

Four commercial LaOCl catalyst precursors have been characterized and their activity for methane oxychlorination was compared. The concentration of OH groups and carbonates was investigated during the chlorination of LaOCl precursors as well as in the final LaCl₃ dominated material. Analytical techniques were used including IR spectroscopy, temperature programmed chlorination, $^{1}H/^{35}Cl$-MAS-NMR spectroscopy, X-ray diffraction and catalytic conversion of CH_4. Evidence is given that the surface functional groups and the catalytic activity is influenced by differences in the chlorination degree of the final LaCl₃ catalysts and hence by the concentration of LaOCl in the final material. XRD and IR study revealed that the catalyst undergoes major transformation to LaCl₃ during the chlorination. The activity of the starting material for the methane oxychlorination reaction decrease in the order SCII > SCIIIB > SCI. The activity strongly correlates with the stability of carbonates hence, less stable carbonates easily transform into lanthanum chloride. Hence, activity depended on a sample that easily converts to the LaCl₃ phase.

1. Introduction

Natural gas is available abundantly in the world. Methane is the major component of the natural gas which can be used efficiently as a fuel or chemical stock. The need to utilize methane as an alternative chemical feedstock is becoming more urgent due to diminishing proven reserves and increasing consumption of crude oil. The acute problem is that 30-60% of the natural gas is concentrated in relatively remote parts of the world; transportation of this gas to the local market is a problem. Therefore, techniques for transformation of methane, in to easy transportable or value added products, such as methanol, ethylene, aromatics, and liquid hydrocarbon fuels are high industrially interested.

The dominant technology used for production of chemicals from methane involves its conversion to a mixture of carbon monoxide and hydrogen. This is usually referred to as synthesis gas or syngas. Synthesis gas can be converted back to liquid hydrocarbons. Although this is the only industrialized technique production of synthesis gas is disadvantageously costly. One promising alternative technology for converting methane to C_2 and higher hydrocarbons could be oxidative coupling of methane. However, the reaction occurs partially on the catalyst surface and partially in the gas phase. The product selectivity decreases with increase in methane conversion and results in a low product yield [1].

Oxidative halogenation of methane or methane oxychlorination (MOC) to methyl halide is another possible technique for transformation of methane. The MOC product, methyl halide can be further processed into valuable chemicals such as methanol, dimethyl ether, light olefins and higher hydrocarbons.

A wide variety of catalysts can be used for the MOC process. Copper-based catalysts have proven to be the most active ones for this reaction though these catalysts are originally used in the industrial oxychlorination of ethylene [2]. Since copper based catalysts are known to be also active for Deacon chemistry [3], the oxidation of HCl to Cl_2, methane activation through liberation of elemental

chlorines is possible. Therefore, methane chlorination proceeds, at least partially, *via* a radical gas-phase mechanism and the selectivity to methyl chloride is usually low at significant methane conversion level [3]. Another drawback is that copper salts are volatile at the usual temperatures required for methane activation. By adulation of KCl, which lowers the melting point of copper chloride and promotes the copper redox steps, the stability of copper catalysts have been greatly enhanced [4-6]. Moreover, in order to prevent melt segregation of copper and potassium chlorides at high reaction temperatures, $LaCl_3$ has been used as a stabilizing promoter [7, 8].

Recently catalyst based on LaOCl which transforms to $LaCl_3$ in the presence of HCl under reaction condition was reported to be active and stable for MOC [9]. The LaOCl catalyst represents a complex system including a broad variety of possible compounds present in it such as La_2O_3 and $LaCl_3$. LaOCl and La_2O_3 are highly sensitive towards CO_2 and water has lot of influence on characteristic of the sample, since water easily adsorbs on the surface of LaOCl and La_2O_3 and easily hydroxylate the surface whereas CO_2 from water and from atmosphere forms carbonate in the sample during the synthesis.

The catalyst is pretreated with HCl before reaction, therefore it is also very important to study the effect of chlorination on the different phases present in LaOCl, since chlorination drastically changes the physicochemical properties of the solid catalyst and directly affecting their catalytic activity.

Furthermore LaOCl material changes dynamically under chlorination condition and continuously equilibrates between the LaOCl and $LaCl_3$ phases. Under chlorination condition this equilibrium shift towards right, i.e., towards bulk chloride. Hence it is interesting to study the phase transformation from LaOCl to $LaCl_3$. What will be the effect of phase transformation on catalytic activity, similarly effect of chlorination duration on different catalyst and their performance for the MOC. Stability of carbonate and hydroxyl group under the chlorination condition this study will be able to answer these questions.

The goal of the present work is to characterize the catalyst extensively during activation, chlorination and under catalytic reaction conditions. The aim of this study will also to correlate the catalyst phase composition with the catalytic performance. For this purpose different analytical techniques including IR spectroscopy, temperature programmed chlorination, ^{1}H/^{35}Cl-MAS-NMR spectroscopy, X-ray diffraction were used to characterize commercial samples. The role of functional groups and surface chemistry in relation to catalytic activity is also studied.

2. Experimental

2.1 Materials

Four commercial LaOCl samples named SCI, SCII, SCIIIB, and GRII were kindly supplied in powder form by Dow Chemical Company USA. The specific surface area of the samples was determined by N_2 adsorption at -196°C on a Micromeritics ASAP 2000 apparatus. Samples were degassed at 400°C for 6h before measurement. The chemical compositions of these samples were analyzed by energy dispersive X-ray spectroscopy (EDX) on a JEOL 500 SEM microscope.

2.2 Powder X-ray diffraction (XRD)

The phase purity of the La-based materials was checked with X-ray diffraction (XRD). XRD patterns of LaOCl samples after 2h chlorination were recorded at RT and phase analysis of the samples was done with a Philips X'pert highscore softwere. All XRD patterns were collected on before and after MOC reaction, XRD patterns of LaOCl samples were also recorded at ambient conditions by Philips X'Pert Pro diffractometer (CuK $_1$-radiation, λ = 0.154056 nm 40 kV/ 40 mA). Measurements were performed on a spinner in the 2θ range from 5° to 75° 2θ (0.05 °/min) with a ¼" slit.

2.3 IR Spectroscopy

The IR spectra of the chlorinated samples in the hydroxyl (3000-4000 cm^{-1}) region were recorded on a Brucker IFS 88 spectrometer at 4 cm^{-1} resolution. The spectrometer was equipped with a flow cell and a vacuum cell and the signals were detected with a MCT detector. In the experiment, about 8 mg sample was pressed into a self-supporting wafer and placed in a gold sample holder in the

center of an evacuated ($<10^{-6}$ mbar) stainless steel chamber equipped with CaF_2 window. The temperature was raised to 400 °C stepwise and a spectrum was recorded at RT, 100, 200, 300, and 400 °C.

2.4 Temperature-programmed chlorination

For temperature programmed chlorination experiment, 250 mg of LaOCl samples was pretreated in 40 ml/min He with a ramp rate 10°C/min to 400°C and maintained at this temperature for 1h. After this treatment the sample was cooled down to 50°C, and then chlorinated with 20% HCl in He. The total flow rate was 50 ml/min and the temperature was raised with a ramp rate of 5°C to 550°C. The chlorine uptake was analyzed by an online Siemens Maxum Edition II gas chromatograph.

2.5 ^{1}H MAS NMR Spectroscopy

For ^{1}H MAS NMR measurements, the samples were activated in vacuum at 453 K and packed into a 4 mm ZrO_2 rotor (^{1}H NMR measurements under nitrogen). The measurements were performed on a Bruker AV500 spectrometer (B_0 = 11.7 T) with a spinning rate of 15 kHz. For the ^{1}H MAS NMR measurements a 90° excitation pulse was applied (1.6   s) and the recycle time was 2.0 s. For calibration of the chemical shift and the total intensity an external adamantane standard was used (= 1.7 ppm).

2.6 Catalytic test

Methane oxychlorination reaction was performed in a conventional fixed bed down stream reactor under atmospheric pressure. The reactor was made up of stainless steel tube (glass lining inside) with 4mm i.d and approximately 43.5 cm long. The catalyst 0.5 g was placed in the middle of the reactor supported by a plug of glass wool. The remaining dead volume of the reactor was filled with the glass beads of size between 0.63 to 0.75 mm to minimize void space. Before each run the catalyst was activated at 550°C for 1h in He to remove adsorbate, like CO_2 and water. After decreasing the temperature to 400°C, a flow of HCl (10 ml/min) was added to the He flow and passed over the catalyst

for 2h, to convert the lanthanum oxychloride catalyst partially or totally to lanthanum trichloride. Then the feed gas flow was switched to a mixture of He, CH_4, HCl, O_2, and N_2 with a ratio of 2:1:1:0.5:0.5. The total flow was 20 ml/min. The catalytic test was performed under integral condition within the temperature range of 400-540 °C. At each temperature the reaction was run for 1.5 h before product analysis by online GC. The lines were heated at 130°C to avoid the condensation of the liquid HCl inside the lines which could result in corrosion and plugging of the lines. Teflon tubing and fitting were used to avoid corrosion due to hydrogen chloride. The outlet of the effluent lines was connected to a 4M NaOH solution to neutralize the HCl and other acidic gases coming out of the reactor. The effluent was further purified by passing through activated charcoal.

The products distribution was analyzed by a Siemens online GC equipped with a thermal-conductivity detector (TCD). Six columns were used for separating product effluent gases.

3. Results

3.1 Effect of chlorination on LaOCl catalysts

The X-ray powder diffraction patterns of LaOCl precursors before and after reaction are presented in Fig 1. The XRD pattern of fresh LaOCl precursor is similar to that reported in the literature [10].
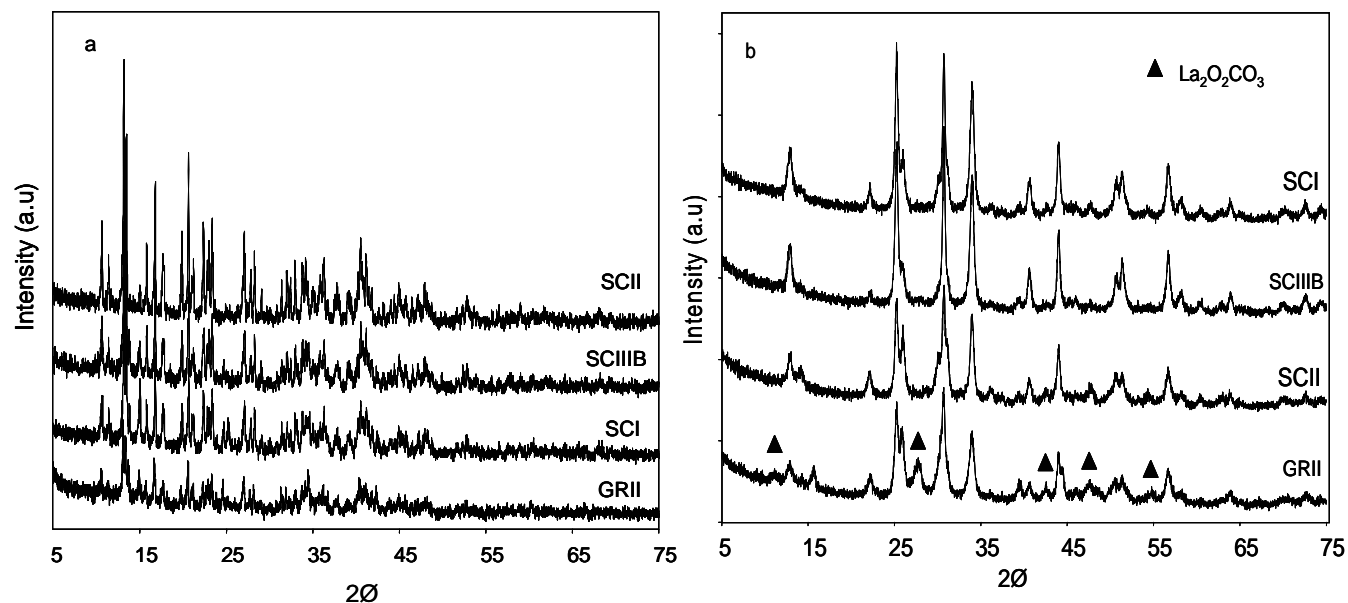
Fig.1. X-ray diffractograms of LaOCl samples a) before reaction b) after reaction recorded at RT

Intense and sharp reflection is observed for SCI and SCIIIB pointing out the high crystallinity of these samples. On the contrary, the XRD patterns of SCII and GRII feature broad reflections of very low intensity. This indicates that SCII and GRII either contain more amorphous phase or have smaller particles size. After reaction LaOCl undergoes major transformation and the typical diffraction peaks of $LaCl_3$ appears. It is found that SCII sample shows intense and sharp peaks of $LaCl_3$ pointing out its high crystallinity. Intensity of the SCIIIB and SCI are relatively lower than for SCII. The most impure sample GRII shows lowest crystallinity among all samples. From the diffraction of the XRD one can assign the order of decrease in crystalinity: SCII > SCIIIB > SCI > GRII.

The influence of chlorination on hydroxyl groups and carbonate is studied by IR spectroscopy. The *in-situ* IR spectra of all chlorinated samples are recorded at 400°C and presented in Fig 2.
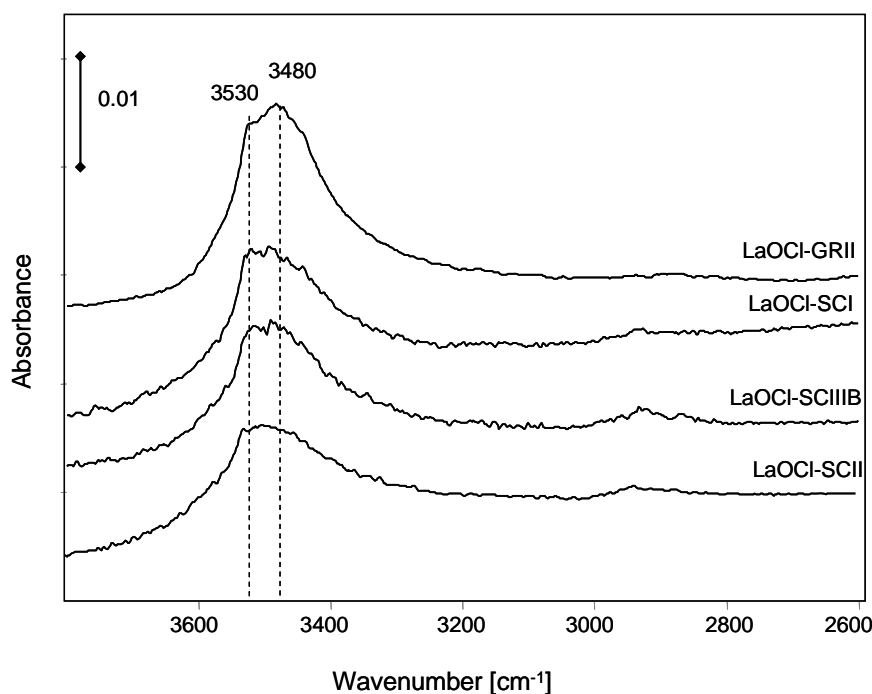
Fig.2. IR spectra of chlorinated commercial LaOCl precursors at 400°C.

The samples show a broad band centered at 3480 cm^{-1} with a shoulder at 3530 cm^{-1}. The band at 3480 cm^{-1} is assigned to the OH stretching vibration of LaO(OH) type species [11-12] and the band at 3530 cm^{-1} attributed to La(OH) species[13]. This indicates that both hydroxyl bands are stable even after chlorination. However intensity of the hydroxyl group decreases sharply compared to the fresh

one. The concentration of hydroxyl group after chlorination decreases in the following order GRII > SCI > SCIIIB > SCII. It is interesting to note that the fresh sample which shows high concentration of hydroxyl group initially shows lower concentration of hydroxyl group after chlorination. The sample which shows initially lower concentration of hydroxyl group shows high concentration of hydroxyl group after chlorination.

Temperature programmed chlorination

Temperature programmed chlorination experiment is performed to measure the uptake of chlorine in all the samples and the results are presented in Fig 3.
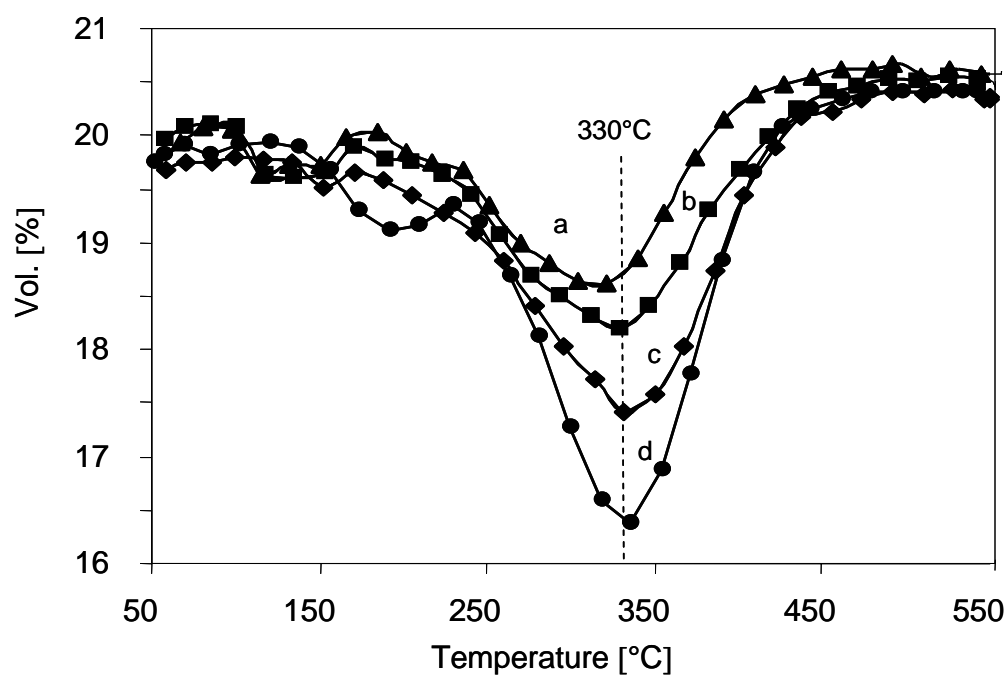
Fig. 3. Temperature programmed chlorination of commercial LaOCl precursor. a) LaOCl SCI b) LaOCl SCIIIB c) LaOCl SCII d) LaOCl GRII

All samples show chlorine uptake maxima at around 330°C. Chlorine uptake is observed at temperature above 200°C and below 450°C. At lower temperature, HCl doesn't react with catalyst while at high temperatures the reaction between HCl and catalyst is already completed. The highest amount of chlorine uptake is observed in GRII sample which is attributed to the presence of large amount of lanthanum dioxycarbonate, which is confirmed from our previous results (Chapter 2 of this thesis). Among the SC samples, SCII sample shows the highest amount of HCl followed by SCIIIB and SCI.

Hence, chlorine uptake of the sample decreases from SCII > SCIIIB > SCI. It is also observed that the uptake of chlorine is coupled with the release of CO_2, which means HCl reacts with Lanthanum carbonate to generate CO_2.

Not surprisingly, GRII which consumes HCl the most releases more CO_2 than other samples. The amount of chlorine uptake of the sample is presented in Table 1.

Table 1. HCl uptake of LaOCl precursor samples.

Samples	HCl uptake [mol/mol LaOCl]
LaOCl SCII	1.34
LaOCl SCIIIB	1.15
LaOCl SCI	0.88
LaOCl GRII	1.62

Phase transformation of LaOCl precursor to LaCl₃

The nature of the catalytic phase and details of catalyst transformation from LaOCl to $LaCl_3$ were examined by XRD during chlorination.

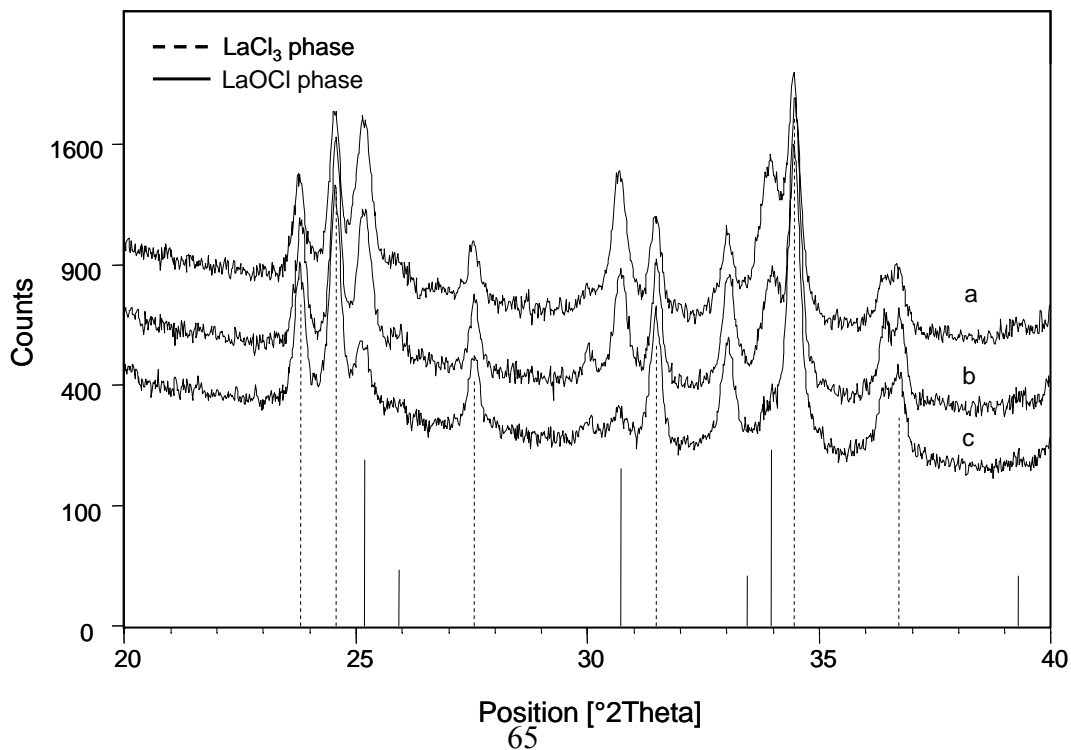Fig.4. XRD diffractograms of chlorinated LaOCl precursors. a) LaOCl SCI b) LaOCl SCIIIB c) LaOCl SCII

All samples transform slowly under chlorination condition to $LaCl_3$. The results are presented in Fig 4. The XRD reflexes for LaOCl phase is shown by solid line while the dashed line represents the $LaCl_3$. All samples measurably transform to $LaCl_3$, this demonstrates that the precursor materials converts to different degrees into $LaCl_3$. LaOCl phase is still present after two hours of chlorination, indicating the need for increasing the chlorination time for the complete transformation of LaOCl to $LaCl_3$. In SCII sample negligible amount of LaOCl phase remains which indicates its labile nature and hence SCII sample is easier to transform to the $LaCl_3$ compared to the other SC samples. SCIIIB sample is the second one followed by SCII, which shows a higher amount of LaOCl compared to the SCII. SCI sample is the most resistant to the transformation and the highest amount of LaOCl phase is present in the sample. Theses differences in the sample can be coupled to the uptake of chlorine in the sample. This in turn depends on the stability of the carbonate in the sample. Samples which have more stable carbonates are more difficult to transform to $LaCl_3$, however samples which have less stable carbonate are easily transformed to $LaCl_3$. From TPR results (not shown) the stability of carbonates in LaOCl precursors is as follow: GRII > SCI > SCIIIB > SCII. SCII sample which has less stable carbonate is easily converted to $LaCl_3$ and shows the maximum extent of transformation to $LaCl_3$ compared to the rest of sample evidenced by XRD. SCII sample shows maximum uptake of chlorine than the rest SC samples.

^{1}H MAS NMR Spectroscopy

To collect more quantitative information on the concentration of hydroxyl group after chlorination, ^{1}H MAS NMR spectra of the LaOCl chlorinated at 500°C is recorded. The spectra of the SC samples are presented in Fig 5. The spectra shows broad signal centered around 5 ppm, which could be assigned to OH groups bound to lanthanum cations [13]. The hydroxyl groups are stable after chlorination treatment and at high temperature. The concentration of hydroxyl groups show the same trends as qualitatively found by IR spectroscopy.
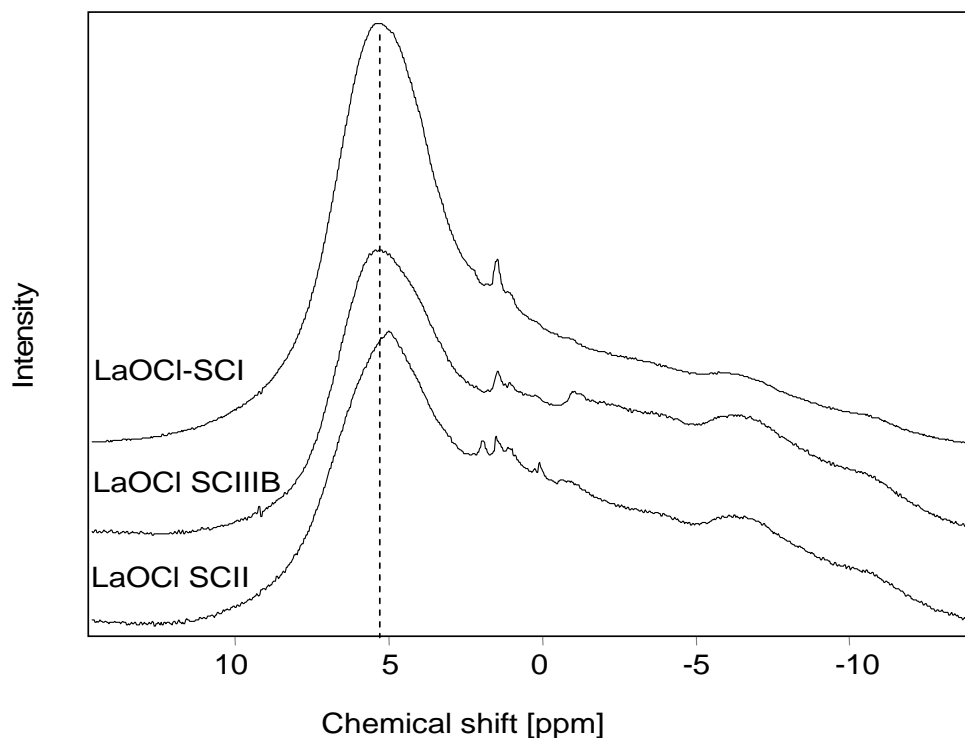
Fig.5. ^{1}H MAS NMR of chlorinated commercial LaOCl precursors recorded in the hydroxyl group.

The concentration of OH groups after chlorination (Table 2) decreases in the order SCI > SCIIIB > SCII.

Table 2. Relative concentration of residual carbonate, hydroxyl group and LaOCl determined by IR, ^{1}H NMR and XRD

Sample	Residual carbonate by IR	Hydroxyl group by ^{1}H NMR	Hydroxyl group by IR	Conc. of LaOCl by XRD
SCII	78	120	105	40
SCIIIB	150	140	136	108
SCI	310	250	210	156
GRII	400	n.a	n.a	n.a

n.a (not available)

Influence of oxygen on hydroxyl groups study by IR spectroscopy and ^{1}H MAS NMR Spectroscopy

IR analysis was used to study the interaction of oxygen with SCII sample at 400°C. After activating the SCII sample in He for 1h, the sample is exposed to 20% O_2 in He. The results are presented in Fig. 6.
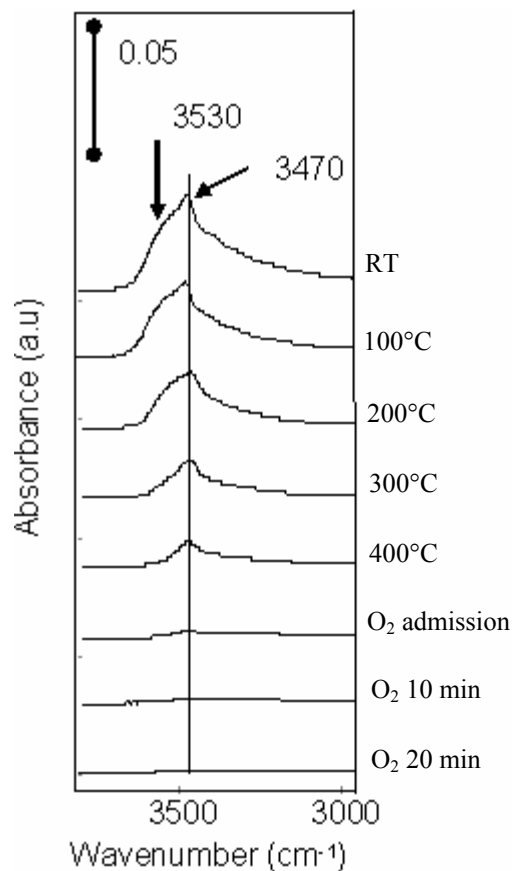
Fig.6. IR spectra of LaOCl SCII shows influence of oxygen on hydroxyl group.

Upon adsorption of oxygen at 400°C, a decrease in intensity of the hydroxyl band is seen. With increase in exposure time further reduction of the hydroxyl band is observed. There is an interaction of hydroxyl groups with gas phase oxygen which leads to a decrease in the concentration of hydroxyl groups by possibly forming water as a product.

To support our observation the interaction of oxygen with hydroxyl group is studied with ^{1}H MAS NMR spectroscopy and the results are presented in Fig.7. The not activated sample shows broad signal centered around 4 ppm. Activation in He leads to a sharp decrease in intensity of the hydroxyl band.
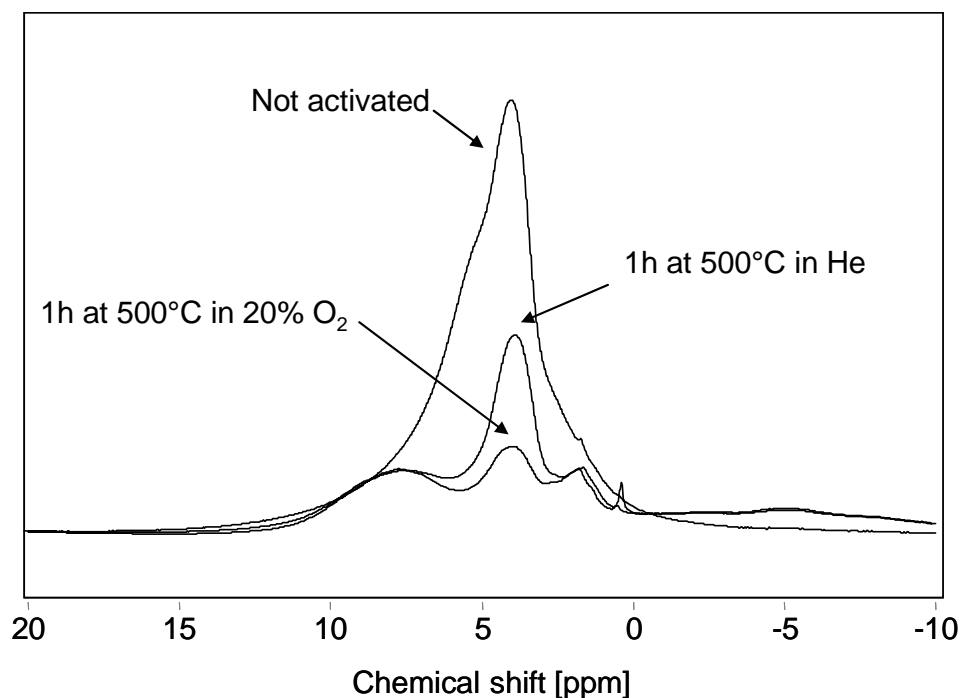
Fig.7. ^{1}H MAS NMR shows influence of oxygen on hydroxyl group in LaOCl SCII.

Further admission of oxygen leads to the gradual decrease of the hydroxyl band, this observation is in good agreement with the IR results.

3.2 Correlation between catalytic activity and concentration of LaOCl

The correlation between the catalytic activity and concentration of LaOCl is presented in Fig 8. The catalytic activity increases with decrease in concentration of LaOCl in the material after chlorination. The order for the catalytic activity is LaOCl SCII > LaOCl SCIIIB > LaOCl SCI. This means that the presence of LaOCl is not beneficial for the catalytic activity and catalyst precursor should be transformed fully or to the maximum extent to LaCl$_3$.
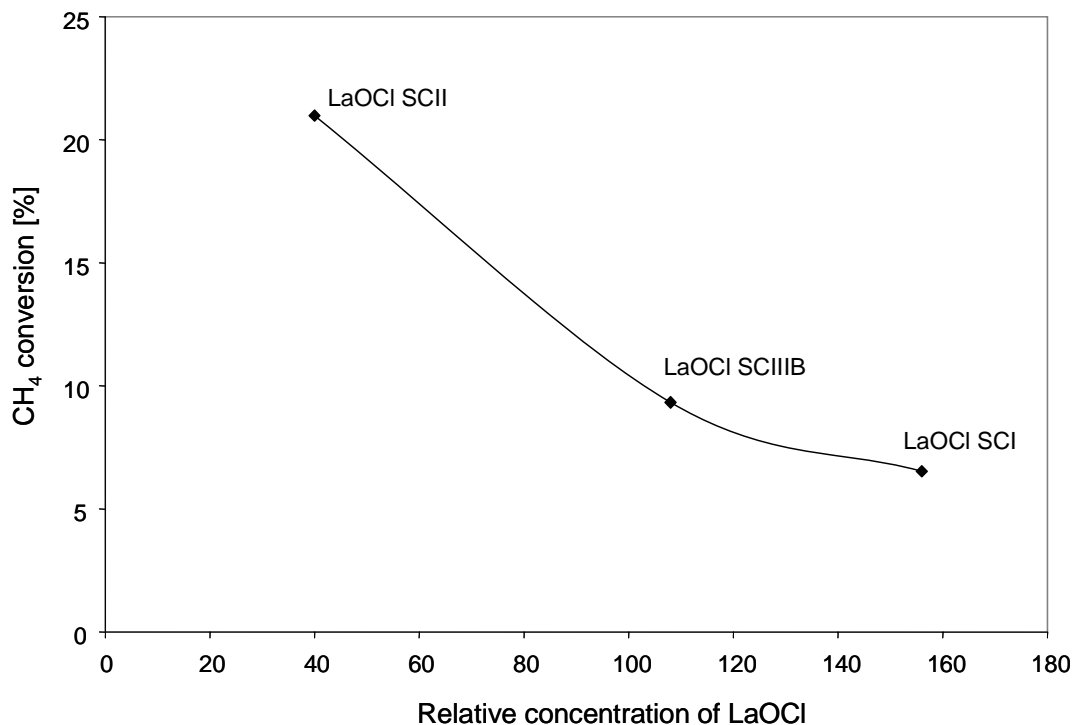
Fig.8. Methane conversion as a function of the relative concentration of LaOCl (determined by XRD)

The amount of LaOCl present after chlorination depends upon two factors. First, the stability of the carbonate in the sample, the less stable carbonate is easily transformed to $LaCl_3$ whereas more stable carbonates are difficult to transform to $LaCl_3$. Second, a increase in chlorination time is extremely helpful to transform these LaOCl precursors to the maximum extent of $LaCl_3$.

Effect of chlorination time on activity

The dependence of activity on chlorination duration of SCII is studied and provided in Fig 9. The catalytic activity increases with increase in chlorination time. As we have seen from the XRD results by chlorination, LaOCl is transformed to a different degree to $LaCl_3$. Increase in chlorination time results in more transformation to $LaCl_3$ which results in an increase in catalytic activity. Hence complete transformation of $LaCl_3$ is useful for an increase in activity. Furthermore, Peringer *et al.* [15] had mentioned that above 490°C the formation of LaOCl takes place due to the partial dechlorination of $LaCl_3$ surface by water and increase in concentration of CO_2 and CO suggest that LaOCl phase contribute to the increase in CO_2 and CO production.

70
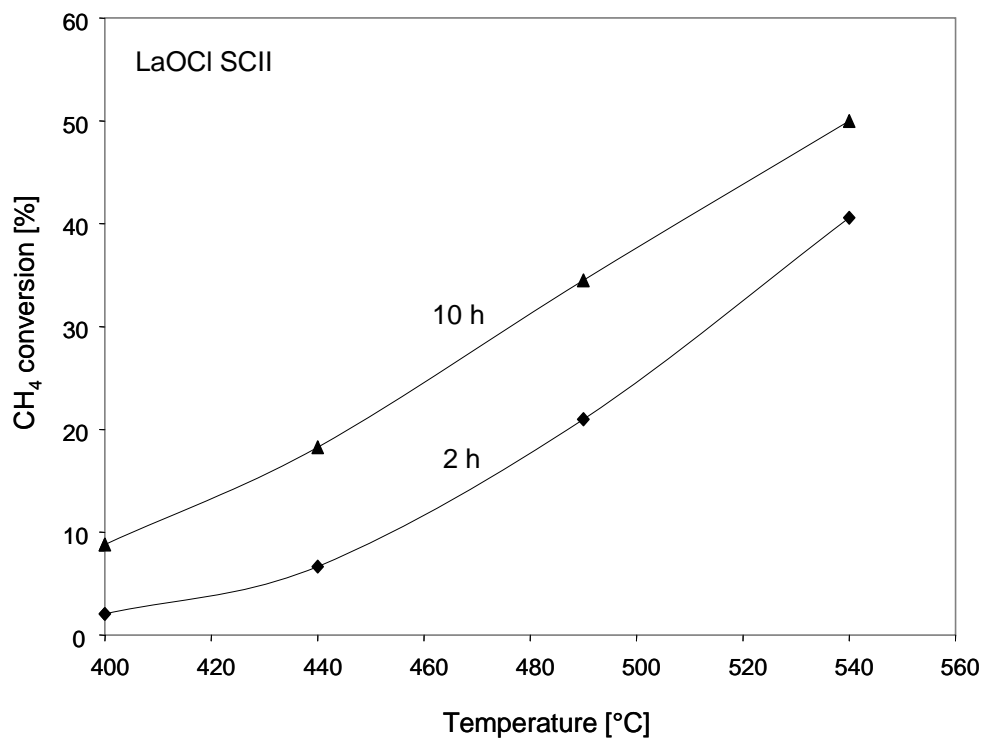
Fig. 9. Effect of chlorination time on methane conversion as a function of temperature

Therefore, presence of LaOCl phase is not beneficial for the selectivity and it necessary to keep catalyst in the chlorinated form. Podkolzin *et al.* [14] mentioned that in order to avoid side reaction it is necessary to keep catalyst in the chlorinated form. This would minimize the number of oxidation sites and raise the energetic barrier for oxidation side reaction.

Effect of chlorination on carbonates

IR spectra of chlorinated sample are recorded in the carbonate region and presented in Fig 10. Surprisingly carbonate bands are visible even after chlorination, which means carbonates are stable under chlorination condition. SCII sample which has less stable carbonate shows little amount of carbonates after chlorination. GRII and SCI sample which have highly stable carbonates show high amount of carbonates after chlorination.
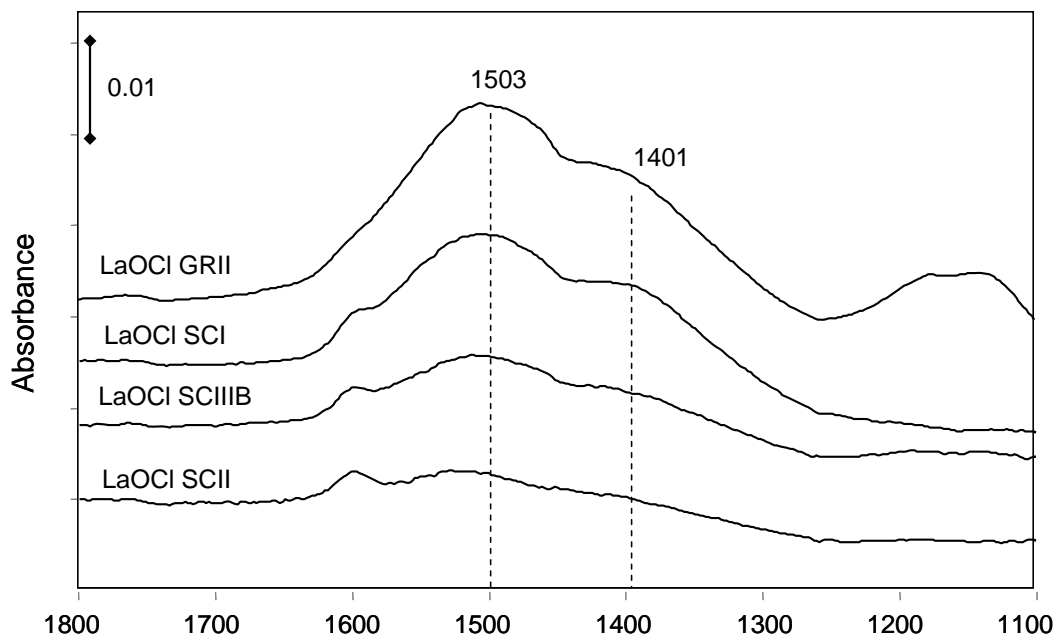
Fig.10. IR spectra of chlorinated LaOCl in carbonate region

These results are consistent with XRD results, which show that SCII sample is easily transformed to $LaCl_3$ under chlorination condition. Theses results are also supports the chlorine uptake results in which SCII sample takes up high amounts of HCl during chlorination and transformed to $LaCl_3$ to high extent compared to other samples. Hence from IR results concentration of carbonates after chlorination follows the order SCII < SCIIIB < SCI < GRII.

4 Discussion

The commercial LaOCl catalysts are not composed of pure LaOCl. Other phases like La_2O_3, $LaCl_3$ and lanthanum carbonates are also present. It is well known that $LaCl_3$, the precursor for LaOCl, is highly sensitive to CO_2. CO_2 from water and atmosphere during synthesis can react with $LaCl_3$ or LaOCl and form lanthanum carbonate. During calcinations or activation lanthanum carbonate decompose to lanthanum monoxy carbonate and dioxycarbonate. At high temperature, they can also transform to lanthanum oxide. These unwanted phases may affect the chlorination. Therefore, it is important to study the stability of these phases under chlorination condition and effect of the resulting phases on catalytic activity.

Second important step is the conversion of LaOCl to LaCl$_3$ under chlorination condition. During our catalytic test, all samples were first exposed to the treatment of HCl, this treatment transforms LaOCl totally or partially to LaCl$_3$ according to the following equilibrium.

$$LaOCl + 2HCl \rightleftharpoons LaCl_3 + H_2O \tag{1}$$

The Influence of chlorination on hydroxyl groups, carbonates and the nature of the catalytic phase and details of catalyst transformation from LaOCl to LaCl$_3$ were examined with XRD, IR and NMR.

Chlorination treatment results in decrease in hydroxyl group as seen from IR and NMR. HCl is acidic and its interaction with basic hydroxyl group leads to the reduction in the hydroxyl group. SCII is the most basic sample (see Table 3) after treatment with HCl it shows lowest amount of hydroxyl groups, GRII sample shows the highest amount of hydroxyl groups.

Table 3: Amount of basic sites determined by CO$_2$-TPD and acid sites determined by ammonia TPD and DMP-TPD.

Sample	Basic sites (μmol g^{-1}) by CO$_2$	Acid sites(μmol g^{-1}) by ammonia	Acid sites(μmol g^{-1}) by DMP
SCII	25.2	2.4	1.7
SCIIIB	13.5	2.9	2.4
SCI	12.4	3.3	2.9
GRII	12.0	3.5	3.1

The difference between the materials is also observed with respect to the uptake of chlorine and the amount of CO$_2$ released. It is important to note that the release of CO$_2$ and the uptake of chlorine are a coupled process that means, higher consumption of HCl corresponds to more pronounced release of CO$_2$. High uptake of hydrogen chloride is important for the activity as the function of catalyst is to provide surface chloride. To test whether catalyst can supply Cl for the reaction, Peringer *et al.* [15] performed a TPR experiment in the absence of HCl, when HCl was eliminated from the feed, the

reaction rate gradually decreases and stabilized at a lower value. This results show that chlorine can be supplied by catalyst, and catalyst is referred as chlorine sheet. Hence, the function of catalyst is to consume large amounts of hydrogen chloride and supply the surface chlorine for the reaction. SCII consumes a high amount of chlorine and shows high activity in the MOC reaction. These chloride ions are nucleophilic and hardly capable of activating methane. Hence, this activation to occur electrophilic oxygen is needed directly or as an intermediate reactant to convert necleophilic chloride into an electrophilic hypochloride OCl^-. Oxygen adsorb on the catalyst dissociatively with the formation of OCl^- surface species. Methane reacts with OCl^- by exchanging a proton for Cl^- and forming a hydroxyl group on the surface. The reaction between the hydroxyl group and gas phase HCl results in formation of gas phase water and restoration on Cl on the surface.

The gradual transformation of LaOCl to $LaCl_3$ is an important step to understand how transformation occurs. XRD results show that all samples convert to different degree under chlorination condition. In this case the stability of the carbonates is necessary to take into consideration. The sample which has more stable carbonates is difficult to transform to $LaCl_3$ while the sample which has less stable carbonate easily transforms to $LaCl_3$. Among all samples SCII samples which has less stable carbonate shows less reflexes of LaOCl and high reflexes for $LaCl_3$ after chlorination. The correlation between the concentration of LaOCl after chlorination and catalytic activity is shown in Fig 8. Results show that activity decreases with increase in amount of LaOCl. Hence for the good activity it is necessary to convert catalyst fully to $LaCl_3$. The results from chlorine uptake and XRD suggest that effective catalyst is the one that consumes high amount of chlorine and transform easily from LaOCl to $LaCl_3$. Peringer *et al.* mentioned that above 490°C partial transformation of the surface from the $LaCl_3$ to LaOCl occurs according to the equation 1.

This results in increase in CO_2 and CO concentration. The active site for the formation of CO_x in oxidative chlorination is likely to be a terminal lattice oxygen atom. Podkolzin *et al.* [14] suggested that in order to minimize deep oxidation of methane in MOC, the reaction should be run over $LaCl_3$ with as

fully as possible chlorinated surface. After the reaction, phases of the catalyst are checked with XRD and $LaCl_3$ is evidenced. The crystallinity of $LaCl_3$ is significantly higher than for LaOCl. The surface area of the catalysts decreased to about 9 m^2/g.

5. Conclusion

Four commercial catalysts are characterized for their bulk and surface properties and tested for their catalytic activity/selectivity in MOC reaction. The following conclusions can be drawn from this study:

XRD analysis suggests that LaOCl undergoes major transformation under chlorination condition to $LaCl_3$. All samples transform to different degrees to $LaCl_3$. SCII shows the highest transformation and SCI lowest. Concentration of carbonates under HCl stream increases in the order LaOCl SCII < LaOCl SCIIIB < LaOCl SCI < LaOCl GRII. Carbonate concentration is related to the concentration of LaOCl in the active catalyst. Catalytic activity is proportional to the concentration of $LaCl_3$ and inverse to the concentration of LaOCl in the activated catalyst.

IR spectroscopy in combination with ^1H MAS NMR was employed to assess the influence of oxygen on hydroxyl groups. It was shown that the presence of oxygen reduces the concentration of OH groups. Concentration of hydroxyl group measured by IR and NMR agree well showing that the most active material has less OH groups. Most likely associated with the lower concentration of LaOCl after chlorination in the better sample. TP chlorination experiments show that LaOCl SCII consumes higher concentration of HCl than LaOCl SCIIIB and LaOCl SCI. All four samples are active for methane oxychlorination and the following activity trend was observed: SCII>SCIIIB>SCI>GRII.

References

[1]   J.H. Lunsford, Catal. Today., 63 (2000) 165.

[2]   B. R. Crum, R. F. J. Jarvis, A. I. T. B. M. Naasz, EP 0720975 A1 1996.

[3]   F. Wattimena, W. M. H. Sachtler, Stud. Surf. Sci. Catal., 7 (1982) 816.

[4]   A. J. Rouco, J. Catal., 157 (1995) 380.

[5]   C. Kenney, Catal. Rev.-Sci. Eng., 11 (1975) 197.

[6]   C. L. Garcia, D. E. Resasco, Appl. Catal., 46 (1989) 251.

[7]   C. L. Garcia, D. E. Resasco, J. Catal., 122 (1990) 151.

[8]   W. J. M. Pieters, W. C. Conner, E. J. Carlson, Appl. Catal**.,** 11(1984) 35.

[9]   A. E. Schweizer, M. E. Jones, D. A. Hickman, US 6452058 B1 2002.

[10]   J. Holsa, M. Lastusaari, J. Valkonen, J. Alloys Compds., 262 (1997) 299.

[11]   B. Klingenberg, M. A. Vannice, Chem. Mater., 8 (1996) 2755.

[12]   M. Nieminen, M. Putkonen, L.Niinisto, Appl. Surf. Sci., 174 (2001)155.

[13]   M. Weihe, M. Hunger, M. Breuninger, H.G. Karge, J. Weitkamp, J. Catal., 198 (2001) 256.

[14]   S. G. Podkolzin, O.V. Manoilova, B.M. Wekhusen, J. Phys. Chem. B., 109 (2005) 11634.

[15]   E. Peringer, S. G. Podkolzin, M. E. Jones, R. Olindo, J. A. Lercher, Top. Catal., 38 (2006) 1.

<p align="center" style="font-size:2em; font-style:italic;">

Chapter 4

Oxidative dehydrogenation of ethane over Dy$_2$O$_3$/MgO supported LiCl containing eutectic chloride catalysts

Abstract

The catalytic oxidative dehydrogenation of ethane was studied with alkali and alkaline earth metal chloride modified LiCl supported on Dy$_2$O$_3$/MgO (MD). Eutectic mixtures of alkali or alkaline earth metal chloride with LiCl were formed on the support surface decreasing so the melting point of the pure LiCl. The lowest melting point, 366 ºC, was found on Li-K-MD. All samples had weak basicity decreasing in the order: Li-K-MD> Li-Sr-MD≈ Li-Ba-MD>Li-Na-MD>Li-MD. With all materials studied physisorbed and chemisorbed CO$_2$ species were detected by *in situ* IR spectroscopy. Bidentate carbonate species dominated on Li-MD while on modified samples both bidentate and unidentate carbonate species were present. The catalyst with lower basicity had higher activity. Catalyst selectivity increased with increasing reaction temperatures and did not vary above a threshold temperature. The ethene selectivity is directly correlated with the melting point of the eutectic melt on the catalyst support.

1. Introduction

Ethene and propylene are important building blocks of chemical industry being currently produced *via* steam cracking of various petroleum fractions. The mature process is operated under severe conditions with disadvantages including thermodynamic limitations, high energy demand, and formation of coke on the catalyst [1]. The olefin market growing at a rate of 3% per year and the continuous rising fuel costs has spurred substantial interest to develop alternative routes to steam cracking [1-3].

Oxidative dehydrogenation (ODH) of light alkanes is one of the most promising alternatives [1-3]. OHD is an exothermic reaction and can be operated at lower temperatures (T < 650º) reducing so the energy input. The feedstock of ODH, light alkanes, is easily available and competitively priced. However, the development of an appropriate catalyst proved to be difficult, since CO_x is thermodynamically favored and the olefins produced are generally more reactive than alkanes. Consequently, catalysts that can, e.g., activate ethane effectively, while maintain high ethene selectivity would be highly desirable.

Catalysts that are active for the ODH of alkanes can be grouped into two categories [3]. The first group materials are reducible metal oxides, based on V and Mo oxides, which can operate at temperatures below 550 ºC [4-11]. The second groups are non-reducible alkali metal-based oxide catalysts that are active at a temperature above 600 ºC [12-22]. Li/MgO is perhaps the most prominent system having been widely studied. While unmodified Li/MgO shows moderate activity [12, 13], the activity of Li/MgO can be significantly increased by addition of small amount of chlorine-containing compounds in the feed or by direct incorporation of chlorine into the catalyst [16, 17]. Environmental concerns exclude the use of chlorine compounds as part of the feed stream. The activity of Li/MgO can be further improved by addition of SnO_2, La_2O_3, Nd_2O_3 or Dy_2O_3 as promoter [18, 19]. Ethene yields up to 77% have been obtained when Dy_2O_3 is used as promoter [19].

From previous study in our group [19], it has been observed that high selectivity is obtained, once the reaction temperature approaching the melting point of LiCl. To further study this phenomenon and the effect of melting point on the ODH of alkanes, a series of catalysts were prepared by adding alkali or alkaline earth metal chlorides to the LiCl/Dy_2O_3/MgO catalyst. Various physicochemical characterization techniques are used together with the catalytic tests for the OHD of ethane in order to establish structure- activity relations.

2. Experimental

2.1. Catalysts preparation

Metal chloride modified LiCl/ Dy_2O_3/MgO catalysts were prepared by wet impregnation. Typically, Dy_2O_3 and MgO powders were added to a solution containing $LiNO_3$, HCl and NH_4Cl (ratio HCl: NH_4Cl = 1:1), and one additional metal chloride (NaCl, KCl, $SrCl_2$, and $BaCl_2$). Then, the slurry obtained was stirred at 80 °C for 2 hours. Subsequently, the water was evaporated under reduced pressure and the residue was dried at 100 °C. All samples were calcined at 350 °C for 4 h followed by calcination at 600 °C for 4 h, except for the unmodified LiCl/ Dy_2O_3/MgO which was calcined at 650 °C. Based on the different metal chloride added, the catalyst was denoted as Li-X-MD (X=Na, K, Sr, and Ba).

In all samples, the atomic ratio of Mg:Dy:Li was 100:2:10. The chloride ion from HCl and NH_4Cl was 20% of MgO. The amount of alkali or alkaline earth metal chloride was added according to eutectic composition with LiCl (see Table1)

Table1. Eutectic compositions and eutectic melting point

Mixture	Eutectic Composition	Eutectic melting Point (°C)
LiCl	-	610
LiCl/NaCl	72:28	554
LiCl/KCl	59:41	353
LiCl/$SrCl_2$	64:36	492
LiCl/$BaCl_2$	75:25	514

79

2.2. Physicochemical characterizations

The metal cation composition of Li, Na, K, Sr, Ba, Mg, and Dy was analyzed by atomic absorption spectroscopy (AAS). The chloride concentration was analyzed by ion chromatography (IC). The specific surface area was determined by N_2 sorption at -196°C (BET method).

The X-Ray diffraction patterns (XRD) were measured with a Philips X'Pert diffractometer using Cu-K$_\alpha$. radiation. *In-situ* high temperature XRD were measured in a Parr chamber HTK 1200 under controlled gas atmosphere with temperature increment of 50 ºC.

TG-DSC measurements were performed with a modified Setaram TG-DSC thermoanalyzer. The initial amount of each catalyst used for the DSC analyses was approximately 15 mg and the temperature was linearly increased from 100 ºC to 700 ºC at a rate of 10 ºC/min.

CO_2 temperature-programmed desorption (TPD) was used to determine the basic properties. The measurement was performed in a dedicated UHV set up connected to a quadrupole mass spectrometer (Pfeiffer Vacuum QME 200). The sample was pretreated at 500 ºC for 1 h followed by adsorption of CO_2 at 100 ºC. After being outgassed for 6h at 100 ºC under 10^{-3} mbar, desorption of CO_2 was monitored by mass spectrometry during heating up to 600 ºC at a rate of 10 ºC/min.

Infrared spectra of adsorbed CO_2 were recorded on a Bruker IFS 88 FTIR spectrometer with a resolution of 4 cm^{-1}. The sample, about 15 mg, was pressed into a self-supported wafer, pretreated at 500 ºC under vacuum (~10^{-5} mbar) for 1 h, and cooled to 30 ºC to record a spectrum. The sample was equilibrated with CO_2 at 0.4 mbar and 1 mbar for 1h before recording the spectra.

2.3. Catalytic tests

The catalytic measurements were performed in a tubular fixed-bed quartz reactor. Typically, 300 mg of the catalyst together with the equal amount of SiC of the same particle size was packed in the reactor. The remaining dead volume was filled with pure SiC, and a quartz bar was inserted downstream to reduce the post-catalytic volume. Prior to each run, the sample was heated to 550 ºC for 1h in He followed by a stability test at 550 ºC for 2h. The composition of the reaction mixture was 8% C_2H_6, 8% O_2 and 84% He. The weight hourly space velocity was 0.8 h^{-1}, if not otherwise stated. To derive the relation between the ethane reaction rate and the space velocity, the space velocity varied from 0.05 to 0.8 h^{-1}.

The oxidative dehydrogenation of ethane was performed in the temperature range 450 -600 ºC. The reaction products were analyzed *on-line* by a Hewlett Packard 6890 series gas chromatograph equipped with an FID and a TCD detector. A Pora Plot Q and a Molsieve column were used for product separation. The main reaction products were C_2H_4, CO, CO_2, and water. The conversion of ethane and selectivity of ethene was calculated on a carbon basis. To determine the contribution of gas-phase reactions, a separate experiment was performed at 600 ºC by using a pure SiC filled reactor. Under this condition, the ethane conversion was less than 1%, which means the gas phase reaction is negligible.

3. Results and discussions

3.1 Chemical compositions and catalyst phases

The elemental composition of the catalysts and the specific surface areas are compiled in Table 2. The atomic ratio of Li/Na, Li/K, Li/Sr, and Li/Ba in the activated samples was identical to the ratio added in the preparation according to the eutectic composition.

Table 2. Catalyst composition and specific surface area

Catalyst	Mg (wt%)	Dy (wt%)	Cl (wt%)	Atomic ratio*				BET - SSA (m^2/g)
				Li/Na	Li/K	Li/Sr	Li/Ba	
Li-MD	46.7	7.7	5.1	-	-	-	-	12.4
Li-Na-MD	43.5	5.4	6.1	2.5(2.6)	-	-	-	9.2
Li-K-MD	42.9	6.8	6.9	-	1.5(1.5)	-	-	2.1
Li-Sr-MD	43.6	6.3	5.1	-	-	1.7(1.8)	-	10.0
Li-Ba-MD	41.8	8.7	7.2	-	-	-	2.9(3.0)	7.3

* Value in the bracket is the ratio of bulk metal chloride eutectic mixture.

As the chloride ion was added in excess and the catalyst treatment temperature, 600 ºC, was relatively low, it is assumed that alkali and alkaline earth metals are present in the catalysts as chloride salts. Therefore, we conclude that eutectic mixtures of alkali or alkaline earth metal chloride and LiCl are present in the catalysts. The specific surface area of the samples Li-Na-MD, Li-Sr-MD, and Li-Ba-MD decreased slightly compared with Li-MD, while the specific surface area of Li-K-MD decreased dramatically, (2.1 m^2/g). As Li-K-MD has a very low melting point (see DSC measurement), the pores of the sample may be blocked by the LiCl/KCl melt during calcination causing the extremely low specific surface area.

XRD was used to characterize the crystalline phases formed in the calcined catalysts. At room temperature, it is very hard to observe crystalline LiCl by X-ray diffraction, as it is strongly hygroscopic. Therefore, the diffractograms of all samples were obtained at 100 ºC under inert atmosphere. As seen in Fig.1, MgO was the dominating crystalline phase and crystalline LiCl and DyOCl were also observed in all samples. However, crystalline Dy_2O_3 was not detected. In a separate experiment, it has been observed Dy_2O_3 diffraction lines when the catalyst calcination temperatures exceeded 650 ºC. Other phases detected are summarized in Table 2. NaCl, KCl, $SrCl_2$, and $BaCl_2$ phases were observed in the samples containing the respective chlorides.

To describe phase transformations under reaction conditions, X-ray diffractograms of pre-activated catalysts were taken *in situ* between 100 ºC and 650 ºC.
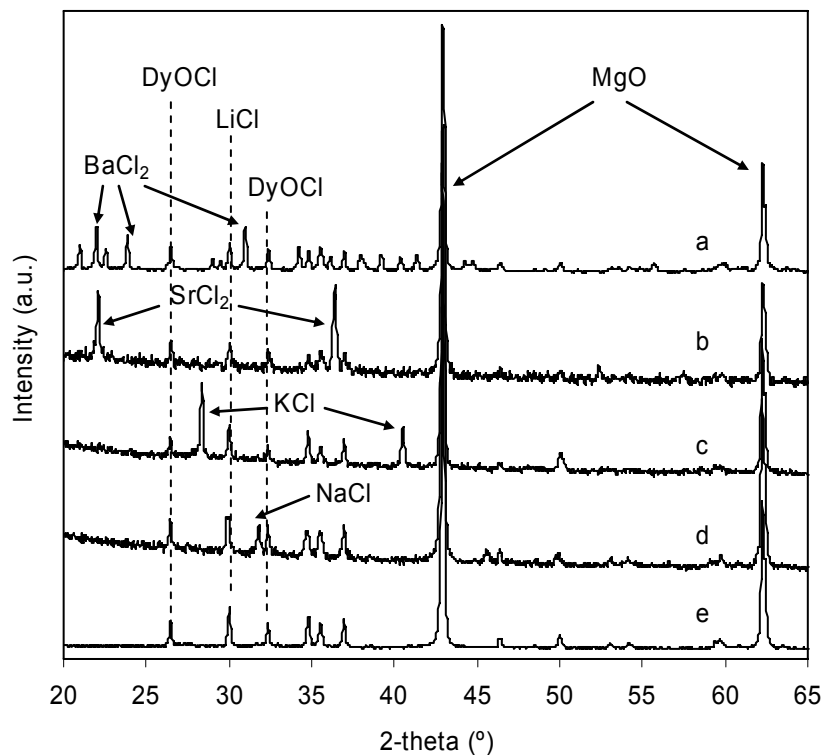
Fig.1. XRD diffractograms obtained at 100 ºC under inert atmosphere: (a) Li-Ba-MD, (b) Li-Sr-MD, (c) Li-K-MD, (d) Li-Na-MD, and (e) Li-MD.
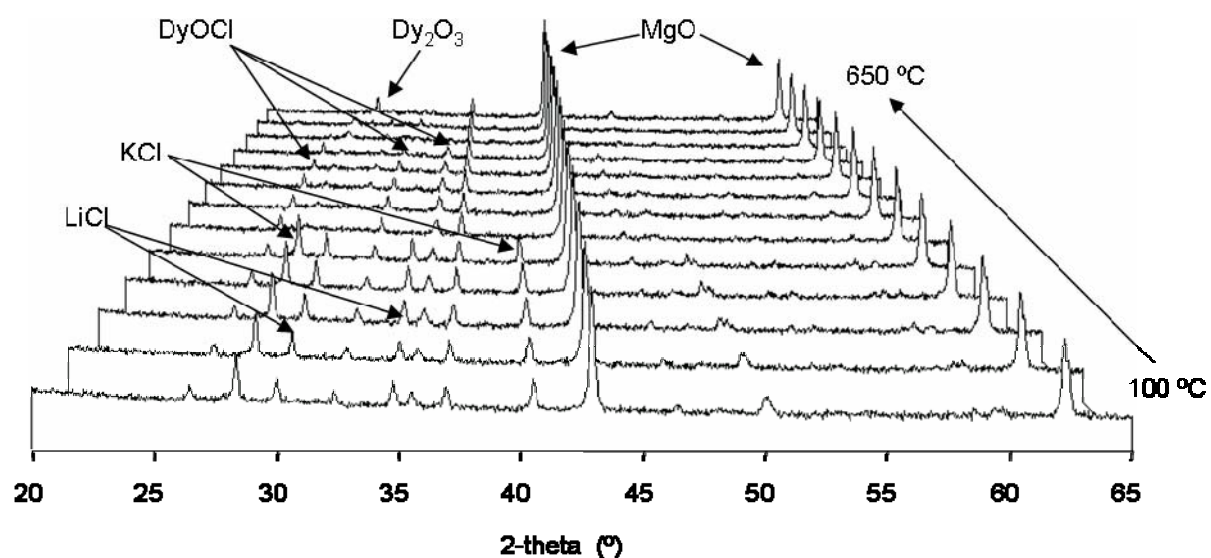

Fig.2. XRD diffractograms of Li-K-MD measured at different temperatures under inert atmosphere (temperature step: 50 ºC)

Fig.2. shows the XRD diffractograms of Li-K-MD catalyst at various temperatures, representative for all Li containing catalysts within this study. MgO was present over the

entire temperature range studied (100 °C to 650 °C). Diffraction peaks of DyOCl disappeared at 600 °C due to decomposition of DyOCl. It is interesting to note that for all Li containing catalysts the XRD reflexes of the alkali and alkaline earth metal chlorides were shifted to higher d-values with increasing temperature. The diffraction peaks of the alkali and alkaline metal chlorides vanished within various temperature ranges (see Table 3 and Fig.2). The diffraction peaks of LiCl and KCl disappeared at approximately 350 °C, a temperature much lower than the melting point either of LiCl (m.p. 610 °C) or KCl (m.p. 771 °C). Obviously, a eutectic mixture of LiCl/KCl was formed.

To investigate the phase transformation in more detail, TG-DSC was used to measure the melting point of the alkali or alkaline earth chloride mixtures with LiCl on the support surface. Fig. 3 shows the DSC signals for all catalysts within the temperature range of 300 °C to 650 °C.
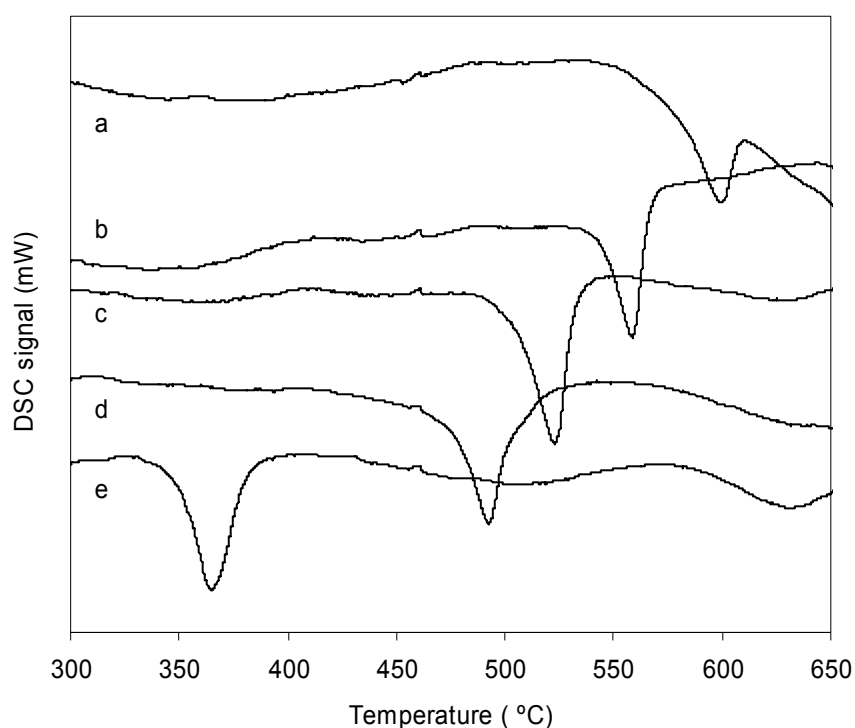

Fig.3. TG-DSC analysis of calcined samples: (a) Li-MD, (b) Li-Na-MD, (c) Li-Ba-MD, (d) Li-Sr-MD, and (e) Li-K-MD.

For pure Li-MD, the observed endothermic signal started to increase at around 550 ºC and reached its maximum at 604 ºC (minimum in the heat flux), indicating that LiCl is transformed to liquid state. The temperature at the highest endothermic signal corresponded to the melting point of LiCl. This value was close to the melting point of pure LiCl (610 ºC). For all other samples, only one phase transformation was observed and the corresponding melting point was much lower than that of LiCl. This is attributed to the formation of eutectic mixtures of alkali chloride or alkaline earth chloride with LiCl. The melting points of the samples together with the thermodynamic value at eutectic composition are shown in Table 3.

Table 3. Main crystalline XRD phases at 100 ºC, melting point (m. p.) estimated by *in-situ* HT-XRD, and m. p. determined by DSC

Catalyst	Phases detected by XRD at 100 ºC	m. p. (HT-XRD) (ºC)	m. p. (DSC) (ºC)	m. p. (thermo.)* (ºC)
Li-MD	MgO, DyOCl, LiCl	550-650	604	610
Li-Na-MD	MgO, DyOCl, LiCl, NaCl	500-600	560	554
Li-K-MD	MgO, DyOCl, LiCl, KCl	350-400	366	353
Li-Sr-MD	MgO, DyOCl, LiCl, $SrCl_2$	450-500	494	492
Li-Ba-MD	MgO, DyOCl, LiCl, $BaCl_2$	500-550	524	514

* Thermodynamic eutectic melting point of the bulk binary mixtures of alkali or alkaline metal chloride with LiCl.

It can be seen that the phase transformation temperatures perfectly coincide with the melting point of the pure bulk metal chloride mixtures. From these experiments, we conclude that the addition of alkali or alkaline earth metal chloride lowers the melting point of the catalyst with respect to $LiCl/Dy_2O_3/MgO$.

3.2 Catalyst acid-base properties

Temperature-programmed desorption of adsorbed CO_2

CO_2 is a suitable probe molecule to determine the basicity of solid catalysts [13, 23]. CO_2 physisorbs and chemisorbs on the surface of a basic solid catalyst. To eliminate the influence of physisorption, all samples were evacuated after adsorption of CO_2 at 100 ºC for 6h. After

this treatment desorption peak detected by the TPD was assigned to the chemisorbed CO_2.

From the TPD profiles in Fig.4, only one broad desorption peak was detected for all samples.
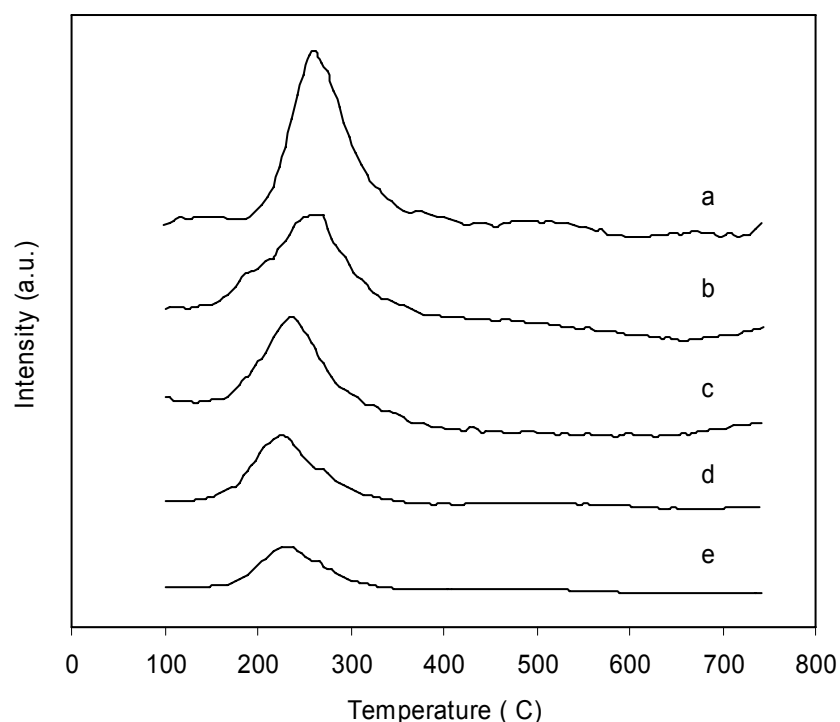
Fig.4. TPD of adsorbed CO_2: (a) Li-K-MD, (b) Li-Sr-MD, (c) Li-Ba-MD, (d) Li-Na-MD, and (e) Li-MD

On the higher temperature side, however, a broadening of the TPD peak was observed.

This indicated that different adsorption species were present and contributed to the adsorption

of CO_2. As shown in Table 4, the total amount CO_2 desorbed was relatively small.

Table 4. Strength and concentration of basic sites derived from TPD of CO_2 and the relative concentration of base sites derived from IR spectra of adsorbed CO_2.

Catalyst	TPD		IR spectroscopy	
	Temp of peak max (°C)	CO_2 adsorbed (mmol/g)	Rel. intensity at CO_2 pressure*	
			1 mbar	0.4 mbar
Li-MD	234	0.16	81	74
Li-Na-MD	234	0.18	95	82
Li-Ba-MD	244	0.22	102	88
Li-Sr-MD	257	0.22	116	95
Li-K-MD	262	0.23	120	108

* Integrated intensities of the bands in the range 1800-1200 cm^{-1}.

The presence of chloride ion in the sample prevents the adsorption of large amounts of CO_2. It was also found that the amount of CO_2 desorbed increased in the order: Li-MD<Li-Na-MD< Li-Ba-MD≈Li-Sr-MD<Li-K-MD. In addition, the temperatures of the desorption maximum were higher for Li-K-MD, Li-Ba-MD, and Li-Sr-MD than for Li-MD and Li-Na-MD. This indicates that first three samples have a higher base strength than the latter two.

Infrared spectra of adsorbed CO_2

The IR spectrum of adsorbed CO_2 is used to characterize Lewis acid and base sites on metal oxides and zeolites. Three types of bands have been observed varying with the nature of the interaction of CO_2 with the catalyst surface [24-27]. These bands include the asymmetric stretching of adsorbed CO_2 (v_3) and the carbonate vibrations between 1800 cm^{-1} and 1200 cm^{-1}.
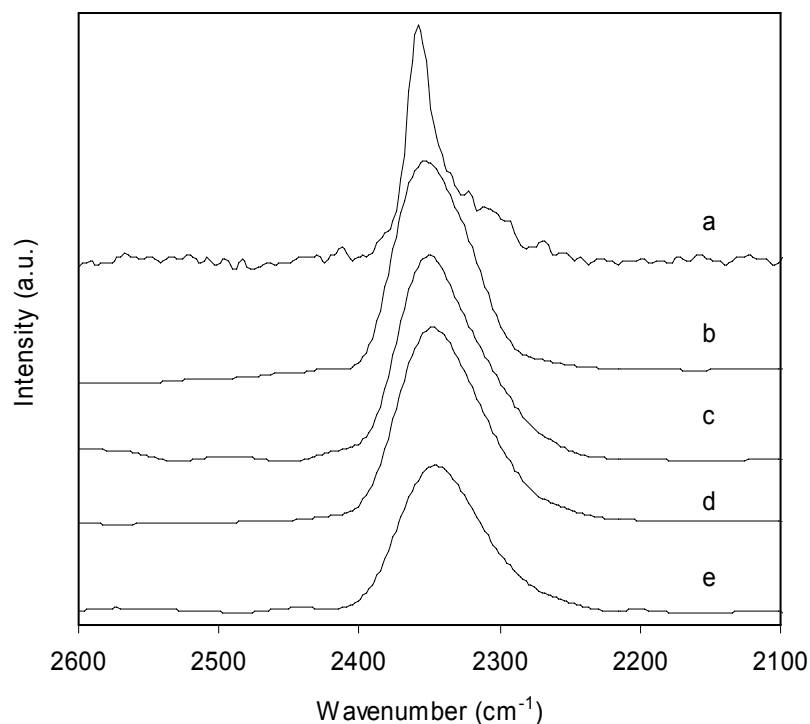
Fig. 5. IR spectra of adsorbed CO_2 (0.4mm equilibrium pressure of CO_2) in the asymmetric stretching region: (a) Li-MD, (b) Li-Na-MD, (c) Li-Ba-MD, (d) Li-Sr-MD, and (e) Li-K-MD.

The IR spectra of adsorbed CO_2 on alkali or alkaline earth metal chloride modified $LiCl/Dy_2O_3/MgO$ catalysts are shown in Fig. 5. The asymmetric vibrations due to molecularly adsorbed CO_2 on Li-MD, Li-Na-MD, Li-Ba-MD, Li-Sr-MD, and Li-K-MD appeared at 2358,

2352, 2350, 2347, and 2344 cm^{-1}, respectively. The v_3 vibration shifts to lower wavenumbers as the ionic radius of the alkali and alkaline earth metal cation increases. This shift is related to the electron pair acceptor strength of the metal cations towards adsorbed CO_2. It implies that the acid strength of the accessible cations decreases in the order Li-MD > Li-Na-MD > Li-Ba-MD > Li-Sr-MD > Li-K-MD. The sequence inversely tracks the increase in interaction with CO_2 observed by TPD of CO_2. It is interesting to note that the sequence of acid strength does not follow exactly the trend expected from an average of the electronegativity of the cations. This is related to the varying concentrations of cations needed to achieve the eutectic mixture and suggests that the individual nature of the cation is not overly influenced be averaging effects in the catalytic material.

The structure of the chemisorbed CO_2 species was investigated by IR spectroscopy of pre-adsorbed CO_2. Fig. 6 shows the IR spectra of the modified and unmodified $LiCL/Dy_2O_3/MgO$ samples after CO_2 adsorption and subsequent evacuation at 30, 200, and 400 ºC. The unmodified sample, Li-MD, exhibits two vibration bands, centering at 1340 and 1620 cm^{-1}, respectively. The former can be assigned to the symmetric O-C-O stretching and the latter asymmetric O-C-O stretching vibration. Both are typical vibration modes of bidentate carbonate species formed on Lewis-acid-Brösted-base pairs (Mg^{2+}-O^{2-} pare site, where Mn+ is the metal cation Mg^{2+} or alkali or alkaline metal cation) [28]. Obviously, bidentate carbonate species dominate on Li-MD. As the temperatures increase, the intensities of these bonds decrease suggesting that the bidentate carbonate species are not stable and therefore the basic sites on Li-MD are not strong. For the modified samples, the IR spectra are more complex. In addition to the bidentate carbonate species, unidentate carbonate species are also detected. Especially for Li-K-MD, Li-Sr-MD, and Li-Ba-MD, vibration bands at 1380-1400 cm^{-1}, assigned to symmetric O-C-O stretching and vibration bands at 1500-1530 cm^{-1}, assigned to asymmetric O-C-O stretching, appear in their spectra. These bands can be ascribed to the unidentate carbonate species which form on isolated surface O^{2-} ions [28].

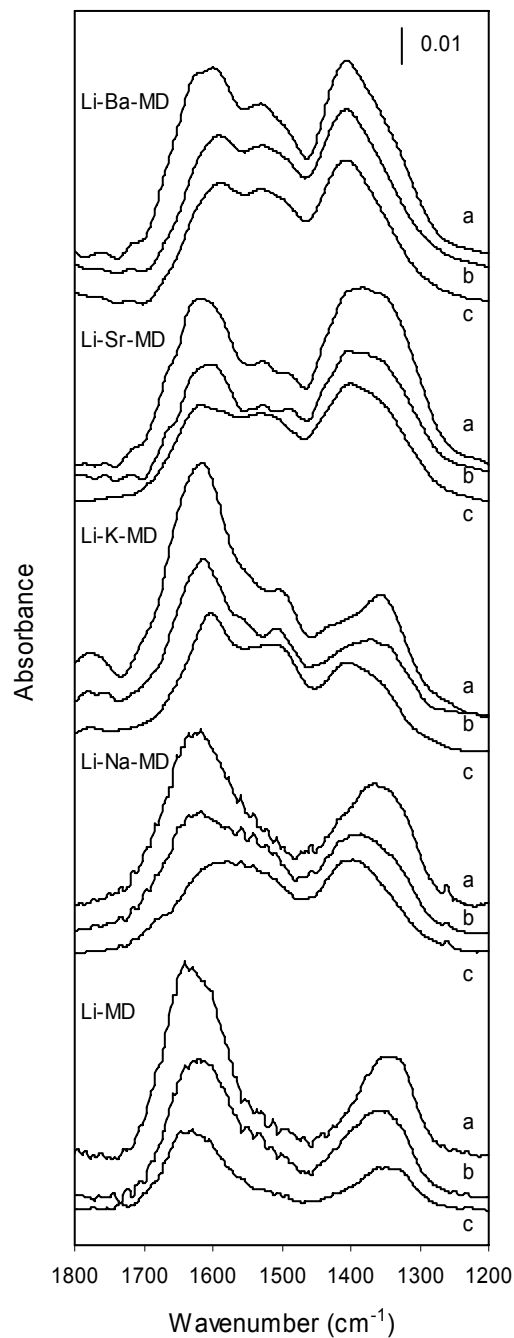Fig.6. IR spectra of adsorbed CO_2 on Li-M-MD catalysts and desorbed under vacuum at different temperatures: (a) 30 ℃, (b) 200 ℃, and (c) 400 ℃

At higher temperatures, the CO_2 bands shift to the unidentate carbonate position, suggesting that the unidentate carbonate species are more stable than the bidentate carbonate species. Therefore, stronger basic sites exist on the surface of these modified samples.

The relative intensity of carbonate bands decreased with decreasing equilibrium pressure, but the bands persisted even after evacuation to 10^{-5} mbar (see Table 4). The integrated value of the intensities of the bands in the range 1800-1200 cm^{-1} on the different samples increased in the order: Li-MD < Li-Na-MD < Li-Ba-MD < Li-Sr-MD < Li-K-MD. This indicates that the base site density increases assuming that the molar extinction coefficient does not vary between these samples.

3.3 Catalytic activity for ODH of ethane

Ethene, CO, CO_2, and H_2O were the main reaction products during the oxidative dehydrogenation of ethane. The ethane conversion and the ethene yield are presented in Fig.7 and Fig.8 as a function of the reaction temperature.
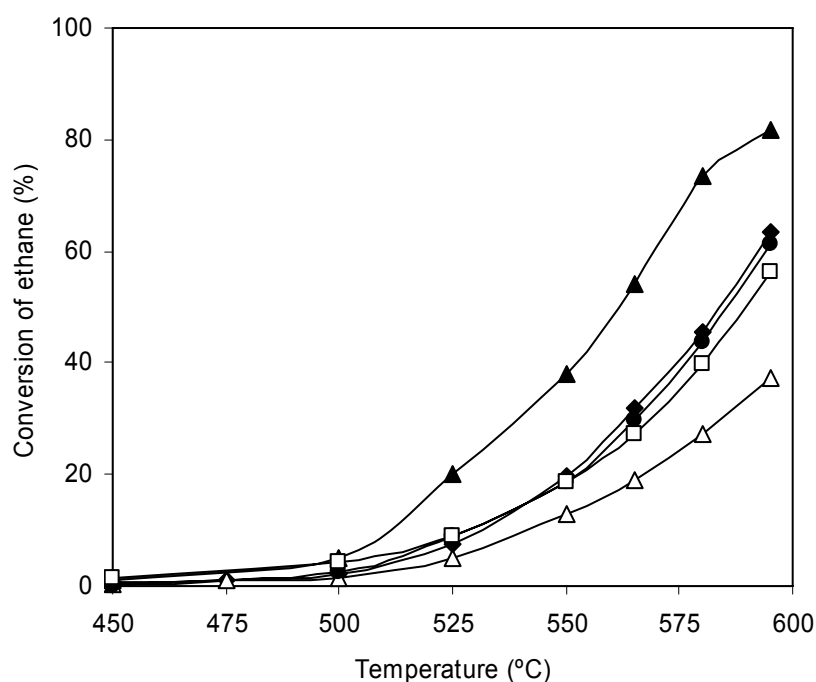

Fig.7. Conversion of ethane at different temperatures over: (▲) Li-MD, (♦) Li-Na-MD, (Δ) Li-K-MD, (●) Li-Sr-MD, and (□) Li-Ba-MD

At the same temperature, the highest activity was found for Li-MD, the lowest for Li-K-MD, and the activities of other samples were in between. For example at 580 °C, the ethane conversion was 73% over Li-MD, 46% over Li-Na-MD, 27% over Li-K-MD, 44% over Li-

Sr-MD, and 40% over Li-Ba-MD. The corresponding selectivity to ethene was 80% (Li-MD),

86% (Li-Na-MD), 96% (Li-K-MD), 91% (Li-Sr-MD), and 88% (Li-Ba-MD).

Fig.8. Yield of ethene at different temperatures over: (▲) Li-MD, (♦) Li-Na-MD, (∆) Li-K-MD, (●)Li-Sr-MD, and (□)Li-Ba-MD

This indicates that addition of the metal chlorides caused a decrease in catalytic

activity and an increase in selectivity. The effect of temperature on the selectivity of ethene is

shown in Fig 9. Li-K-MD presented the highest selectivity and its selectivity retained at

around 96% in the temperature range from 450 ºC to 595 ºC. For other catalysts, the ethene

selectivity increased with temperature and then became constant, when the temperature

approached certain value. A further increase of the temperature did not change the product

distribution. It is important to note that the temperature, at which the high and constant

selectivity was obtained, coincides with the temperatures at which spreading/melting of the

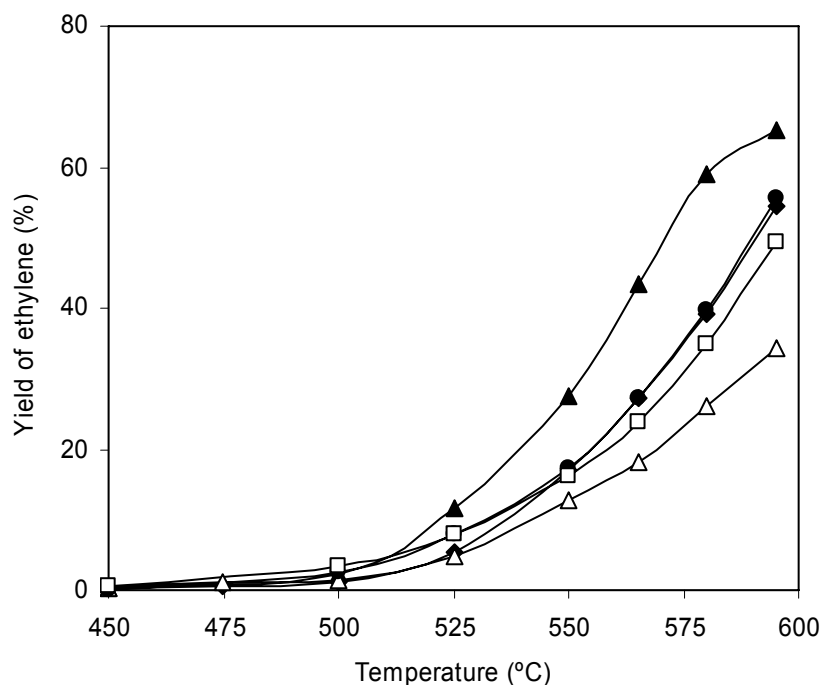alkali and alkaline earth metal chloride phases was experimentally observed.
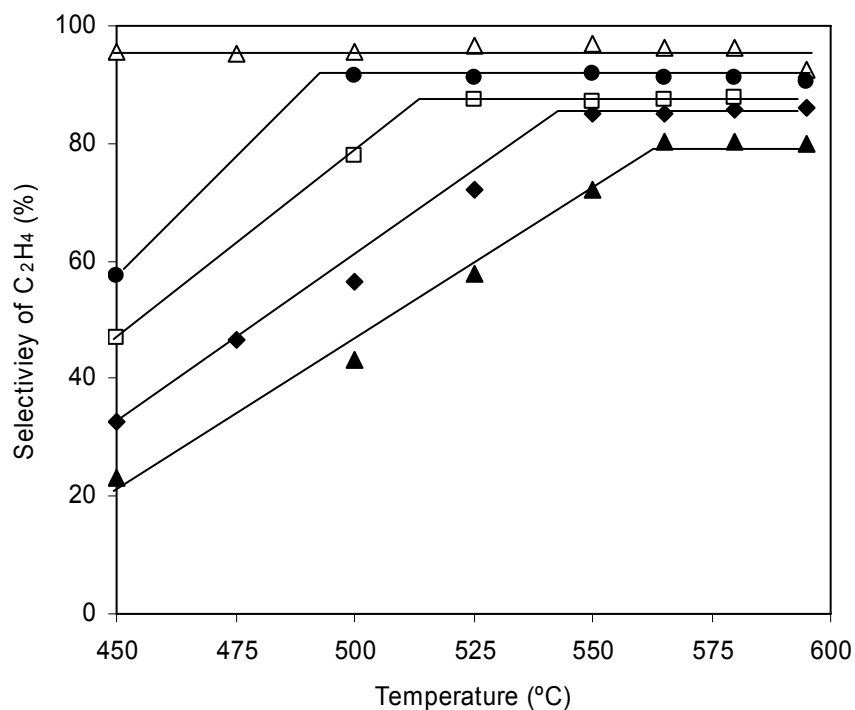
Fig.9. Selectivity of ethene at different temperatures over: (▲) Li-MD, (♦) Li-Na-MD, (Δ) Li-K-MD, (●) Li-Sr-MD, and (□) Li-Ba-MD.

It is also remarkable that the lower melting points induce higher ethene selectivity. By adding alkali or alkaline earth metal chloride, the constant ethene selectivity increased from 80% for Li-MD to 96% for Li-K-MD. The possible reasons for the effect of melting point on the ethene selectivity is speculated to be related to the easier desorption of ethyl radicals formed on the catalyst surface and weaker adsorption of ethene in molten state.

The ethane reaction rate as a function of weight hourly space velocity at 550 ºC is shown in Fig.10. The results show clearly that the catalysts were operated under strong diffusion limitations for the most of the space velocities tested. At the highest SV, the rates were approximately constant, so that one can assume the absence of external limitations. Internal limitations were checked according to the Weisz-Prater criterion. The Weisz-Prater number was found to be much lower than 1.5. Thus, the internal diffusion limitations are considered to be negligible.
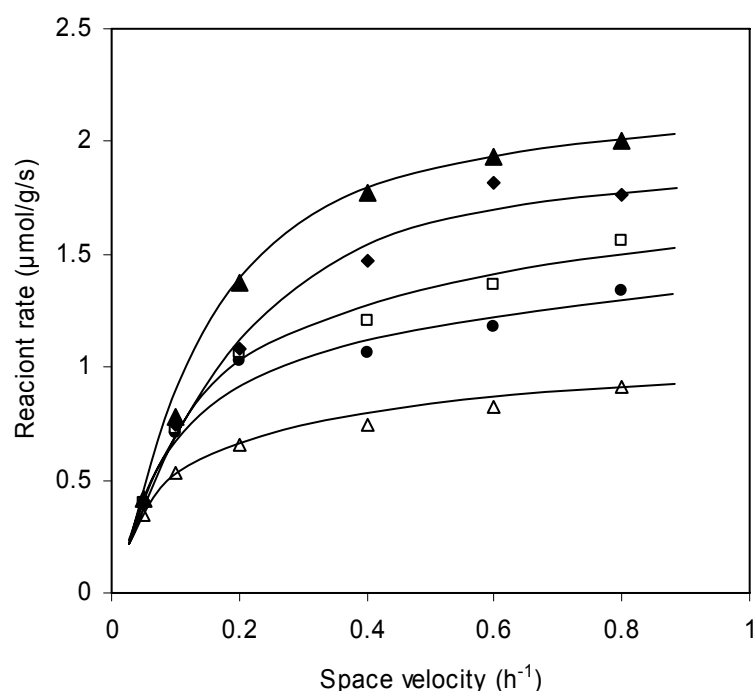
Fig. 10. Ethane reaction rate as a function of weight hourly space velocity at 550 °C: (▲) Li-MD, (♦) Li-Na-MD, (□) Li-Ba-MD, (●) Li-Sr-MD, and (e) Li-K-MD.

In the absence of diffusion limitations, the ethane reaction rate decreased in the order: Li-MD > Li-Na-MD > Li-Ba-MD > Li-Sr-MD > Li-K-MD. The catalytic activity was, thus, directly correlated with the strength of the accessible Lewis acid sites and inversely correlated with the basicity as determined by TPD of adsorbed CO_2. In this context, it is interesting to note reported that Wang et al. [17], in contrast reported that a highly basic catalyst intrinsically is more effective in activating an alkane, but is more easily poisoned by CO_2 formed as byproduct in the oxidative dehydrogenation.

4. Discussion

It has been concluded that the unusually high selectivity for oxidative dehydrogenation of ethane over LiCl based catalysts is related to the molten state of LiCl in the active catalyst [19]. Thus, it is a logical step to explore other low melting eutectic mixtures with respect to these properties and to relate the acid/base properties of these materials to the activity and selectivity for oxidative dehydrogenation of ethane. In order to prepare practical catalysts, the

molten salts have to be supported on a relatively inert support, forming a thin layer on its surface. In this contribution, we report the preparation, characterization and catalytic properties of such supported binary eutectic mixtures of LiCl with alkali and alkaline earth metal chlorides.

Let us establish first that the eutectic mixture exists on the catalyst and that it is molten under reaction conditions. Indirect evidence for the existence of the molten eutectic mixture comes from the elemental analysis. The atomic ratio of Li/Na, Li/K, Li/Sr, and Li/Ba (see Table 2) agrees well with that of the composition suggested by the thermodynamic composition of the eutectic mixture. More direct evidence is provided by *in-situ* high temperature XRD. In the XRD diffractograms, the XRD peaks of the alkali or alkaline metal chlorides shifted to higher *d*-values with increasing temperature (Fig. 2) and disappeared finally at a certain temperature (Table 3, Fig3). This indicates an expansion of the corresponding alkali or alkaline metal chloride lattice as well as spreading and/or melting of the metal chloride crystallites at the catalyst surface at a defined temperature. Most important is that the theoretical melting points of pure bulk LiCl, LiCl/NaCl, LiCl/KCl, LiCl/SrCl$_2$, and LiCl/BaCl$_2$ are within the estimated melting temperature regions, determined by the disappearance of XRD diffraction peaks (Table 3). Thus, it is concluded that the disappearing peaks are affiliated with the melting of the solid metal chloride phases. Calorimetry provides the most direct conclusive evidence (see Fig.3), as the onset temperature and melting point can be clearly observed. The melting points of all samples determined by calorimetry coincide perfectly with those reported in the literature [29]. Taking all three pieces of evidence together, it is safe to conclude that indeed the supported eutectic melt has been formed on the MgO surface.

The effect of supported eutectic melt on catalytic activity was studied for the ODH of ethane. The catalytic experiments (Fig. 7 and Fig. 8) indicate that the addition of alkali or alkaline earth metal cations decreased the catalytic activity, but increased the selectivity. To

explore the reasons, the acid-base properties of these materials were determined by TPD and by IR spectra of adsorbed CO_2. The TPD of CO_2 (Fig.4) indicates that the addition of alkali and alkali earth metal cations leads to stronger adsorption of CO_2. The IR spectra of linearly adsorbed CO_2 shows, however, that the addition of alkali and alkali earth metal cations decreases the strength of the accessible Lewis acid sites. Thus, both experiments (see Table 4) complementary suggest that the acid strength of the accessible Lewis acid sites increases, while the base strength of samples decreases in the order Li-K-MD < Li-Sr-MD < Li-Ba-MD < Li-Na-MD < Li-MD. So, the introduction of metal cations with low electronegativity such as Na^+, K^+, Sr^{2+}, and Ba^{2+} leads to a more basic surface, while the acid strength of the action decreases. Both experiments also suggest that the original MgO surface covered to a significant fraction with the melt, but that oxide fractions are either still available or that parts of the chloride is converted back to surface carbonates. It is worth noting that with increasing size of the cation CO_2 tends to form more unidentate carbonates (see Fig. 6). As this seems to be more stable strong adsorption CO_2 may lead to blocking some active sites lowering so catalytic activity.

Thus, while we note that the stronger Lewis acid cations lead to higher catalytic activity, we cannot rule out that the poisoning of CO_2 is the cause of lower activity of the more basic catalyst, i.e., those with a lower eutectic melting temperature. Lunsford *et al.*[16,17], who had used Cl^- as a modifier reached such a conclusion when studying the influence of the surface acid/base properties of Li^+-MgO-Cl^- in the ODH of ethane. Contrary to the effect on catalytic activity, addition of alkali or alkaline metal chloride has a remarkable positive effect on the catalyst selectivity. As shown in Fig. 9, the ethene selectivity increased with the increasing temperature, when the reaction temperatures were below melting point. Once the reaction temperature approached or exceeded the chloride melting point, constant selectivity was obtained and maintained up to 595 ºC. Remarkably,

the level of this constant ethene selectivity is directly correlated with the melting point of the catalyst (Fig.11).
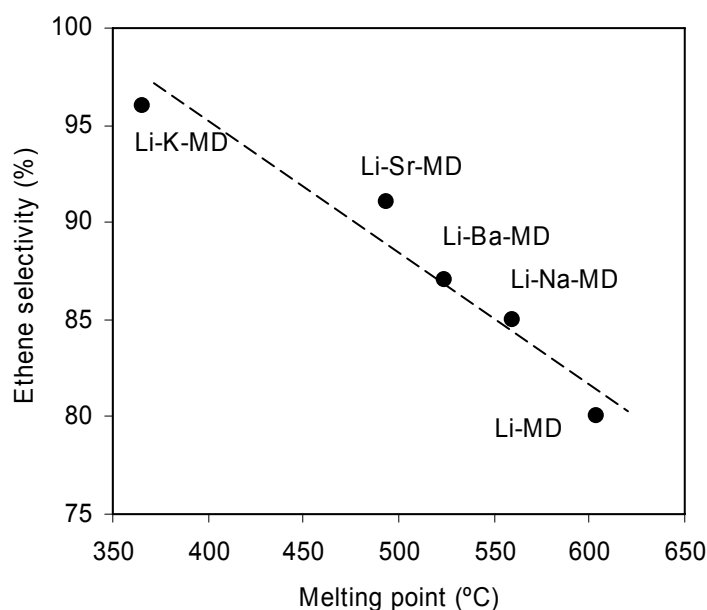
Fig.11. Correlation between the melting point of the eutectic melt and the maximum ethene selectivity

Catalysts with a lower melting point have a higher selectivity. Swaan *et al.* [20] reported that a Li/Na/MgO catalyst showed a selectivity of 86% to ethene at 38% conversion for the ODH of ethane while the Li/MgO catalyst showed a selectivity of 80% at the similar conversions. The authors speculated that the increased selectivity over Li/Na/MgO catalyst is related to a molten layer of $LiNaCO_3$ forming a eutectic with a melting temperature of 490 ºC. Thus, it seems that the liquid state under reaction conditions has a beneficial effect on the catalyst selectivity whatever the active phase may be. Tentatively, we attribute the higher selectivity of the molten catalysts to weaker adsorption of ethene on the mobile surface, which in turn suppresses further oxidation of the formed olefins. In essence, the mobility of exposed cations will reduce the strength of bonding to the double bond of the olefin. The diffusion of the alkali metal cations from the surface into the bulk is suggested to lead to the weakening in the π-C_2H_4-Me^+ interaction, as ethene has a very low solubility in the polar melt. It should be

noted that for the supported salts studied the lower the melting point the weaker the π-C_2H_4-Me^+ interaction.

5. Conclusion

Addition of alkali or alkaline earth metal chloride to the $LiCl/Dy_2O_3/MgO$ catalyst markedly affects the melting point as well as the acid and base strength. Direct and indirect physicochemical characterizations suggest that a eutectic melt is formed with all combinations. In practice, alkali or alkaline earth metal chloride addition to supported LiCl leads to a much lower melting point compared to pure supported LiCl.

In parallel TPD of adsorbed CO_2 showed that these additions lead to samples with moderate to weak base strength, its strength decreasing in the order Li-K-MD > Li-Sr-MD > Li-Ba-MD > Li-Na-MD > Li-MD. IR spectra of molecularly adsorbed CO_2 show that that the Lewis acid strength increased in that order. Chemisorbed CO_2 was found to be stabilized as unidentate and bidentate carbonate species on the modified catalysts.

The catalysts containing additional alkali and alkali earth metal chlorides showed lower activity for ODH of ethane than the parent Li-MD. However, they had very high ethene selectivity reaching a constant and high level once the reaction temperatures exceed the melting point. The selectivity in this state is the higher the lower the melting point and the higher the base strength is reaching up to 96% ethene selectivity was obtained with Li-K-MD. Tentatively, this is related to the easier desorption of the olefins. In parallel, however, the activity of the catalysts decreased, which is speculated to be related to the larger and weaker acidic accessible cations in the modified catalysts or the stronger poisoning by more stable carbonates.

References

[1]   M. M. Bhasin, J. H. McCain, B. V. Vora, T. Imai, P. R. Pujado, Appl. Catal. A: Gen., 221 (2001) 397.

[2]   M. A. Banares, Catal. Today, 51 (1999) 319.

[3]   F. Cavani, F. Trifiro, Catal. Today, 24 (1995) 307.

[4]   P. Botella, A. Dejoz, J. M. L. Nieto, P. Concepcion, M. I. Vazquez, Appl. Catal. A: Gen, 298 (2006) 16.

[5]   P. Botella, E. Garcia-Gonzalez, A. Dejoz, J. M. L. Nieto, M. I. Vazquez, J. Gonzalez-Calbet, J. Catal., 225 (2004) 428.

[6]   J. M. L. Nieto, P. Botella, M. I. Vazquez, A. Dejoz, Chem. Commun. (2002) 1906.

[7]   D. Siegel, J. Biophys., 45 (1986) 399.

[8]   E. M. Thorsteinson, T. P. Wilson, F. G. Young, P. H. Kasai, J. Catal., 52 (1978) 116.

[9]   W. Ueda, N. F. Chen, K. Oshihara, Chem. Commun. (1999) 517.

[10]   E. Heracleous, A. A. Lemonidou, J. Catal., 237 (2006) 162.

[11]   E. Heracleous, A. F. Lee, K. Wilson, A. A. Lemonidou, J. Catal., 231 (2005) 159.

[12]   E. Morales, J. H. Lunsford, J. Catal., 118 (1989) 255.

[13]   J. A. Roos, S. J. Korf, R. H. J. Veehof, J. G. van Ommen, J. R. H. Ross, Catal. Today, 4 (1989) 441.

[14]   J. B. M. S. S. Hong, Catal. Lett., 40 (1996) 1.

[15]   S. Sugiyama, N. Kondo, K. Satomi, H. Hayashi, J. B. Moffat, J. Mol. Catal. A: Chem., 95 (1995) 35.

[16]   S. J. Conway, J. H. Lunsford, J. Catal., 131 (1991) 513.

[17]   D. J. Wang, M. P. Rosynek, J. H. Lunsford, J. Catal., 151 (1995) 155.

[18]   S. J. Conway, D. J. Wang, J. H. Lunsford, Appl. Catal., 79 (1991) L1.

[19]   S. Gaab, M. Machli, J. Find, R. K. Grasselli, J. A. Lercher, Top. Catal., 23 (2003) 151.

[20]   H. M. Swaan, A. Toebes, K. Seshan, J. G. van Ommen, J. R. H. Ross, Catal. Today, 13 (1992) 629.

[21]   S. B. Wang, K. Murata, T. Hayakawa, S. Hamakawa, K. Suzuki, Catal. Lett., 62 (1999) 191.

[22]   S. B. Wang, K. Murata, T. Hayakawa, S. Hamakawa, K. Suzuki, Chem. Commun. (1999) 103.

[23]   J. A. Lercher, C. Gründling, G. Eder-Mirth, Catal. Today, 27 (1996) 353.

[24]   R. Bal, B. B. Tope, T. K. Das, S. G. Hegde, S. Sivasanker, J. Catal., 204 (2001) 358.

[25]   F. Solymosi, H. Knozinger, J. Catal., 122 (1990) 166.

[26]   S. B. Waghmode, R. Vetrivel, S. G. Hegde, C. S. Gopinath, S. Sivasanker, J. Phys. Chem. B, 107 (2003) 8517.

[27]   J. A. Lercher, C. Colombier, H. Noller, Z. Phys. Chemie NF, 131 (1982) 111.

[28]   V. K. Díez, C. R. Apesteguia, J. I. Di Cosimo, J. Catal., 240 (2006) 235.

[29]   Gmelins Handbuch der anorganischen Chemie, 8 (1970).

Chapter 5

Summary

Summary

This thesis addresses two reaction part A) Oxy chlorination of methane (OCM) and part B) Ethane oxidative dehydrogenation (ODH).

A) Methane is the major component of the natural gas which can be used efficiently as a fuel or chemical stock. Oxidative halogenation of methane or methane oxychlorination (MOC) to methyl halide is an attractive technique for transformation of methane into methyl halide which can be further processed into valuable chemicals.

Recently it was found that catalysts based exclusively on LaOCl, which is converted to $LaCl_3$ in the presence of HCl under reaction conditions, were active, selective, and importantly stable for oxidation chlorination. However the effect of chlorination on the different phases present in LaOCl, the role played by different kinds of basic sites and their optimal concentration and strength have not been studied in detail. Therefore the aim of this work is to characterize the LaOCl catalyst extensively during activation, chlorination and under catalytic reaction conditions and also try to correlate the catalyst phase composition with the catalytic performance.

The catalysts precursor studied are commercial LaOCl catalysts provided by Dow Chemical Company, USA. The phase purity of the LaOCl sample are checked with XRD. XRD analysis reveals that sample GRII is the most impure one among all samples with high amount of lanthanum dioxycarbonate present. This is also evident from EDX analysis having the highest La/Cl ratio 2.82. IR spectroscopy technique is used to identify the different types of hydroxyl species present on the surface of the sample. Two types of hydroxyl groups are present on SC samples which can be assigned to LaO(OH) and La(OH) type species. Additional hydroxyl group due to $La(OH)_3$ type species are present on GRII sample. The nature and concentration of different acid sites were determined by using TPD of DMP (2,6-dimethylpyridine) and ammonia. TPD of adsorbed ammonia and DMP showed that only one type of weak acid sites presented on all sample surfaces and strength of Lewis acid sites

decreased in the following order GRII>SCI>SCIIIB >SCII. Basic sites were identified by using CO_2 as probe molecule. Three desorption peaks were detected in CO_2 TPD measurement, indicating the existence of three different basic sites. The concentration of total basic sites was exactly opposite to the sample's acid sites. IR spectra indicated that different types of carbonate species were formed after adsorption of CO_2. From IR and TPD results, it was concluded that monodentate and bidentate carbonates were the main species and the minor species was the hydrogen carbonate.

Finally, the four commercial LaOCl samples were tested for the methane oxychlorination. For methane oxychlorination reaction methyl chloride is the primary product followed by methylene chloride, CO, and CO_2 as secondary products and trace amount of $CHCl_3$ and CCl_4 as minor by-products. It was found that the SCII sample was the most active catalyst for MOC reaction followed by SCIIIB and SCI. A direct dependence of activity on basicity (conc. of O^{2-} sites) is observed for all samples. Hence it is postulated that the more active SCII sample takes a higher amount of HCl during chlorination, which leads to a substitution of the O^{2-} basic sites by Cl^-. The substituted Cl^- added to the surface is suggested to be labile and is therefore responsible for a higher activity for methane oxychlorination. It is believed that activity depends upon the number of chlorine terminated lattice sites on the surface and a mechanism with OCl* as the active species has been suggested.

The catalyst is pretreated with HCl before reaction. It is interesting to study the phase transformation from LaOCl to $LaCl_3$ and to find correlation between the catalyst phase composition with the catalytic performance. Different analytical techniques including IR spectroscopy, temperature programmed chlorination, $^1H/^{35}Cl$-MAS-NMR spectroscopy, X-ray diffraction were used to characterize the commercial samples. XRD and IR study revealed that the catalysts undergo major transformation to $LaCl_3$ during the chlorination. It was found that the surface functional groups and the catalytic activity is influenced by differences in the chlorination degree of the final $LaCl_3$ catalysts and hence by the concentration of LaOCl in

the final material. It was found that the activity of the starting material for the methane oxychlorination reaction decrease in the order SCII > SCIIIB > SCI. The activity strongly correlates with the stability of carbonate, hence less stable carbonate easily transform into lanthanum chloride. Hence the activity depends on a sample that easily converts to the $LaCl_3$ phase.

B) ODH is an attractive technique for the production of olefins. It is an alternative method to the dehydrogenation reaction and provides great advantages over non-oxidative process based on engineering and economic consideration

To explore the possibility of tailoring a catalyst that is highly selective at lower temperature. A series of catalyst were prepared by adding alkali or alkaline earth metal chloride to the $LiCl/Dy_2O_3/MgO$ catalyst. The prepared catalysts were thoroughly characterized by using various techniques.

The specific areas of the prepared sample were measured by BET. It is observed that the specific surface area of the Li-Na-MD, Li-Sr-MD, Li-Ba-MD decreased slightly compared with Li-MD, while the specific surface area of Li-K-MD decreased dramatically. The pores of the sample may be blocked by the LiCl/KCl melt during calcinations causing the extremely low surface area since Li-K-MD has a very low melting point.

XRD was used to characterize the crystalline phases formed in the calcined catalysts. It reveals that MgO was the dominating crystalline phase and the crystalline phase LiCl and DyOCl were also observed in all samples. Other phases NaCl, KCl, $SrCl_2$, and $BaCl_2$ phases were observed in the samples containing the respective chloride.

To study phase transformation under reaction condition *in situ* X-ray diffraction of pre-activated catalysts were recorded between 100°C and 650°C. As the temperature increases it is found that the diffraction peaks of the alkali and alkaline earth metal chloride vanish within various temperature range. Most important is that the theoretical melting points of pure bulk LiCl, LiCl/NaCl, LiCl/KCl, $LiCl/SrCl_2$ and $LiCl/BaCl_2$ are within those temperature

ranges. Therefore, it is concluded that the disappearing reflexes are affiliated with the melting of the solid metal chloride phases.

TG-DSC techniques are used to investigate phase transformation in more detail. For pure Li-MD, the observed endothermic signal started to increase around 550°C and reached its maximum at 604°C, this indicates that LiCl is transformed to liquid state. The temperature at the highest endothermic signal corresponded to the melting of LiCl. This value agrees well to the melting point of pure LiCl (610°C). For all other samples, only one phase transformation was observed and the corresponding melting point was much lower than that of LiCl. This is attributed to the formation of eutectic mixtures of alkali chloride or alkaline earth chloride with LiCl. It was observed that phase transformation temperature perfectly coincides with the melting point of the pure bulk metal chloride mixture. From theses experiment it is concluded that addition of alkali and alkaline earth metal chloride lowers the melting point of the catalysts with respect to $LiCl/Dy_2O_3/MgO$.

The concentration of basic sites was quantified by using Temperature-Programmed Desorption of adsorbed CO_2. Only one broad peak was detected for all samples. This peak is assigned to desorption chemisorbed CO_2. It was observed that addition of alkali and alkaline earth metal chloride increases the basicity of the sample. Li-K-MD, Li-Ba-MD, Li-Sr-MD samples have a higher basic strength. The concentration of Lewis acid and basic sites were determined by IR spectroscopy of adsorbed CO_2. The asymmetric vibration due to molecularly adsorbed CO_2 appeared on alkali and alkaline earth metal chloride modified catalysts around 2300 cm^{-1}. The v_3 vibration shifts to lower wave numbers as the ionic radius of the alkali and alkaline earth metal cations towards adsorbed CO_2. This shift is related to the electron pair accepter strength of the metal cations towards adsorbed CO_2. It implies that the acid strength of the accessible cations decreases in the order Li-MD > Li-Na-MD > Li-Ba-MD > Li-Sr-MD > Li-K-MD. This sequence inversely tracks the increase interaction with CO_2 observed by TPD of CO_2. IR spectroscopy used to determine structure of CO_2 adsorbed

in the carbonate region. IR spectroscopy reveals that bidentate carbonate species dominate on Li-MD sample. For the modified samples, in addition to bidentate carbonate species, unidentate carbonate species are also detected. From the relative intensity of carbonate bands the basicity increases in the order Li-MD < Li-Na-MD < Li-Ba-MD < Li-Sr-MD < Li-K-MD. Finally, the catalysts were tested for the ethane oxidative dehydrogenation reaction. The highest activity was found for Li-MD, the lowest for Li-K-MD, and the activities of other samples were in between. The effect of temperature studied on selectivity, ethene selectivity increased with temperature and become constant once the temperature approach the melting point. The temperature, at which the high and constant selectivity was obtained, coincides with the temperature at which spreading/melting of the alkali and alkaline earth metal chloride phases was experimentally observed. It is remarkable that the lower melting points induce higher selectivity. The possible reasons for the effect of melting point on the ethene selectivity is speculated to be the easier desorption of ethyl radicals formed on the catalysts surface and weaker adsorption of ethene in molten state. The ethane reaction rates decreased in the order Li-MD > Li-Na-MD > Li-Ba-MD > Li-Sr-MD > Li-K-MD. The catalytic activity was directly correlated with the strength of the accessible Lewis acid sites and inversely correlated with the basicity.

Zusammenfassung

Diese Doktorarbeit behandelt zwei Teile: Teil A) Oxychlorierung von Methan (OCM) und Teil B) Oxidative Dehydrierung von Ethan (ODH).

A) Methan ist der Hauptbestandteil von Erdgas, und kann als Treibstoff oder als Ausgangsstoff für die chemische Industrie verwendet werden. Die oxidative Chlorierung von Methan zu Methylhalogeniden ist eine viel versprechende Technik für die Umsetzung von Methan zu Methylhalogeniden, die vielfältig weiterverarbeitet werden können.

Erst kürzlich wurde entdeckt, dass Katalysatoren, die ausschließlich aus LaOCl bestehen und unter Reaktionsbedingungen mit HCl zu LaCl$_3$ umgewandelt werden können, aktiv, selektiv und vor allem stabil sind für die oxidative Chlorierung von Methan. Jedoch ist der Einfluss der Chlorierung auf die in LaOCl vorhandenen verschiedenen Phasen, die Rolle der verschiedenen basischen Zentren, deren optimale Konzentration und Stärke, noch nicht im Detail bekannt. Deshalb ist es das Ziel dieser Arbeit LaOCl während der Aktivierung, der Chlorierung und unter Reaktionsbedingungen zu charakterisieren. Außerdem soll versucht werden die Zusammensetzung des Katalysators aus verschiedenen Phasen mit dem katalytischen Verhalten zu korrelieren.

Als Katalysatorvorläufer wurde kommerzielles LaOCl verwendet, das von Dow Chemical Company, USA, bereitgestellt wurde. Die Phasenreinheit der LaOCl Proben wurde mit XRD überprüft. Die XRD Analyse zeigte, dass die GRII Probe die Probe mit der höchsten Verunreinigung mit Lanthandioxokarbonat ist. Dieses Ergebnis wurde auch durch die EDX Analyse bestätigt, die zeigt, dass GRII das höchste La/Cl Verhältnis von 2.82 besizt. IR Spektroskopie wurde verwendet, um verschiedene Arten von Hydroxylgruppen auf der LaOCl Oberfläche zu identifizieren. Auf den SC Proben konnten zwei verschiedene Hydroxylgruppen identifiziert werden, LaO(OH) und La(OH). Außerdem wurden bei GRII konnten noch weitere Hydroxylgruppen des La(OH)$_3$ Typs nachgewiesen. Die Art und die Konzentration der verschiedenen Säurezentren wurde mit DMP-TPD (2,6-Dimethylpyridin)

und NH$_3$-TPD bestimmt. Die Temperaturprogrammierte Desorption von Ammoniak und DMP zeigen, dass auf allen Probenoberflächen nur eine Art von schwach aziden Zentren vorhanden ist. Die Stärke der Lewis Säurezentren sinkt in der folgenden Reihenfolge GRII>SCI>SCIIIB>SCII. Basische Zentren wurden mit CO$_2$ als Probenmolekül identifiziert. In der Temperaturprogrammierten Desorption von CO$_2$ wurden drei verschiedene Peaks detektiert, was auf die Anwesenheit von drei verschiedenen basischen Zentren hinweist. Die Reihenfolge der Konzentration aller basischen Zentren ist genau gegensätzlich der Reihenfolge der Säurezentren. Mit IR Spektroskopie konnten nach der CO$_2$ Adsorption verschiedene Karbonatspezies nachgewiesen werden. Die IR und TPD Ergebnisse zeigen, dass einzähnige und zweizähnige Karbonate als Hauptspezies vorliegen und in geringen Mengen Hydrogenkarbonat.

Alle vier kommerziellen Katalysatoren wurden für Methan Oxychlorierung getestet. In der Methan Oxychlorierung ist Methylchlorid das Primärprodukt, gefolgt von Methylenchlorid, CO und CO$_2$ als Sekundärprodukte und Spuren von CH$_3$Cl und CCl$_4$ als Nebenprodukte. SCII hat sich als der aktivste Katalysator für die MOC Reaktion herausgestellt, gefolgt von SCIIIB und SCI. Eine direkte Abhängigkeit der Aktivität mit der Basizität (Konzentration der O^{2-} Stellen) wurde für alle Proben beobachtet. Daher wird postuliert, dass bei der aktivsten Probe, SCII, die die größte Menge an HCl während der Chlorierung aufnimmt, ein Austausch der O^{2-} Basenzentren durch Cl$^-$ stattfindet. Das substituierte Cl$^-$ Atom wird als instabil angenommen und ist daher verantwortlich für die höhere Aktivität bei der Methan Oxychlorierung. Es wird angenommen, dass die Aktivität von der Anzahl der Chlor-begrenzten Stellen and der Oberfläche abhängt. Als aktive Spezies im Mechanismus wird OCl* vorgeschlagen.

Der Katalysator wird mit HCl vorbehandelt, daher ist es von Interesse die Phasenumwandlung von LaOCl zu LaCl$_3$ zu untersuchen und eine Korrelation zwischen der Phasenzusammensetzung und dem katalytischen Verhalten zu finden. Verschiedene

Analysetechniken wie IR Spektroskopie, Temperaturpogrammierte Desorption, ^{1}H/^{35}Cl-MAS-NMR Spektroskopie, Röntgenbeugung wurden verwendet um die kommerziellen Proben zu charakterisieren. XRD und IR zeigten, dass sich die Katalysator größtenteils zu LaCl$_3$ umwandelten. Es konnte gezeigt werden, dass die Funktionellengruppen und die katalytische Aktivität von verschiedenen Graden der Chlorierung von LaCl$_3$ beeinflusst werden und dadurch auch durch die Konzentration von LaOCl im endgültigen Material. Es konnte gezeigt werden, dass die Konzentration des Startmaterials für die Methan Oxychlorierungsreaktion in der folgenden Reihenfolge sinkt: SCII>SCIIIB>SCI. Die Aktivität korreliert mit der Stabilität der Karbonate (Konzentration der Karbonate), da sich gering stabile Karbonate leichter in Lanthanchloride umwandeln. Daher hängt die Aktivität davon ab wie leicht sich die Probe in die LaCl$_3$ Phase umwandeln.

B) ODH ist eine attraktive Technik für die Produktion von Olefinen. Es ist eine alternative Methode zur Dehydrierung und bietet basierend auf technischen und ökonomischen Überlegungen große Vorteile gegenüber nicht-oxidativen Prozessen.

Eine Reihe von Katalysatoren wurde durch Zugabe von Alkali- oder Erdalkalimetalchloriden zu LiCl/Dy$_2$O$_3$/MgO Katalysatoren synthetisiert. Die hergestellten Katalysatoren wurden mit verschiedenen Techniken charakterisiert. Die spezifischen Oberflächen der hergestellten Katalysatoren wurden mit N$_2$ Adsorption gemessen. Es wurde beobachtet, dass die spezifische Oberfläche von Li-Na-MD, Li-Sr-MD nur schwach sinkt im Vergleich zu Li-MD, während die spezifische Oberfläche von Li-K-MD dramatisch sinkt. Da Li-K-MD einen sehr geringen Schmelzpunkt hat, werden wahrscheinlich die Poren der Proben während der Kalzinierung durch die LiCl/KCl Schmelze blockiert, was die überaus geringe Oberfläche verursacht. Mit XRD wurden die kristallinen Phasen, die im kalzinierten Katalysator gebildet werden, untersucht. Es hat sich gezeigt, dass MgO die dominierende Phase ist, weiterhin wurden auch LiCl und DyOCl Phasen in allen Proben nachgewiesen. Ander Phasen wie NaCl, KCl, SrCl$_2$ und BaCl$_2$ Phasen wurden in den entsprechenden Proben beobachtet.

Die Umwandlung unter Reaktionsbedingungen eines zuvor aktivierten Katalysators wurde *in situ* mit XRD zwischen 100°C und 650°C untersucht. Mit steigender Temperatur verschwinden die Beugungsreflexe der Alkali- und Erdalkalimetallchloride innerhalb verschiedener Temperaturbereiche. Am interessantesten ist es zu erwähnen, dass der theoretische Schmelzpunkt von reinem LiCl, LiCl/NaCl, LiCl/KCl, LiCl/$SrCl_2$ und LiCl/$BaCl_2$ innerhalb dieser Temperaturbereiche liegt. Daraus wird gefolgert, dass die Abnahme der Reflexe mit dem Schmelzen der Metallchloridphase zusammenhängt.

Die Phasenumwandlung wurde mit TG-DSC genauer untersucht. Bei purem Li-MD wurde die Abnahme des beobachteten endothermen Signals erstmals um 500°C beobachtet und ein Maximum wird bei 604°C erreicht, was auf das Schmelzen von Lidl hinweist. Dieser Wert stimmt mit dem Schmelzpunkt von reinem LiCl (610°C) überein. Für alle andern Proben, wurde nur eine Phasenumwandlung beobachtet und der entsprechende Schmelzpunkt ist viel niedriger als der von LiCl. Dies wird auf die Bildung einer eutektischen Mischung von Alkali- oder Erdalkalimetallchloriden mit LiCl zurück geführt. Aus diesem Experiment wird geschlossen, dass die Zugabe von Alkali- und Erdalkalimetallchloriden den Schmelzpunkt im Bezug zu LiCl/Dy_2O_3/MgO verringert.

Die Konzentration der basischen Zentren wurde ebenfalls mit der Temperaturprogrammierten Desorption von CO_2 bestimmt. Für alle Proben wurde nur ein breiter Peak beobachtet. Dieser Peak wird physisorbiertem CO_2 zugeschrieben. Die Zugabe von Alkali- und Erdalkalimetallchloriden erhöht die Basizität der Proben. Li-L-MD, Li-Ba-MD, Li-Sr-MD sind stärker basisch. Die Konzentration der Lewissäurezentren und Basenzentren wurde auch mit IR Spektroskopie von adsorbierten CO_2 untersucht. Die asymmetrische Schwingung des molekular adsorbierten CO_2 der mit Alkali- und Erdalkalimetallchloriden modifizierten Katalysatoren erscheint um 2300 cm^{-1}. Die v_3 Schwingung ist zu niedrigeren Wellenzahlen verschoben, da der Ionenradius der Alkali- und Erdalkalimetallkations?. Diese Verschiebung steht im Bezug zur

Elektronenpaarakzeptorstärke der Metallkationen bezüglich des adsorbierten CO_2. Das impliziert, dass die Säurestärke der zugänglichen Kationen in der folgenden Reihenfolge sinkt: Li-MD>>Li-Na-MD>Li-Ba-MD>Li-Sr-MD>Li-Sr-MD>Li-K-MD. Diese Reihenfolge ist genau umgekehrt zum Anstieg in der beobachteten Wechselwirkung mit CO_2 in der CO_2-TPD. Mit IR Spektroskopie wurde die Struktur des adsorbierten CO_2 in der Karbonatregion untersucht. Für die veränderten Proben wurden neben zweizähnigen Karbonatspezies auch einzähnige Karbonatspezies detektiert. Von der relativen Intensität der Karbonatbande kann auf die Basizität geschlossen werden, die in der folgenden Reihenfolge ansteigt: Li-MD<Li-NaMD<Li-Ba-MD<Li-Sr-MD<Li-K-MD.

Die präparierten Katalysatoren wurden auch für die oxidative Dehydrierung von Ethan getestet. Die höchste Aktivität zeigte Li-MD und die geringste Aktivität zeigte Li-K-MD. Die Aktivitäten der anderen Katalysatoren liegen dazwischen. Die Untersuchung des Effektes der Temperatur auf die Selektivität hat gezeigt, dass die Ethylenselektivität mit steigender Temperatur steigt und konstant wird, sobald die Temperatur den Schmelzpunkt erreicht hat. Die Temperatur, bei der die höchste und konstante Selektivität erreicht wurde fällt mit der Temperatur zusammen bei der die Verteilung/Schmelzen der Alkali- und Erdalkalimetallchloridphase experimentell beobachtet wurde. Ein möglicher Grund für den Einfluss des Schmelzpunktes auf die Ethylenselektivität könnte die leichtere Desorption des Ethylenradikals, das auf der Katalysatoroberfläche gebildet wird, und die schwächere Adsorption von Ethan im geschmolzenen Zustand sein. Die Ethanreaktionsrate sinkt in der folgenden Reihenfolge: Li-MD>Li-Na-MD>Li-Ba_MD>Li-Sr-MD>Li-K-MD. Die katalytische Aktivität korreliert direkt mit der Stärke der zugänglichen Lewissäurezentren und korreliert indirekt mit der Basizität.

LIST OF PUBLICATIONS

1. Oxidative dehydrogenation of ethane over Dy_2O_3/MgO supported LiCl containing eutectic chloride catalysts
    Balkrishna B. Tope, Yongzhong Zhu and Johannes A. Lercher
    (communicated to *Topics in catalysis*)

2. Surface Acidity and Basicity of La_2O_3, LaOCl, and $LaCl_3$ Characterized by IR Spectroscopy, TPD, and DFT Calculation
    O. V. Manoilova, S. G. Podkolzin, **B. B. Tope**, J. A. Lercher, E. E. Stangland, J. M. Goupil, B. M. Weckhuysen
    Journal of Physical Chemistry B **2004,** *108***, 15770-15781**

3. Alkali loaded silica, a solid base: Investigation by FTIR Spectroscopy of adsorbed CO_2 and its catalytic activity
    Rajaram Bal, **B. B. Tope**, T. K. Das, S. G. Hegde and S. Sivasanker
    Journal of Catalysis **2001,** *204***, 358-363**

4. A mechanistic approach to phenol methylation on $Cu_{1-x}Co_xFe_2O_4$: FTIR study
    T. Mathew, M. Vijayaraj, S. Pai, **B. B. Tope**, S. G. Hegde, B. S. Rao and C. S. Gopinath
    Journal of Catalysis **2004,** *227***, 175-185**

5. Acid- Base properties of $Cu_{1-x}CO_xFe_2O_4$ ferrospinels: FTIR investigation
    Thomas Mathew, **B. B. Tope**, N. R. Shiju, B. S. Rao, S. G. Hegde, C. S. Gopinath
    Physical Chemistry Chemical Physics **2002,** *4***, 4260-4267**

6. Vapour Phase O-methylation of dihydroxybenzenes with methanol over cesium loaded silica, a solid base
    Rajaram Bal, **B. B. Tope** and S. Sivasanker.
    Journal of Molecular Catalysis A: Chemical **2002,** *182***, 161-171**

7. Tertiary butylation of phenol over HY and dealuminated HY zeolite
    R. Anand, R. Maheswari, K. U. Gore, **B. B. Tope**
    Journal of Molecular Catalysis A: Chemical **2002,** *3780***, 1-7**

CONTRIBUTIONS TO SYMPOSIA/CONFERENCES

1. Oxidative dehydrogenation of ethane over supported chloride catalyst
    B. Tope, S. Gaab, Y. Zhu, R. Olindo, and J.A. Lercher
    DGMK-Conference "Oxidation and Functionalization: Classical and Alternative Routes and Sources, Milan, 2005, Italy.

2. Oxidative Synthesis of Methylchloride from Methane
    E. Peringer, **B. Tope**, R. Olindo, O. Manoilova, S Podkolzin, B. Weckhuysen and J.A. Lercher
    DGMK-Conference "Oxidation and Functionalization: Classical and Alternative Routes and Sources, Milan, 2005, Italy.

3. FT-IR, TPD and DFT studies on the acid-base properties of La_2O_3, LaOCl and $LaCl_3$ catalysts
O. V. Manoilova, S. G. Podkolzin, **B. Tope**, S. Gaab, J. A. Lercher, J. M. Goupil, C. Binet, T. Visser and B. M. Weckhuysen
Conference on Interfaces and Colloidal Systems, Giens, France.

4. Acid-Base properties and Catalytic Application of Cobalt-Zinc Ferrites
T. Mathew, K. Sreekumar, **B. Tope,** S. G. Hegde and B. S. Rao
International Symposium on Acid-Base Catalysis IV (ABC IV) May 7-12-2001 at Matsuyama, Japan.

5. Vapour Phase O-methylation of dihydroxybenzenes with methanol over cesium loaded silica, a solid base
R. Bal, **B. B. Tope**, T. K. Das, S. G. Hegde and S. Sivasanker
Fifteenth Indian National Symposium on Catalysis and Second Conference of the Indo-Pacific Catalysis Association CATSYMP-15 & IPCAT-2 at National Chemical Laboratory, Pune, India.